FINAL REPORT

PARTS III AND IV
The Study of Space Communications Spread Spectrum Systems

REPORT 88-3

PREPARED FOR THE DEPARTMENT OF COMMUNICATIONS
UNDER DSS CONTRACT NO. 36001-6-3530/0/ST

Department of Electrical Engineering
Queen's University at Kingston
Kingston, Ontario, Canada

FINAL REPORT

PARTS III AND IV
The Study of Space Communications Spread Spectrum Systems

REPORT 88-3

PREPARED FOR THE DEPARTMENT OF COMMUNICATIONS
UNDER DSS CONTRACT NO. 36001-6-3530/0/ST

UNLIMITED
CRC-DP-CR-88-002
DND-SUPPORTED
Refer All Requests
to L. Mason or
CRAD/DSIS

DND SUPPORTED CONTRACT REPORTS

SECTOR	BRANCH	DATE
DGSTA	DSAT	14-12-88

1. DND CR NO. CRC-DP-CR-88-002	2. DSS CONTRACT NO. 36001-6-3530	
3. TITLE: THE STUDY OF SPACE COMMUNICATIONS SPREAD SPECTRUM SYSTEMS (Part I, II, III & IV)		4. DATE March, 1988
5. CONTRACTOR Queen University		
6. SCIENTIFIC AUTHORITY L. Mason	7. LOCATION CRC/DSAT	8. TEL. NO. 998-2855

9. CONTRACTOR REPORT CLASSIFICATION:

LIMITED [ ] UNLIMITED [xxx]

* REASONS FOR CLASSIFICATION:

10. NO. OF COPIES SUBMITTED TO LIBRARY: 3 copies each

SECURITY CLASSIFICATION OF FORM
(highest classification of Title, Abstract, Keywords)

DOCUMENT CONTROL DATA

(Security classification of title, body of abstract and indexing annotation must be entered when the overall document is classified)

1. ORIGINATOR (the name and address of the organization preparing the document. Organizations for whom the document was prepared, e.g. Establishment sponsoring a contractor's report, or tasking agency, are entered in section 8.)

Department of Electrical Engineering,
QUEEN'S UNIVERSITY,
KINGSTON, Ontario, Canada. K7L 3N6

2. SECURITY CLASSIFICATION (overall security classification of the document. including special warning terms if applicable)

Unclassified.

3. TITLE (the complete document title as indicated on the title page. Its classification should be indicated by the appropriate abbreviation (S,C,R or U) in parentheses after the title.)

"The Study of Space Communications Spread Spectrum Systems"
Part III - Synchronization of a Frequency Hopped, Spread Spectrum, Space Communications System
Part IV - Detection of a Sinusoidal Signal with a Wideband Discrete Frequency Distribution

4. AUTHORS (Last name, first name, middle initial. If military, show rank, e.g. Doe, Maj. John E.)

Part III - Simmons, Stanley J.
Part IV - McLane, Peter J., Hopkins, Wendy Lee, Beaulieu, Norman C.

5. DATE OF PUBLICATION (month and year of publication of document)

March, 1988.

6a. NO. OF PAGES (total containing information. Include Annexes, Appendices, etc.)

108 + 38

6b. NO. OF REFS (total cited in document)

31 + 6

7. DESCRIPTIVE NOTES (the category of the document, e.g. technical report, technical note or memorandum. If appropriate, enter the type of report, e.g. interim, progress, summary, annual or final. Give the inclusive dates when a specific reporting period is covered.)

Final Report, Parts III and IV.

8. SPONSORING ACTIVITY (the name of the department project office or laboratory sponsoring the research and development. Include the address.)

Communications Research Centre, Department of Communications, 3701 Carling Avenue,
P.O. Box 11490, Station 'H', OTTAWA, Ontario. K2H 8S2

9a. PROJECT OR GRANT NO. (if appropriate, the applicable research and development project or grant number under which the document was written. Please specify whether project or grant)

32A99

9b. CONTRACT NO. (if appropriate, the applicable number under which the document was written)

DSS Contract 36001-6-3530/0/ST

10a. ORIGINATOR'S DOCUMENT NUMBER (the official document number by which the document is identified by the originating activity. This number must be unique to this document.)

Report 88-3, Department of Electrical Engineering, Queen's Univ., Kingston, Ont.

10b. OTHER DOCUMENT NOS. (Any other numbers which may be assigned this document either by the originator or by the sponsor)

11. DOCUMENT AVAILABILITY (any limitations on further dissemination of the document, other than those imposed by security classification)

(x) Unlimited distribution
( ) Distribution limited to defence departments and defence contractors; further distribution only as approved
( ) Distribution limited to defence departments and Canadian defence contractors; further distribution only as approved
( ) Distribution limited to government departments and agencies; further distribution only as approved
( ) Distribution limited to defence departments; further distribution only as approved
( ) Other (please specify):

12. DOCUMENT ANNOUNCEMENT (any limitation to the bibliographic announcement of this document. This will normally correspond to the Document Availabilty (11). However, where further distribution (beyond the audience specified in 11) is possible, a wider announcement audience may be selected.)

No Limitation.

13. ABSTRACT (a brief and factual summary of the document. It may also appear elsewhere in the body of the document itself. It is highly desirable that the abstract of classified documents be unclassified. Each paragraph of the abstract shall begin with an indication of the security classification of the information in the paragraph (unless the document itself is unclassified) represented as (S), (C), (R), or (U). It is not necessary to include here abstracts in both official languages unless the text is bilingual).

PART III: This part deals with uplink synchronization in a frequency-hopped multiple-access satellite system. Uplink synchronization encompasses the acquisition (and tracking) of parameters required to allow the detection of frequency-hopped user transmissions at a satellite that performs frequency-dehopping and detection processing. Since this synchronization process will require feedback to the user, the issues of downlink format and synchronization need to be addressed, but to a lesser extent. We first define the system under consideration along with the assumptions that are employed. A downlink format is defined, and an associated downlink synchronization procedure is described. Various aspects of uplink synchronization are then outlined, and options for system implementations and strategies are presented. As a baseline, an ideal "simplest possible" system (having lowest synchronization complexity) is then described. Finally, we look at the synchronization implications of the schemes suggested by Kolba.

PART IV: This part examines the detection of sinusoidal signals of which only the signal frequency is unknown. It is assumed that the signal will be transmitted at one of N discrete, orthogonal frequencies and that the detector knows the frequency distribution. A goal of the report is to establish the detection performance limits for the interception of slow frequency hopped signals. Optimum and near-optimum receivers, both coherent and noncoherent, are developed for the signal structure noted above, assuming an additive white Gaussian noise environment. In particular, we consider the case when N is large, a situation appropriate for slow frequency-hopped, spread spectrum communications where N is the processing gain. We determine N and a corresponding threshold SNR such that operation of an interception receiver is impractical below this SNR.

14. KEYWORDS, DESCRIPTORS or IDENTIFIERS (technically meaningful terms or short phrases that characterize a document and could be helpful in cataloguing the document. They should be selected so that no security classification is required. Identifiers, such as equipment model designation, trade name, military project code name, geographic location may also be included. If possible, keywords should be selected from a published thesaurus. e.g. Thesaurus of Engineering and Scientific Terms (TEST) and that thesaurus identified. If it is not possible to select indexing terms which are Unclassified, the classification of each should be indicated as with the title.)

Part III

Frequency hopped spread spectrum, processing satellite, uplink synchronization, downlink synchronization.

Part IV

Frequency hopped spread spectrum modulation, interception receiver, probability of detection, probability of false alarm, coherent receiver, non-coherent receiver, maximum likelihood receiver, processing gain.

FINAL REPORT

PARTS III AND IV

The Study of Space Communications Spread Spectrum Systems

REPORT 88-3

PREPARED FOR THE DEPARTMENT OF COMMUNICATIONS

UNDER DSS CONTRACT NO. 36001-6-3530/0/ST

1. Part III - Synchronization of a Frequency Hopped, Spread Spectrum, Space Communications System, by S. J. Simmons, pages 1 - 37.
2. Part IV - Detection of a Sinusoidal Signal with a Wideband Discrete Frequency Distribution, by Peter J. McLane, Wendy Lee Hopkins and Norman C. Beaulieu, pages 1 - 154.

Department of Electrical Engineering

Queen's University

Kingston, Ontario, Canada

February 1988

SYNCHRONIZATION OF A FREQUENCY HOPPED, SPREAD SPECTRUM, SPACE COMMUNICATIONS SYSTEM

by

S. J. Simmons

REPORT 88-3

FINAL REPORT PART III

PREPARED FOR THE DEPARTMENT OF COMMUNICATIONS

UNDER DSS CONTRACT NO. 36001-6-3530/0/ST

"The Study of Space Communications Spread Spectrum Systems"

Queen's University

Kingston, Ontario, Canada

February 1988

TABLE OF CONTENTS

PART III - Synchronization of a Frequency Hopped, Spread Spectrum, Space Communications System

PART III - Synchronization of a Frequency Hopped, Spread Spectrum, Space Communications System

INTRODUCTION

This part of the report deals with uplink synchronization in a frequency-hopped multiple-access satellite system. Uplink synchronization encompasses the acquisition (and tracking) of parameters required to allow the detection of frequency-hopped user transmissions at a satellite that performs frequency-dehopping and detection processing. Since this synchronization process will require feedback to the user, the issues of downlink format and synchronization need to be addressed, but to a lesser extent. High-level data formats and associated protocols (e.g. for network management) are not considered.

We first define the system under consideration along with the assumptions that are employed. A downlink format is defined, and an associated downlink synchronization procedure is described. Various aspects of uplink synchronization are then outlined, and options for system implementations and strategies are presented. As a baseline, an ideal "simplest possible" system (having lowest synchronization complexity) is then described. Finally, we look at the synchronization implications of the schemes suggested by Kolba [1,2] for demand-assignment of satellite resources in a system with a large number of users.

1. SYSTEM UNDER CONSIDERATION

1.1 General

It is assumed that this is principally a point-to-point communications system based on circuit switching. Users communicate through a processing satellite that dehops user uplink transmissions, and creates suitably formatted TDM frames for transmission on the downlink. Call setup is assumed to be handled through some central controller. This controller may be a ground station, or may in fact be on board the satellite itself. Users send call

requests to the controller using the same uplink channels that they use for the subsequent call; these requests therefore enjoy the same antijam protection as normal user transmissions. Channel assignments for the users may be fixed or reconfigurable by a central controller overseeing demand assignment. To keep things simple, we initially assume a fixed assignment scheme with dedicated uplink/downlink slots for each user. The implications of demand-assigned systems are dealt with in section 6.

We assume that when user A is not engaged in a call or a call request, the satellite places the data detections from user A's uplink slot into user A's downlink slot. This "loopback" mode is assumed to be the default; it provides the feedback which is crucial to initial synchronization. The type of feedback information provided for this synchronization, and the format with which it is delivered, are considered later.

Once synchronization is achieved, the user can send the appropriate control codes to command the satellite to reconfigure to route subsequent transmissions to the central controller (who will in turn command subsequent reconfigurations needed for the call). Once the call is complete, hangup codes from the initiating party can be relayed by the satellite to the central controller, and the call connection terminated. This implies that the reconfiguration control on the satellite must be capable of accepting commands directly from each user, as well as from the central controller. This method also implies that the satellite must be continually decoding signals from each user's slot, looking for control codes. It will therefore be necessary to avoid hangup codes in normal transmissions. In addition, we must make negligible the probability that the satellite randomly detects the code for exiting loopback mode when a user is not yet synchronized (or is not even transmitting). This can be assured by making these codes long.

Alternatives do exist, such as dedicating a (possibly time-shared) channel for each user to send requests to the (ground-based) central controller. That

is, we might specify that for some small percentage of the time during loopback or regular calls, the satellite will instead route the user transmissions to the central controller. Such time-division multiplexing embeds a control channel in the normal user transmissions. By shifting the responsibility of looking for control codes to a ground-based controller, the processing burden on the satellite could be reduced. The method outlined in the previous paragraph has only been adopted so that the discussion is simpler and more concrete; all of the important principles and problems are still revealed.

1.2 The uplink

Uplink users are arranged in an FDMA format, with each user employing a non-coherent M-ary modulation (FSK is assumed). Users hop their carrier frequencies as a group (as shown in Fig. 1) over a very wide band (approximately 1 GHz). The carrier phase is not preserved across hops. The hopping pattern which the users' frequency synthesizers follow is produced by a pseudo-random sequence generator with a period which can be in excess of several days. The hopping rate employed (e.g. 20 kHz) is sufficient to thwart frequency-follower jammers.

Users can be separated into two groups. Low-rate users (e.g. 2400 bps) are distinguished by several (or many) hops occurring during one symbol duration. Conversely, high-rate users (e.g. 1.5 Mbps) transmit many symbols per hop. We assume for the lower rate users that there are an integer number of Q hops per symbol, and that the symbol boundaries are aligned with hop transitions. For the higher rate users, we also assume alignment of hopping transitions and symbol boundaries, this time with an integer number of symbols per hop. If this is not the case, the first and last symbols of a hop cannot be used (which is a possible option). For the lower rate users, the hopping rate determines the effective bandwidth of the signal, and puts a lower limit on the frequency spacing of their FSK tones. For example, a hopping rate of 20

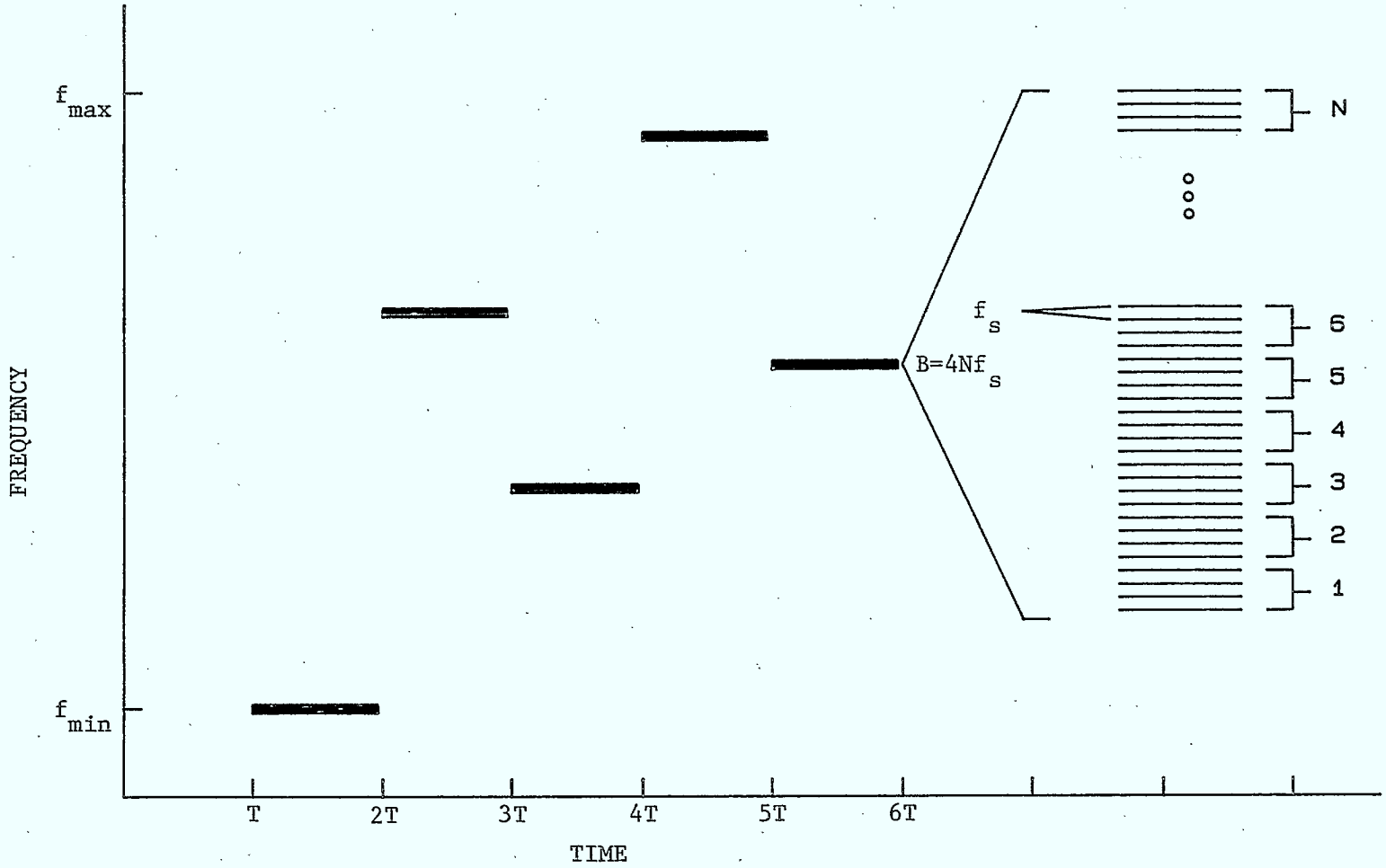

Fig. 1. Frequency-hopping of group of N users using 4-ary FSK.

kHz means that the FSK tones of each user must be spaced at 30 kHz to 40 kHz to be accurately discriminated at the satellite.

Uplink beam sharing is a possibility [2]. One or several agile high-gain uplink antennae can provide coverage to a large number of spot zones on a time-multiplexed basis. This scheme allows user ground terminals to operate at lower EIRP's, so that smaller transmitting antennae can be used (and/or lower power transmitter amplifiers). Users must know when the satellite antenna is pointed to receive signals from their zone (accounting for earth-to-satellite propagation delay), or at least, they must be able to discover this window by trial-and-error search. Such a trial-and-error procedure could be accommodated by simply adding one more parameter to the uplink synchronization search discussed later. This beam-sharing option poses no additional fundamental problems, and simply implies longer waits for access to satellite resources. It is therefore not considered further.

1.3 The downlink

The downlink follows a TDM format and the composite signal may or may not be protected by spectrum spreading. If spectrum spreading is employed here, the first step at the receiver is to synchronize to this spreading sequence and despread. This is a conventional synchronization problem and so is only briefly considered here. Downlink spreading may be a requirement to protect against jamming. Jamming the weak satellite signals may not be overly difficult when users employ low-gain antennae with correspondingly poor direction discrimination.

The downlink is served by a single high-gain agile antenna that provides a narrow spot beam that hops from zone to zone. This arrangement again allows users to employ smaller (lower-gain) receive antennae, but its primary purpose is to reduce the required satellite transmitter power. The downlink TDM format is assumed to be as in Figure 2. One frame is composed of the intervals during

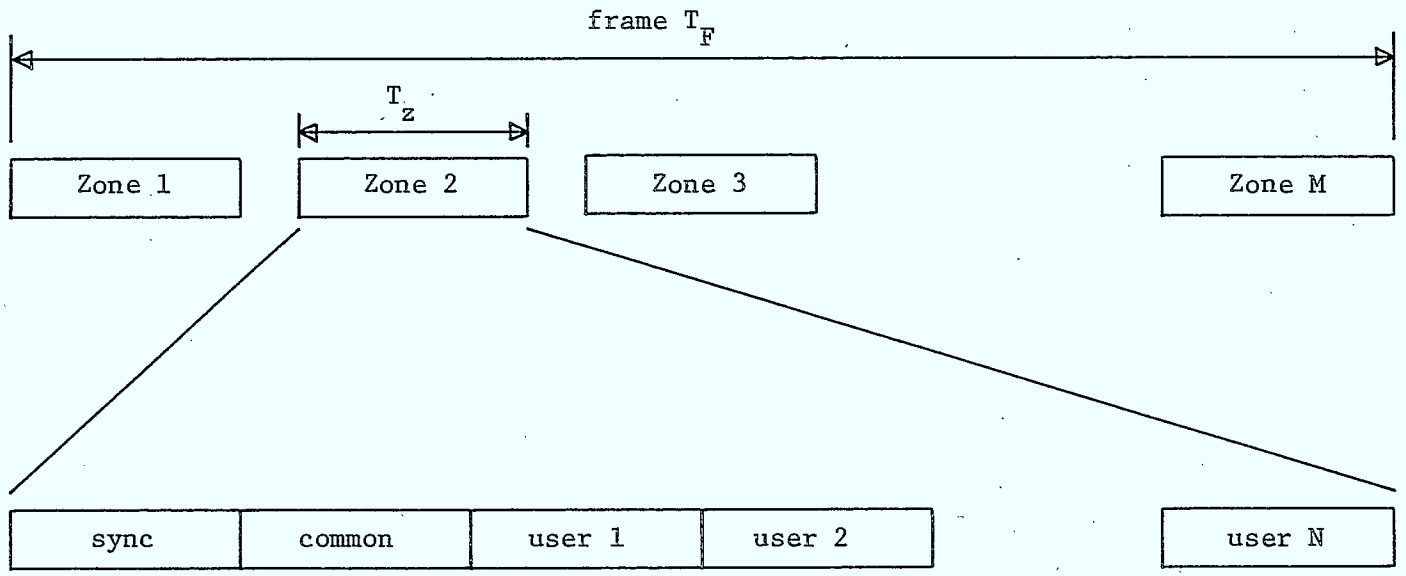

Fig. 2. Downlink TDM frame format.

which the downlink antenna beam hops to each of the coverage zones. While dwelling on a zone, a conventional sync pattern is transmitted, followed by data slots for the users, as well as a common information slot in which the satellite may transmit control messages or data which facilitate initial synchronization and tracking. Users look for the sync pattern, then "read" data from their assigned time slots. As in a normal TDMA satellite system, the sync pattern creates the time reference for the user time slots that follow.

2. DOWNLINK SYNCHRONIZATION

We assume initially that the downlink TDM signal is not spread. Each user receives signal energy only during the time that the downlink beam is dwelling on the user's zone. For example, with 20 fully active zones, users see signal energy for about 5% of the time; some small percentage is needed to allow beam repositioning.

To perform initial acquisition for an unspread signal, the following procedure may be employed. Users energy-detect over a sliding window of length T_z (or smaller), where T_z is the dwell time on the zone. Once received energy exceeds a threshold, the window is frozen. Now the received energy may be monitored as the window position is varied, with step sizes reduced at each iteration, until the best alignment with the satellite dwell time is found. The final window position should then be advanced slightly to ensure that the sync burst at the start of the frame does not fall outside the window. The windowed signal is then passed to phase and bit-timing recovery circuits. Once these parameters are acquired, the data is decoded, and a search for a unique sync word in the sync burst is begun using a sliding binary correlator [3]. This will reliably detect the sync word even in the presence of isolated bit errors. When the sync word is acquired, the user can identify his time slot and pick out the data destined for him. In addition, any common data supplied

by the satellite can be recovered. Note that the initial steps of this procedure may require averaging over several frames. The windowing is used to avoid presenting just noise (and possibly jamming signals) to the sync circuits when the satellite beam is pointed elsewhere.

Note that unlike a conventional TDMA system having TDM both on the uplink and on the downlink, we do not need bit-timing symbols dedicated to each user. All data bursts for the ground users are exactly aligned to common timing marks since these bursts are contained in slots formed by the satellite from its internal clock; there is only this single timing reference. This also means that the signals from subsequent beam hops are easily combined in the carrier and bit-timing recovery loops. All that is needed is a simple gating waveform as in Figure 3.

If the downlink signal is spread, synchronization is more complicated. When spectral spreading is used, the (average) signal level may be well below the noise level at the output of the front-end filters. In this case, straight energy detection over a sliding window may be of no use. Instead, a sequential search for the spreading code sequence (and correct carrier frequency) would be performed, with steps on the order of half of a chip for trial code phases (with DS spreading), or half of a hop (with FH spreading). The fact that there may be no signal for a large percentage of the time (while the downlink beam is elsewhere) will affect the search strategy.

In a typical sequential search, an attempt is made to despread the received signal using a locally generated reference with trial values for code phase and carrier frequency. The envelope of the despread waveform is detected at some intermediate frequency after filtering to the bandwidth of the data modulation. This energy is then integrated over an observation interval of T_I. If the result exceeds a predetermined threshold, a possible detection of aquisition is declared, otherwise the trial values of code phase and carrier frequency are stepped, and the process repeated. With such a method applied

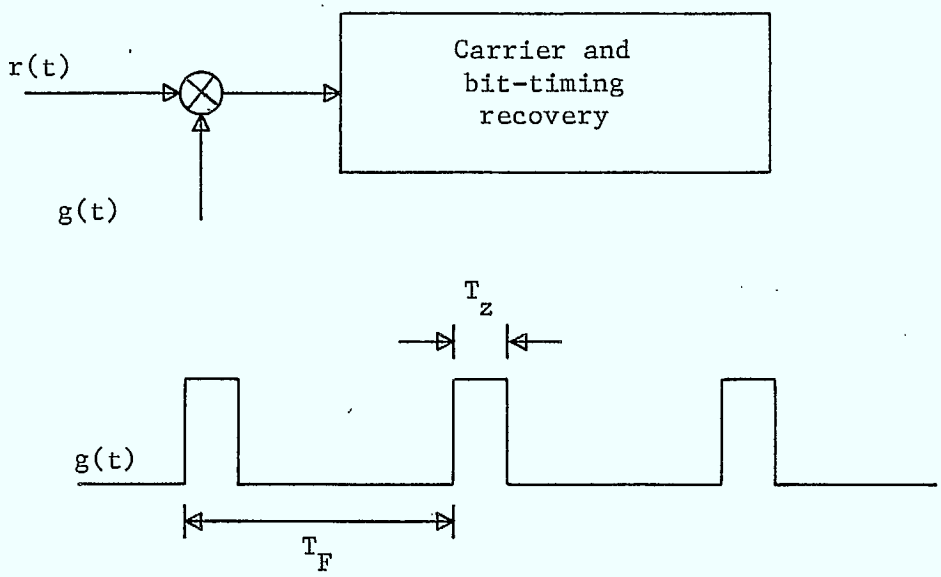

Fig. 3. Gating for downlink synchronization.

with downlink beam-hopping, care must be taken to avoid basing decisions on the integration output when the signal was either completely absent or only present for a fraction of T_I. Simply making T_I larger than T_F is not acceptable; in that case we are guaranteed to see signal energy, but only for T_Z, a small fraction of the total integration time. Detection thresholds would have to be low, and this implies a high probability of false alarm. A better approach is to still window the received signal with a window of duration T_Z before despreading and integrating. The window position becomes one more search parameter. If (T_F/T_Z) trial values for window position are searched while holding the other parameters fixed, we are sure to have at least half the signal energy (i.e. over at least time $T_Z/2$) pass through the window at one of these (T_F/T_Z) trial positions. The integration time T_I may still span several frames (if necessary to develop adequate SNR) at a single trial value for the window position.

There are of course a number of different alternatives to fixed-integration-time detection [5,6] (e.g. continuous sweep, multiple dwell times, sequential detection), but all should incorporate windowing to increase the SNR. One final alternative that can be mentioned is matched-filter detection. A bandpass filter is matched to the transmitted signal over (a portion of) the code sequence. In this scheme, two detection circuits are used, one with the wrong code to act as a reference, and the other to search for the correct code. When the output of the searching circuit exceeds the output of the reference, a possible detection is declared. The use of a reference avoids reliance on a threshold that depends on a-priori unknown signal to noise (or jamming) ratios. The use of the matched filter means that a sliding-window effect is created, where the window is the length of the matched-filter response. If the signal energy from a single dwell time T_Z is sufficient for detection, then there is

no need to combine across multiple frames. If this is not the case, however, this approach could not be used.

Once synchronization to the spreading code is achieved, a tracking loop is switched in, and the transmitted data can be recovered. Here again, it will be necessary to arrange for a tracking implementation that can ignore inputs except during the time that the downlink beam dwells on the user zone. The position of this dwell window actually becomes one of the parameters to be tracked.

It should be mentioned that the expected length of the search time for all of the above methods depends on the initial uncertainty in the parameters to be acquired, the most important of which is spreading-code phase. Even if there is zero a-priori knowledge of this parameter, exhaustive search is still possible as long as the period of the spreading code sequence is not excessive. Unlike the uplink situation where an extremely long period is needed to prevent jammers from predicting the next hop, a more modest sequence period can be used for DS spreading on the downlink, allowing aquisition from zero a-priori knowledge of code sequence phase.

3. UPLINK SYNCHRONIZATION: ACQUISITION

The following are identified as the parameters to be acquired (and tracked) to allow the satellite processor to successfully demodulate user transmissions from the ground:

(a) Hopping sequence phase, i.e., the proper point in the long pseudo-random hopping pattern. (coarse sync)

(b) Hopping clock phase, i.e., the alignment of hop transitions of the uplink signal arriving at the satellite with those created by the dehopper on board the satellite. (fine sync)

(c) Carrier frequency. There may be significant errors due to Doppler shifts, initial errors in the frequency synthesizers, and drift. (coarse and fine sync)

There is one other parameter that can be mentioned. For low-rate users, each transmitted symbol spans several hops. The satellite may provide processing that combines received energy over these several hops. In that case, the ground user will have to establish the correct hop at which a new symbol should be started. If there are Q hops per symbol, each of Q possibilities needs to be tried. We will not mention this again in what follows; it should be clear that these Q trials would just represent one additional step in the searching procedure.

3.1 Hopping sequence phase/coarse carrier frequency

The acquisitions of these two parameters are tightly bound together. In effect, they create a two-dimensional search space over the regions of uncertainty. System implementation choices will determine the size of the uncertainty regions and ultimately the time for acquisition.

The initial uncertainty in the hop sequence phase has two components. The first is due to the user's uncertainty about the sequence phase inside the satellite at some absolute time t^*. The second is due to the uncertainty in the propagation delay from the user terminal to the satellite. This second component is directly proportional to the uncertainty in the range to the satellite, which depends on how accurately the user knows both his own position and that of the satellite. If the propagation delay is known to an uncertainty of T_p, this translates into an error in hopping sequence phase of T_p/T_h hops, where the hopping rate $R_h = 1/T_h$. With an assumed hopping rate of R_h = 20 kHz,

every 50 microseconds of timing uncertainty translates into an uncertainty of one hop in hopping sequence phase.

We deal first with the former uncertainty component, and assume, quite generally, that the pseudo-random sequence is produced, both in the satellite and in the ground stations, by a finite state machine (the "sequencer") realized as a clocked digital circuit. There appear to be two distinct system implementation options that determine the initial uncertainty in the current sequence phase of the satellite sequencer. In the first option, the user's (slave) sequencer box is initially synchronized by physical connection to a master unit. Depending on the method used, it may be necessary to wait until the master sequence is ready to repeat (i.e. up to several days) to give a start signal to the replica sequencer box. Small errors in the clock frequency will cause phase error to accumulate from that point on (until the next synchronization with the satellite is achieved). This master unit must be in close synchronization with the sequencer in the satellite to avoid passing on errors to the slave sequencers. The only way that this appears possible is if both the master and satellite contain highly stable clocks, and the master unit frequently resynchronizes to the satellite after its launch to prevent large clock-drift errors from accumulating. For example, assuming R_h = 20 kHz, and clock stabilities on the order of one part in 10^6, after 50 seconds the sequencers may be out of step by one hop. With one part in 10^9, an additional two hops of error can accumulate every day.

There is, however, an alternative that does not rely on physical connection to a master unit (our second option). Since the "state" of the satellite's finite-state-machine sequencer at any one time is implicit in the value of the internal storage elements (latches or flip-flops), it is possible to keep users' sequencers updated by transmitting this state information to the ground users <u>on the satellite downlink</u>. By setting the latches or flip-flops

to the same values in his replica sequencer circuit, a user acquires synchronization. Such side information must, of course, be protected. This is ensured if the downlink is encrypted or if the sequencer circuit utilizes a secret key (bit-string) in the formation of the hopping pattern (for example a cipher-block chained encryption device [4]). Only with the right key is the state information of any use. Such encryption devices are capable of generating extremely long pseudo-random sequences, and are well-suited to this application.

All bits necessary to describe the state can be sent in one frame, and a new state sent with each frame (in the "common" slot of Fig. 2). Alternatively, the bits could be spread out over several frames so that fewer bits are needed in each frame (to lower the overhead of the "common" slot). Users can load this state into their replica sequencers, adjust for the delay in sending all bits of the state from the time the state was sampled, and adjust for round-trip delay. If these delays are known to within a few hops, then the maximum initial error in the hopping sequence phase may be only a few hops.

As mentioned earlier, the uncertainty in propagation delay is directly proportional to the uncertainty of the range to the satellite. For example, to create a phase uncertainty of one hop with R_h = 20 kHz, the range uncertainty must be (50 μsec)(3 X 10^8 metres/sec) = 15 kilometres. With a geostationary satellite, the satellite is typically within a sphere of 100 km of its nominal position, representing a phase uncertainty of about 6 hops maximum in this example. This range uncertainty can be made even smaller by continually updating the users' knowledge of the position of the satellite. Knowing their own position, a simple calculation then gives the users the corresponding propagation delays. Satellite positional data can be given to the users in the "common" slot of the downlink frames. The satellite positional data can be transmitted to the satellite by a master station; presumably one will be in

charge of station-keeping commands to the satellite. The problem here is for the master station to accurately determine the satellite position. Typical methods employ triangulation calculations based on ranging performed by cooperating earth stations. Such methods are vulnerable to jamming. In any event, the satellite can continue to broadcast its last known position, which should not change significantly until the next update becomes possible.

The second parameter which must be acquired to achieve coarse synchronization is carrier frequency. The ability to perform rapid frequency hopping appears to create a frequency accuracy problem for the user's frequency synthesizers. For example, low-data-rate users would transmit one of M tones separated in frequency by about 40 kHz when a hopping rate of R_h = 20 kHz is used. These tones will be transmitted by a carrier frequency of nominally 40 GHz (EHF), but selectable over a 1 GHz hopping band. To achieve placement of such signals to an accuracy on the order of 1/10'th the tone separation (4 kHz) implies frequency synthesizer accuracy on the order of 1 part in 10^7 over a 1 GHz range, with a new frequency selected every 50 microseconds.

It is difficult to say what is a reasonable initial frequency uncertainty for these frequency synthesizers. If users maintain adjacent positions within the hopping group (Fig. 1) across hops, this will constrain the maximum allowable initial frequency uncertainty. In this case, a frequency error on the order of user spacing in the group can cause the synchronization attempts by one user to interfere excessively with his immediate neighbours (assuming they are already synchronized, and are using the satellite). To allow higher initial frequency errors, a different assignment of users to positions in the group would be needed. If we permute the relative positions of the users from hop to hop (there is really no reason why we can't), then even in the face of large frequency errors by a user first attempting to synchronize, another user will only be "hit" during a fraction of the hops. Since combining across hops is used by the satellite processor to deal with jamming anyway, these random

"hits" may be completely tolerable. In effect, with this permutation strategy, users attempting synchronization with large initial carrier frequency errors will simply appear as another source of jamming.

Of course, carrier frequency accuracy and misalignment is much less serious for the higher-rate users whose frequency separations are higher by at least two orders of magnitude. It may be safe to assume then that initial frequency errors are insignificant for all but the low-rate users, since frequency synthesizers for the higher rate users will almost certainly be of better quality, and therefore have initial frequency uncertainties that are no higher.

We may also use the "common data" downlink slot to help users adjust their frequencies before attempting synchronization. Satellite current centre frequency value may be digitized and also sent in the common downlink slot (1 bit per frame may be sufficient). Users compare this to their own reference and adjust accordingly. This will keep initial frequency synthesizer error to a minimum. To be able to use this data, the ground users must accurately know the frequency of the satellite onboard clocks that produce the reference for the dehopping carrier frequency, and that were used to make this onboard measurement. They can get this information indirectly if the downlink TDM frame duration is some exact multiple of the satellite clock. Users can measure the duration of the frame to a high accuracy, and therefore calibrate the satellite data. One problem here is that both the user and the satellite will not be able to directly measure the frequencies produced by their synthesizers. It is only possible to measure the frequencies of clocks that are used in some frequency-multiplication scheme to derive the final carrier. It could be that such "open-loop" measurements are very inaccurate, so that they may be of no use at all. In that case, there would be no choice but to resort to closed-loop measurements requiring feedback from the satellite that gives an indication of the quality of alignment of the carriers.

In addition to frequency drift between the satellite and ground frequency references, carrier frequency error can be caused by Doppler shift with mobile user terminals. At a nominal frequency of 40 GHz, a user terminal speed of 100 km/hr translates into a Doppler frequency shift of about 4 kHz. Compared to other sources of frequency error, this component seems relatively unimportant, even for the low-data-rate users. This component could, however, become important if user terminals are located on aircraft, where the frequency error can be an order of magnitude larger. In that case, it may become necessary to predict the Doppler effect knowing the relative motion of the satellite and user antennae, and to compensate accordingly.

3.1.1 Search Strategies

There are many possible search strategies for acquiring initial coarse synchronization [5, 6]. The two dimensional search space is divided into N cells, with the trial carrier frequencies in adjacent cells separated by Δf_c, and the trial hopping sequence phases in adjacent cells separated by a fraction of a hop (or possibly a full hop).

In all strategies, we set the hopping sequence phase, and carrier frequency, to the trial values for a given cell, and observe the effect of these choices. We leave the form of the "observation" unspecified for the moment. Depending on the result of the observation, we either declare a possible aquisition and observe for a longer time, or change to a new cell and repeat the observation. This declaration typically is made by comparing the observation to a predetermined threshold. If a possible detection turns out to be incorrect, we say that the initial detection was a false alarm. If we fail to declare a possible detection in the correct cell, we say that a missed detection has occurred. If, after the increased observation time following a possible detection, we are satisfied that we are in the correct cell with a

high probability, aquisition is declared, and we switch over to a fine-acquisition mode. This mode allows fine adjustments to be made to the carrier frequency and hopping clock phase in order to achieve better alignment. Finally, a tracking mode may be entered which adjusts for relative drifts in these parameters between the satellite processor and the user equipment (fine-acquisition and tracking are usually indistinguishable in conventional spread-spectrum systems).

The simplest strategy involves looking at all cells in sequence, and observing for the same amount of time at each cell. If acquisition is missed after visiting all cells, we simply start over. This is a fixed-observation-time serial search. As an alternative, a variable-observation-time approach may be adopted. A fast initial sweep over all cells with small dwell (observation) time at each can be performed, with possible acquisition detections being explored for longer times, in a hierarchical fashion. If the initial sweep fails, it is repeated with the dwell time increased. As a variation, more time can be spent on those cells closest to the expected value of the sequence phase, and $\Delta f = 0$, since the likelihood of larger drifts and errors is correspondingly smaller. Alternatively, a more formal sequential probability ratio test (SPRT) can be employed. In the SPRT, we compute $\Gamma_K = p_s(\underline{r}_K)/p_n(\underline{r}_K)$ where p_s and p_n are, respectively, the probability distributions of received observation sequence $\underline{r}_K$ (of length K samples) given signal present, and given noise-only present. This likelihood ration Γ_K is compared to upper and lower thresholds selected to produce desired values of probabilities of false alarm p_{fa}, and of detection p_d. If the ratio falls between the thresholds, the test is repeated with the (K+1)'th sample r_{K+1} added.

The choice of search strategy depends on the size of the initial uncertainty regions. The more complicated strategies generally yield shorter average acquisition times, but those that use a-priori information (e.g. SNR's,

or probability distributions for carrier frequency or code phase error) can be sensitive to errors in this a-priori information. If the initial uncertainties are small, a single serial search with detection threshold set for the desired p_{fa} and p_d might be used. For very large uncertainty regions, the SPRT may be desirable. For moderate uncertainty regions, a variable-dwell-time search procedure may be sufficient.

A method for scanning through a range of hop sequence phases is now described. The arrangement is shown in Figure 4, and allows selection of a trial phase to within one full hop. As before, we assume that the hopping sequence is produced by a clocked digital circuit. The pseudo-random sequence generator (PNG) can be clocked by ϕ, the nominal clock, or by ϕ^{++}, a high speed clock. In addition, the clock input can be disabled so that the outputs of the PN generator do not change. A block of k bits from the output of this PNG is clocked separately into a buffer register that feeds the frequency synthesizer to select one of 2^k frequencies. A block of k=32 bits is sufficient to specify one of $2^{32} \sim 10^6$ different frequencies. This is sufficient to span a hop band of 1 GHz with placement of the carrier to 1 kHz. To produce a hopping rate of R_h, the nominal clock rate of the PNG is then kR_h.

The procedure to be followed is now outlined. Assuming an initial uncertainty of $\pm H$ hops in hop sequence phase, we initially switch to ϕ^{++} to run the sequencer "ahead" by H hops. Since the nominal clock rate of the sequencer will be relatively low for the hop rates ($R_h \sim 20$ kHz) and number of frequencies ($k < 32$) of interest, a ϕ^{++} clock at ten times the frequency of ϕ (about 6.5 MHz for the example) is well within the capabilities of modern digital circuits. While this run-up is being performed, the input register at the synthesizer is still being reloaded at the nominal hop rate R_h, so that the carrier frequency is still hopping, albeit to "random" frequencies. After the

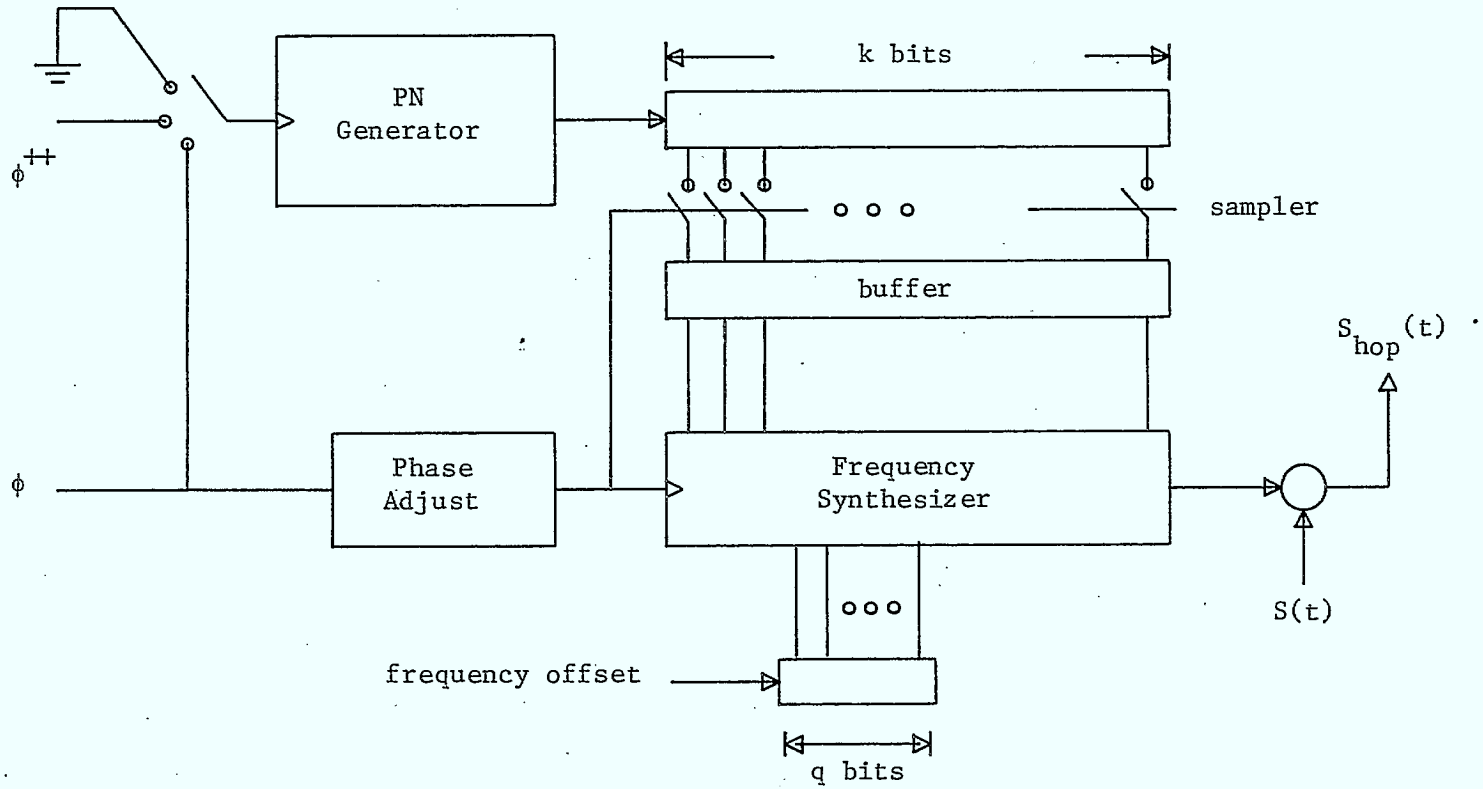

Fig. 4. System for adjusting hopping sequence phase and clock, and carrier frequency.

PNG has advanced H hops ahead of nominal, its clock input is then returned to ϕ. Now we can drop back by one hop (relative to the satellite) by disabling the clock input for one hop, and then returning it to ϕ for an interval of I hops duration, the observation time at the current hop sequence phase.

During this time, we observe the downlink return (which we have previously assumed is directed to us in a loopback mode) and either declare acquisition or continue the procedure to examine the next hop phase. The maximum observation time to cover the initial uncertainty band of 2H possible hop sequence phases is then $2H \cdot I \cdot T_h$ seconds. Of course, the choice of observation interval I is determined by the search strategy adopted. This procedure may be repeated for each of the trial values of carrier frequency (separated by Δf_c) in the band of initial uncertainty. Alternatively, the search may be done in the opposite order, with the different trial values of carrier frequency being tested while holding at one trial value of hopping sequence phase. The order is unimportant.

To search over different frequencies, we must be able to offset the frequency produced by the synthesizer in steps of Δf_c. This control is produced by specifying a q-bit block to select a multiple of the offset Δf_c. This is also shown in Fig. 4. Finally, it should be mentioned here that there is, in principle, no reason why the k bits shown in Fig. 4 cannot be put through a permutation mapping that is unique to each user so that their position in the hopping group can be permuted from hop to hop. This was mentioned earlier as a possible technique which would tolerate greater initial frequency error for users first attempting to synchronize. One practical disadvantage of this method is that it may be harder to keep the users frequency-aligned in the group if this extra permutation is attempted. That is, with non-ideal (but identical) frequency synthesizers, less stringent requirements may be placed on

the synthesizers if the relative frequency change in the carrier from hop to hop is identical for all users.

3.1.2 Detection of Acquisition

At each trial value of hopping sequence phase and carrier centre frequency, we must decide if acquisition has been achieved. Figure 5 depicts the alignment of the carrier hops with the satellite dehopping carrier, when the hopping phases are within one hop. Note that a serial search of possible hop sequence phases must produce an alignment at some trial phase that causes at least 1/2 of the signal energy to be properly dehopped by the satellite and pass through the satellite IF filters. In the worst case then, there will be a 3 dB loss of signal energy (at IF) at proper alignment for this coarse acquisition phase. Notice also that the transmitted user tone is "gated" before IF filtering which will produce spectral spreading and some additional loss after filtering to the data bandwidth. This spreading and additional loss will only be appreciable for the lower-data-rate users whose transmitted tone separation is comparable to the hopping rate, and therefore of the same order as the spreading effect.

The effect of this coarse alignment is very different for the low rate and high rate users. For the low-rate users, the data symbol transmitted is constant over several hops. A 3 dB loss in signal energy at IF translates directly into a 3 dB loss after filtering to the tone (data) bandwidth. For the high rate users, however, there are many symbols per hop; we assume that a block of S symbols is transmitted by tones using M-ary FSK during each hop. The gating effect due to hopping clock misalignment will cause a fraction of these S tones to completely disappear after IF filtering. At some trial hop sequence phase, however, at least half of the data tones will pass through the "gate", and appear at the demodulator. Outside of the gate interval, only noise will appear at the demodulator input.

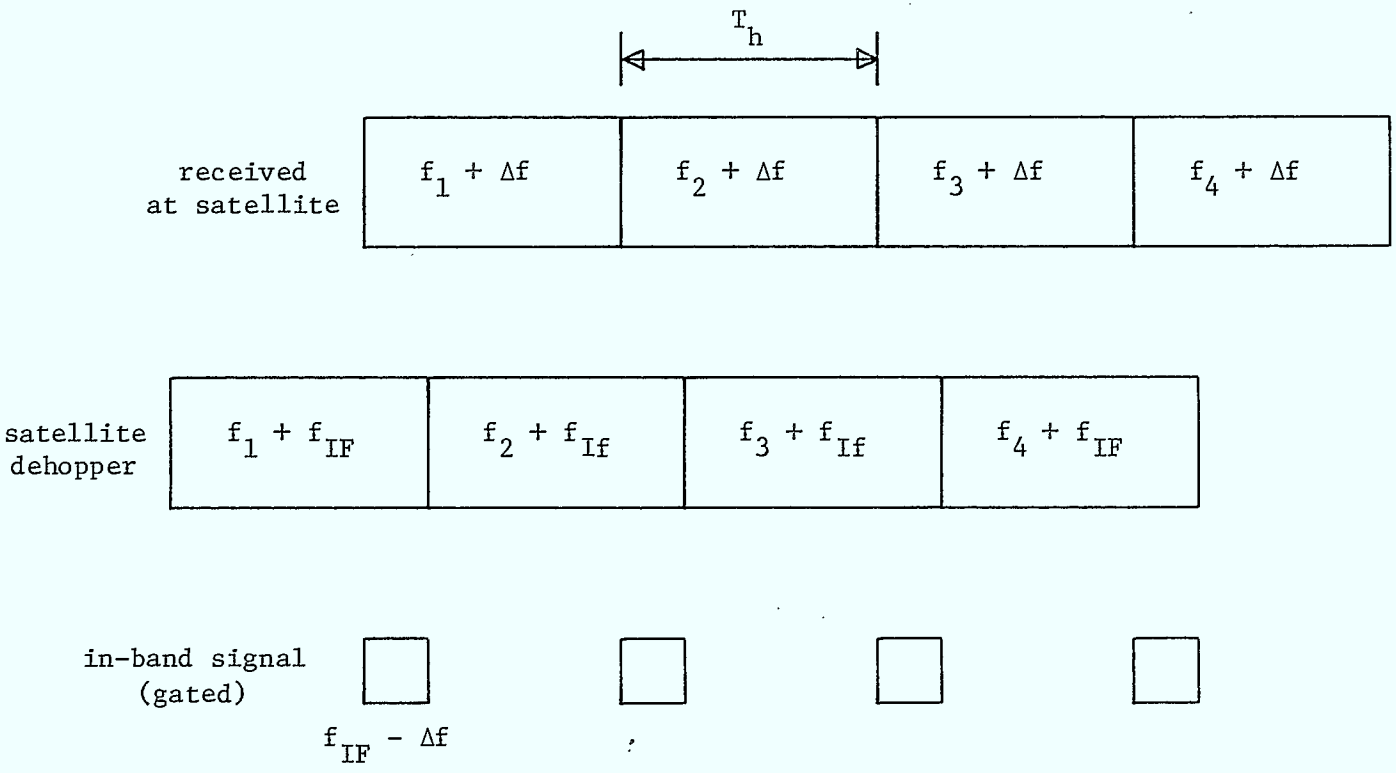

Fig. 5. Effect of misaligned hopping clock phase.

Carrier centre frequency misalignment will reduce (or possibly eliminate) the signal component that appears after filtering to the data bandwidth. As mentioned earlier, this frequency error has a much greater effect on the lower-data-rate users. For example, with FSK tone spacing of 40 kHz, a 40 kHz frequency error will cause the satellite to interpret the received signal as the tone adjacent to the one actually transmitted. A smaller frequency error will cause both loss of energy at the desired tone frequency after processing, and spillover of energy into adjacent frequency slots. For a medium-data-rate user (e.g. 1.5 MHz), the much larger FSK tone spacing makes a 40 kHz error insignificant. We assume that Δf_c is chosen to produce a maximum 3 dB loss at the desired tone frequency when the best frequency cell is found. This implies very different choices for Δf_c for low rate and high rate users.

There are several options for the downlink return information during this initial coarse acquisition phase. The type of information needed depends on whether the users are low rate (several hops per symbol) or high rate (many symbols per hop).

For the high-rate users, the choice seems most clear; we can simply have the satellite return the same information as it sends to the intended user when forwarding a normal point-to-point call. Let us assume initially that there is no degradation due to carrier frequency error. The only loss then is due to hopping clock misalignment when the hopping sequence phase is correct. As mentioned above, this causes the complete loss of some of the symbols in the block of S symbols for each hop. This can be exploited by the high-rate users to detect coarse aquisition. If they transmit a block of S symbols, and look for the satellite return on the downlink (loop-back mode), they will know that coarse aquisition has been achieved when runs of S/2 (or longer) consecutive correct symbols are seen on the downlink. Of course, because of the non-zero error rate even when the user signals are reaching the satellite demodulator, we would have to allow some errors in these runs. For example, we might

declare a run when 95% of the symbols in a sliding window of S/2 symbols are correct.

In the event of degradation due to filtering in the presence of significant frequency error in the correct cell, the error rate may be significantly higher, and the threshold for declaring coarse acquisition must be lower. For example, if the Δf_c carrier error causes the error rate in decoding by the satellite processor to increase to one symbol in four (for example), we may set the threshold to declare coarse acquisition as long as runs are seen in which 70% of the symbols are correct. For high reliability, we may then require that such runs must be seen in the same positions over many consecutive hops.

For the low-rate users, the best choice for downlink information to be returned in loopback mode is less clear. One option is to have the satellite transmit a hard decision (1 or 0) on the presence or absence of the tone which is being transmitted by the user (one of M tones). This tone can be the same one throughout the synchronization procedure, and can be established beforehand so that the satellite knows which tone to look for. The decision threshold may be set to give some desired tone detection probability in the presence of maximum uplink fading and full band jamming. The ground user can then use these tone-detection decisions in a SPRT test, or, in a simpler strategy, these decisions may simply be counted over an observation of I hops, and the count compared to a threshold.

As an example, the design threshold for this latter search might yield probabilities of tone detection, given tone present (with 3 + 3 = 6 dB loss due to hopping phase and carrier frequency misalignment) and tone absent, of $p(td|1) = .8$ and $p(td|0) = .1$, respectively. If we look for 5 or more detections in 10 hops, this will yield a false alarm probability of $P_{fa} \sim 10^{-3}$ and a probability of detection of acquisition of $P_d \sim .966$ (from standard binomial

distribution calculations). Of course the detailed calculations of $p(td|0)$ and $p(td|1)$ in the presence of jamming will be complicated. With Gaussian noise only, these probabilities form a set of well known curves. The presence of partial-band jamming and frequency misalignment errors introduce further complications.

Note that the previous strategy requires 1 bit per hop or Q bits per symbol transmitted, where Q is the number of hops spanned by one symbol from a low-rate user. If we plan to use all of this data, this will require a expansion of the normal data rate assigned to a user slot on the downlink compared to the normal downlink return of $\log_2 M$ bits per symbol transmitted. This may be acceptable if the satellite knows when the user is trying to synchronize; the extra data would only be needed for brief and infrequent synchronization attempts. The very nature of the system, however, implies that the satellite cannot have this knowledge, so this data-rate expansion is unacceptable. For this reason, it would be necessary to gather this data for only a fraction of the hops (say every second or third hop) to keep the rate on the downlink the same.

Other options include having the satellite perform combining across several hops (as it normally does) before declaring the presence or absence of the tone (maintaining $\log_2 M$ bits per symbol), or having the satellite make soft decisions so that more bits of information can be returned (again we would have to gather this for only a fraction of the hops).

Finally, it should be mentioned that the round-trip delay to the satellite may greatly contribute to the length of the synchronization time. This will be the case if we wait the full round-trip delay for the downlink observation before stepping the hopping sequence phase (or carrier frequency) to a new cell. To avoid this delay, we can perform a group of adjustments in rapid succession, and then wait for the round-trip delay for the corresponding group of observations. If there are K adjustments in each group, this can cut the

overall synchronization time by almost a factor of K. This strategy applies equally to the fine-synchronization adjustments discussed in the next section.

3.2 Hop clock phase / fine carrier frequency

The procedures described above will yield a coarse synchronization to within one half of a hop and within $\Delta f_c/2$ carrier frequency error. We then wish to adjust the hop clock phase, and frequency synthesizer centre frequency, in small increments of Δt and Δf, and receive downlink data about the quality of the alignment. Again, the strategy for fine alignment will be quite different for the high-rate and low-rate users.

We will start again with the high-rate users. It seems best to achieve carrier frequency alignment first. As we step the frequency closer to proper alignment, this will be reflected by a decreased error rate in the downlink return symbols. It is a simple matter to locate the best carrier frequency alignment, as this yields the lowest error rate. As mentioned before, this may be a non-issue if we assume that the initial frequency errors will be sufficiently small to cause negligible degradation for high-rate users. Now the hopping clock phase can be fine-adjusted. As we step closer to proper alignment, more of the S symbols for a hop will make it through the "gate", and the successful detection of these symbols is easily monitored on the looped-back downlink return. It seems unreasonable to expect alignment to a fraction of a bit to allow the first and last bits of a hop to be recovered. A simpler strategy is to just discard the first and last δ (dummy) bits, and seek alignment to just δ bits of accuracy. This loss of bits will represent only a small loss in effective transmission rate if there are many bits per hop. Note that the satellite demodulator circuits can still extract symbol-timing to a fraction of a symbol as required to demodulate the user signal.

For the low-rate users, achieving fine alignment is complicated if the satellite sends only hard decisions about tone detections on the downlink. One

possibility is to have the satellite send soft decisions on the synchronizing tone where this data is a quality measure, for example, the output of an energy detector quantized to one of several levels. Now the user can see the effect on detected energy as the carrier frequency is fine-adjusted. Again, it will be necessary to use only a fraction of this data to prevent bandwidth expansion on the downlink.

Another possibility is to estimate the proper fine alignment from only hard-decision tone detection data as assumed above. In this case, the hop clock phase or carrier frequency may be stepped by Δ sequentially until a target rate of missed detections (e.g., 4 missed out of 10) is exceeded. The clock phase or carrier frequency may then be stepped in the opposite direction until missed detections again occur in excess of this target rate. Proper alignment may then be estimated to lie exactly half way between these two extremes. Of course, this procedure will take longer than an alternative employing multiple-bit alignment-quality data transmitted by the satellite. The procedure is aided, however, by the fact that there should be a reasonably sharp threshold effect at which the rate of missed detections rises quickly with increased frequency misalignment.

4. UPLINK SYNCHRONIZATION: TRACKING

Once acquired, parameters will drift toward loss of synchronization during normal data transmission. This may be avoided by tracking, that is, by monitoring and adjusting the fine alignment.

In the system as described so far, the default is for the satellite to always direct the detections from a user's uplink slot back into that same user's downlink slot when the user is not engaged in a call ("loopback mode"). This situation will therefore be present during coarse and fine synchronization to give the necessary feedback for the user attempting to synchronize. Once

synchronized, the user will transmit the necessary codes to request a reconfiguration of the satellite to "normal mode" for that user, and the satellite will then route the transmissions from that user to the network controller which can perform a call setup. From this point on, the user no longer has any feedback on his alignment, making tracking a difficult proposition. This contrasts sharply with the tracking problem in a conventional spread spectrum system in which we have full access to the signal emerging from the dehopper. In this conventional system, a tracking loop is employed [5].

If we assume that drifts over the duration of a typical call are tolerable, then when the call finishes, the satellite can revert to the loopback mode, and fine adjustments can again be carried out by the user. If the drift is not tolerable, then adjustments must be made in the middle of a call. This may be made possible by reserving some small percent of the transmission time for loopback mode. For example 10 out of every 1000 hops might be in loopback mode, ten for each user involved in the call. This does complicate the control on board the satellite to some degree, and involves one more level of synchronization (at the data-format level) so that the satellite and sending user know which hops are for loopback, and so that the receiving user knows which bits in the downlink should be discarded.

We can use a different approach to give feedback to the user. Low rate supplementary channels could be paired with each user's data slot in the downlink frames. This channel can be supported by only a small increase in the duration of a user's assigned slot. In these channels, the satellite would provide low-rate users alignment-quality data (e.g., energy detector output quantized to b bits) averaged over many hops. For the high-rate users, the data on these low-rate supplementary channels might be the first δ, and last δ, symbols from every k'th hop. The user can compare these to the data symbols actually transmitted to see if errors are starting to occur, implying loss of fine adjustment (in either hopping clock phase or carrier frequency).

In either case, the ground terminal could use this data in a tau-dither [5,6] type of scheme to make adjustments to hopping clock phase and carrier centre frequency. This can be envisaged as a tracking loop that accounts for the long round-trip return delay. Because the loop time constant will be large compared to the hop duration T_h, the data rate of these supplementary channels need only be a fraction of the user data rate, and can represent a small overhead.

One final alternative provides the feedback indirectly, but more transparently. Parity check bits may be embedded in the user data streams. If user A is talking to user B, and drifts toward loss of synchronization, this will show up as errors in the data. User B can then request that user A adjust his parameters to try for better alignment. This is also a feedback loop, but it has a much slower response time than the previous scheme. It also requires an extra level of synchronization in the data streams to identify which bits are data and which are check bits (although it is likely that such error-detection or correction capability will already be present in the system).

5. SIMPLEST SYSTEM

Given the previous discussion, it is now possible to identify a system which makes acquiring uplink synchronization as simple (and as fast) as possible for the ground user. Again, it will be necessary to consider the low-rate and higher-rate users separately.

For both the low-rate and higher-rate users, this system shares the following attributes:

(a) All users know the round-trip delay to the satellite to within a small fraction of a hop. At a hopping rate of 20 kHz, this implies range accuracy on the order of 1 km. Range determination is aided by satellite positional data provided in the "common data" downlink slots.

(b) The internal state of the pseudo-random sequencer in the satellite is periodically transmitted on the downlink in the "common data" slot of the frames. Users load this state into their replica sequencers, and coarse adjust for delays by running their sequencers ahead by the appropriate number of clocks.

(c) The satellite hopping clock phase is aligned with the boundaries of the frames of the TDM downlink. Given (a), this allows the users to fine-adjust the clock phase of their hoppers to within a fraction of a hop.

(d) Satellite current centre frequency is digitized and also sent in the common downlink slot. Users compare this to their own reference and adjust accordingly. This will keep initial frequency synthesizer error to a minimum.

(e) Relative motion is known accurately so that Doppler shifts can be calculated, and the transmitted carrier frequency adjusted accordingly.

(f) As an alternative to (d) and (e), the satellite can provide continuous data on alignment quality of the carrier frequencies over low rate supplementary downlink slots for each user. This may be used both for acquisition and tracking.

For low-rate users, if the initial frequency uncertainty provided by (d) is sufficiently small, then no further synchronization procedures are needed. This is a very ideal situation, and is unlikely to be achieved in practice. The major question is whether it is possible to adjust the frequency synthesizers accurately in the "open-loop" method of (d). It seems much more likely that (f) above will be needed.

For high-rate users, frequency errors are much less critical, and initial errors will either have negligible effect, or will be rapidly corrected using (f) above. It is errors in hopping clock phase that may become more critical for the higher rates (lower symbol durations). If there are many symbols per

hop, a simple strategy (mentioned earlier) is to treat the first and last δ symbols in each hop as expendable "dummy" positions, so that (a) above is sufficient.

6. DEMAND-ASSIGNMENT-NETWORK CONSIDERATIONS

So far, it has been assumed that there is a fixed assignment of satellite resources to each user, that is, each user can count on a dedicated uplink frequency slot and a dedicated downlink time slot. This means that these resources are "always there" for a user who wishes to attempt synchronization. We further assumed that when the user was not engaged in a call, the satellite redirected all detections from the user's uplink slot back into the user's downlink slot (the default "loopback mode") to create the feedback necessary for achieving synchronization. In this section, we briefly consider the effect of non-fixed or demand-assigned uplink (and downlink) slots.

In [1] and [2], Kolba describes a scheme for embedding control channels in the uplink and downlink slots that allow both demand-assignment and network control. The arrangement is shown in Fig. 6. On the uplink, control channels c_1 and c_2 are created by time sharing the uplink FDM frequency slot with the normal data traffic. Channel c_1 is intended for transparent network communications, and is not considered here. Channels c_2 are for access control. On the downlink, channels c_3 are created as extra time slots in the downlink frame. These c_3 channels carry the responses from the access controller (which may be located either in the satellite or on the ground) to the requests for access made in the uplink c_2 channels. In the demand-assigned network, there are many more users than uplink and downlink slots so that these slots must be time-shared between the users on a demand-assignment basis. The advantage here is that many more users can be supported by the same satellite resources if these users each require access for only a small percentage of the time. Users make

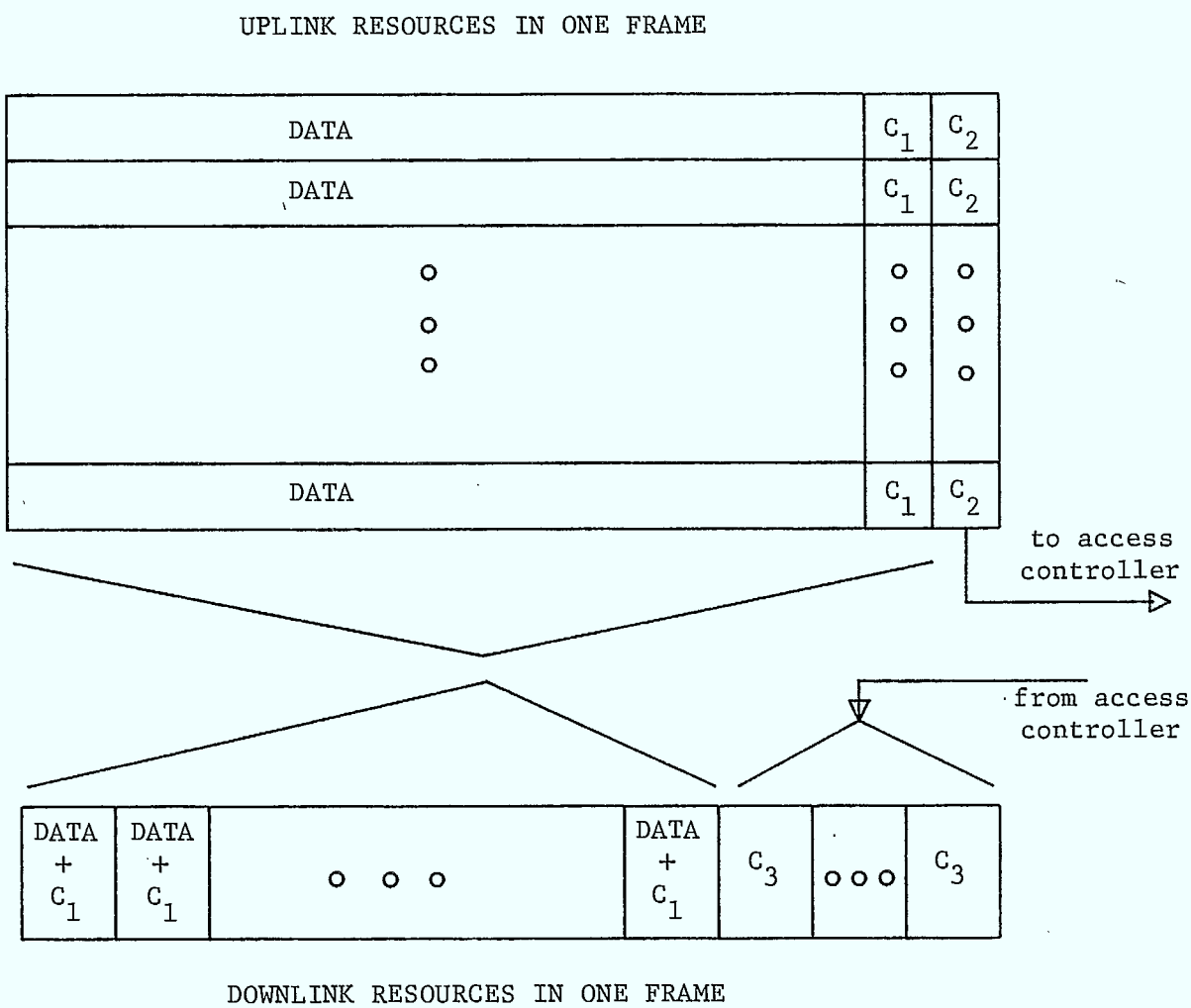

Fig. 6. Kolba's scheme for demand-assigned access control [1], [2].

requests for access over the c_2 control channels, and look for acknowledgements over the return c_3 channels. For example, 10 users may be assigned to share uplink frequency slot #1. These 10 users will then all use the same c_2 slot at this uplink frequency, and all look for acknowledgements in the corresponding downlink c_3 slot. Some method of sharing this c_2 slot must be used.

Kolba suggests two methods for using these access-request channels. The first method is to perform a straight time-division multiplex. In the example above, each of the 10 users would only have access to every 10'th c_2 slot. To achieve lower average waiting times for access to this control channel, Kolba also suggests a random-access protocol; whenever a user wishes to make an access request, he immediately transmits the request over the c_2 channel to which he is assigned. In the event that two users attempt simultaneous access to c_2, their transmissions collide at the satellite, the access controller will fail to see either request, and the users see no request acknowledgement over the return c_3 slot.

The method used has implications for the ability of users to first synchronize to the satellite. It should be emphasized that open-loop synchronization, as hinted at by the "simplest" systems of the last section, is probably not possible. To perform closed-loop synchronization, feedback from the satellite is essential. Since the satellite does not know when users will attempt to synchronize, some satellite resources that will allow feedback for synchronization must be dedicated to each user. In this demand-assigned environment, these dedicated resources must be the time-shared c_2 and c_3 channels. If the round-robin time-multiplex of these channels is adopted, each user can count on access to c_2 and c_3 at well defined instants of time. We now specify the default to be that the satellite redirect the uplink detections for

a user's c_2 slots into the corresponding c_3 slots for that user. Users synchronize by transmitting into c_2 and receiving feedback over c_3.

This poses one complication that is not present for the fixed-assignment system assumed earlier in the report. In the fixed-assignment scheme, each user has his own dedicated uplink frequency, and can begin transmitting on that frequency at any time without concern for what other users are doing. With demand-assignment, however, many users share the same uplink frequency and c_2 assignments. While one user is assigned the data portion of the uplink frame, the others can access the control portion c_2 only. To avoid interfering with the active user, other users must accurately know the time instant at which c_2 starts. By specifying the uplink frame duration to be some multiple of the downlink frame, and specifying that the boundaries of these uplink and downlink frames be aligned (at the satellite), users can infer the starting position of the uplink frame, and therefore the position of c_2, from their accurate knowledge of the downlink frame boundaries. This does, however, require accurate knowledge of the propagation delay to the satellite. A user who is not synchronized may not know this delay accurately. It may therefore be necessary to allow some guard time around the c_2 slot, and let the users consider the accurate timing of their c_2 transmissions to be just one more parameter to be discovered by the synchronization search procedure. The size of these guard bands depends on the maximum user uncertainty in the round-trip propagation delay. The extra overhead introduced by these guard bands can be kept small by increasing the specified duration of the uplink frame (which impacts on the average time a user has to wait for his turn at the c_2 slots).

When the user achieves synchronization, the appropriate codes can be sent to the satellite to reconfigure the c_2 and c_3 usage for that user back to

normal mode, i.e. to route c_2 data to the access controller, and return its responses over c_3 to the user. This again implies user access to the satellite reconfiguration controls as for the fixed-assignment system assumed earlier.

It can now be seen that a random-access strategy is not possible for these control channels. The only way to provide the dedicated resources that each user needs for initial synchronization is to share these control channels on a round-robin basis. Of course it is possible to come up with a modification of Kolba's system to allow random-access for users who are already synchronized, and provide dedicated round-robin access to all users on different control channels for synchronization purposes. This would only be useful, however, if we assume that users will not drift out of synchronization over the periods when there are not using the network, and are therefore not receiving any feedback about the quality of their alignment.

This discussion shows that synchronization can still be accommodated in a demand-assigned environment. Because low-bandwidth control channels are shared on a round-robin basis for this purpose, synchronization in this system can be expected to take substantially longer than in a fixed-channel-assignment system.

REFERENCES

[1] D.P. Kolba, "Generalized control and networking for EHF Satellite Communication Systems", AIAA 9th Communications Satellite Systems Conference, San Diego, CA., March 1982.

[2] D.P. Kolba, "System aspects of scanning beams for widely distributed users", International Telemetering Conference, San Diego, CA., October 1981.

[3] W.W. Wu, "Elements of Digital Satellite Communication: Volume I", Computer Science Press, Rockville, Maryland, 1984.

[4] D.E. Denning, "Cryptography and Data Security", Addison-Wesley, Reading, MA., 1982.

[5] R.E. Ziemer and R.L. Peterson, "Digital Communications and Spread Spectrum Systems", Macmillan, New York, N.Y., 1985.

[6] M.K. Simon, J.K. Omura, R.A. Scholtz and B.K. Levitt, "Spread Spectrum Communications: Volume III", Computer Science Press, Rockville, Maryland, 1985.

DETECTION OF A SINUSOIDAL SIGNAL WITH A WIDEBAND DISCRETE FREQUENCY DISTRIBUTION

by

Peter J. McLane

Wendy Lee Hopkins

Norman C. Beaulieu

REPORT 88-3

FINAL REPORT PART IV

PREPARED FOR THE DEPARTMENT OF COMMUNICATIONS

UNDER DSS CONTRACT NO. 36001-6-3530/0/ST

"The Study of Space Communications Spread Spectrum Systems"

Queen's University

Kingston, Ontario, Canada

February, 1988

ABSTRACT

This report examines the detection of simusoidal signals of which only the signal frequency is unknown. Particularly, it is assumed that the signal will be transmitted at one of N discrete, orthogonal frequencies and it is further assumed that the detector knows the frequency distribution exactly. A goal of the report is to establish the groundwork necessary to find the detection performance limits for the interception of slow frequency hopped signals.

Optimum and near-optimum receivers, both coherent and noncoherent, are developed for the signal structure noted above, assuming ideal conditions and an additive white Gaussian noise environment. It is found that the maximum likelihood receiver gives a near equivalent performance to the optimum, or average likelihood, receiver. Also, noncoherent detection gives an additional loss of 1 to 2 dB over coherent detection methods. The effects of frequency offset and a priori knowledge are also examined. The former results in a performance degradation while the latter gives a performance improvement.

Most of the report considers a modest number of discrete frequencies, N, in the frequency distribution. The final chapter considers the case when N is large: the case that occurs in most frequency hopping systems. The properties given above are shown to hold for large N. It is also shown how to determine N such that the interceptor's detection probability corresponds to his false alarm rate, thus rendering the detector scheme impractical. This represents a fundamental performance limit for interception receivers for frequency-hopped, spread-spectrum modulation.

TABLE OF CONTENTS

LIST OF TABLES

LIST OF FIGURES

GLOSSARY OF NOTATION

A - signal amplitude

A_j - weights of the Gaussian Quadrature Rule

b - decision threshold for the optimum coherent receiver

c,d - arbitrary limits used in the description of the Gaussian Quadrature Rule

d^2 - signal to noise ratio; defined as the signal energy divided by the noise spectral height

D - positive diagonal matrix with nonzero elements equal to r_{ii}^2

E - signal energy

$E(x)$ - expectation or mean of x: $\bar{x} = E(x)$

$f(\alpha_i)$ - probability that e^{α_i} exceeds the decision threshold, assuming α_i is smaller than β

$g(\alpha_i)$ - probability that e^{α_i} exceeds the decision threshold, assuming α_i is smaller than ρ

H_0 - noise only hypothesis

H_1 - signal plus noise hypothesis

$h(\alpha_i)$ - probability that e^{α_i} exceeds the decision threshold, assuming α_i is smaller than β

$I_o(x)$ - zero-order modified Bessel function of the first kind

$I_{N-1}(x)$ - N-1 - order modified Bessel function of the first kind

k_i - integer constant relating ω_i to the frequency separation

j - $\sqrt{-1}$; imaginary number

J - triadiagonal matrix

L - sum of lognormal random variables

L_c - $\frac{2A}{N_0} \int_0^T r(t) \cos \omega t \, dt$

L_{ci} - $\frac{2A}{N_0} \int_0^T r(t) \cos \omega_i t \, dt$

L_s - $\frac{2A}{N_0} \int_0^T r(t) \sin \omega t \, dt$

L_{si} - $\frac{2A}{N_0} \int_0^T r(t) \sin \omega_i t \, dt$

$L(r)$ - likelihood ratio

$\mathcal{L}$ - sufficient statistic for the low SNR receiver

ℓ - sufficient statistic : ℓ_{H0} is ℓ on H_0; ℓ_{H1} is ℓ on H_1

ℓ_i - a decision statistic dependent on the output of the ith detector: ℓ_{i0} is ℓ_i on H_0; ℓ_{i1} is ℓ_i on H_1

M - number of moments used by the Gaussian Quadrature Rule

m_{ij} - element in the ith row and jth column of the matrix M

m^*_{ik} - transformation of the elements of M and R^*, defined in Appendix B

m_x - mean of X

M - moment matrix

n_i - components of the orthogonal expansion of the noise

N - number of frequencies the signal may be transmitted at

$\underline{N}$ - noise vector

$n(t)$ - additive white Gaussian noise

$\frac{N_0}{2}$ - noise spectral density in W/Hz

P_D - probability of detection

P_{Di} - probability that a signal of angular frequency, ω_i, will be detected

P_F - probability of false alarm

P_i - assumed probability that ω_i is the frequency of the received signal

$\hat{P}_i$ - true probability that ω_i is the frequency of received signal.

P_M - probability a signal is not detected ("miss")

$p_x(X)$ - probability density function of the random variable, X

$P_x(X|H_0)$ - the probability density function of the random variable, X, when noise only is present

$P_x(X|H_1)$ - the probability density function of the random variable, X, when a transmitted signal is present

$P_r(\underline{R}|H_1,\omega)$ - probability density function of the received signal when a transmitted signal is present as a function of the signal frequency, ω

$P_r(\underline{R}|H_1,\theta)$ - probability density function of the received signal when a transmitted signal is present as a function of the phase, θ

$P_r(\underline{R}|H_1,\theta,\omega)$ - probability density function of the received signal when a transmitted signal is present as function of the phase, θ, and the frequency, ω

q - sufficient statistic of noncoherent maximum likelihood receiver; $q^2 = L_c^2 + L_s^2$

q_i - $q_i^2 = L_{ci}^2 + L_{si}^2$: q_{i0} is q_i on H_0; q_{i1} is q_i on H_1

q_i - eigenvector of J

q_{1i}^2 - first component of the ith eigenvector of J

$Q(x)$ - cumulative normal distribution function

$Q(a,b)$ - Marcum Q-function

$Q_N(a,b)$ - generalized Q-function

Q_D - probability of detection for a signal of known frequency

Q_F - probability of false alarm for a signal of known frequency

$r(t)$ - received signal

r_i - components of the orthogonal expansion of the received signal

R - decomposition of moment matrix M, defined in Appendix B

$\underline{R}$ - received signal vector

R^* - upper triangular matrix

s_i - components of the orthogonal expansion of the transmitted signal

$\underline{S}$ - signal vector

$\text{sinc}(x)$ - $\frac{\sin \pi x}{\pi x}$

$s(t)$ - transmitted signal

T - received signal duration

t_j - nodes of the Gaussian Quadrature Rule

x_i - random variables

$w_e(x)$ - symmetrical lognormal function

z_i - logarithm to the base 10 of x_i

α_i - the natural logarithm of the decision statistic, ℓ_i

β, ρ - probability region boundaries

δ - fraction of frequency separation that ω_r is offset from ω_1

$\Phi(x)$ - probability that a normal random variable is greater than x

γ - decision threshold for coherent maximum likelihood receiver

η - decision threshold

$\Psi_x(v)$ - characteristic function of the random variable x; Fourier transform of the probability density function of x.

λ_i - eigenvalue of J

μ_i - ith moment of a random variable

μ_i^* - ith moment of a symmetrized lognormal random variable

$\mu_i(n)$ - ith moment of a sum of of n random variables

θ - phase

σ_x^2 - variance of X

ω - angular signal frequency

ω_i - one of the discrete values taken on by the signal frequency

ω_{max} - the largest signal frequency

ω_{min} - the smallest signal frequency

ω_o - $\omega_r - \omega_i$

ω_r - frequency of the received signal

ABBREVIATIONS

AWGN	- Additive White Gaussian Noise
CRTC	- Canadian Radio-television and Telecommunications Commission
dB	- decibel ($10 \log_{10} x$)
FCC	- Federal Communications Commission (United States)
FH	- Frequency Hopping
GQR	- Gaussian Quadrature Rule
PN	- Pseudonoise or direct sequence
ROC	- Receiver Operating Characteristic
SAW	- Surface Acoustic Wave
SNR	- Signal-to-Noise Ratio

CHAPTER 1

INTRODUCTION

1.1 INTRODUCTION

In the last fifteen years, spread spectrum communications has been receiving increased interest in the open literature. Aside from military applications, more and more civilian uses are being developed. Examples can be found in [1-5].

Spread spectrum signals have several forms: frequency hopping (FH), pseudonoise or direct sequence (PN), and time hopping. Time hopping is generally used with either FH or PN signalling but will not be discussed in this thesis. The first two forms are the most commonly used and are similar in that the frequency of the transmitted signal is altered by a pseudo-random sequence. For FH signals, this sequence selects the carrier frequency while for PN signals, the sequence generates a phase that is used to modulate the message. Excellent tutorials on spread spectrum communications can be found in [1] and [2].

Among the many attractive properties of spread spectrum signals, from a user's point of view, is its low probability of interception [5]. Since the signal power for the PN signals is spread across the transmission bandwidth to resemble noise (hence the name), and FH signals have their power transmitted in a narrow bandwidth, PN signals have a lower probability of interception. However, FH signals have a much wider transmission bandwidth and superior antijamming properties. Therefore, some systems will choose FH signalling over PN.

With spread spectrum communications coming into greater use, it is

only natural that the question of interception by an unfriendly receiver has arisen. This is not only of interest to the military. Spread spectrum signal interception is becoming a greater concern to communications regulatory boards, such as the CRTC in Canada, and the FCC in the United States.

The interception problem is difficult since the transmission spectrum is typically 20 GHz wide, with each user having a bandwidth of 20 kHz. If a discrete frequency distribution is assumed, and the receiver uses a filter matched to each frequency, ten thousand filters would be required to detect the user spectrum while covering the entire spread spectrum. This indicates a great deal of complexity at the receiver. However, approximately 50 SAW Fourier transform devices could accomplish this task.

To solve the problem, it becomes necessary to answer the following question. Given that a sinusoid of one of N possible frequencies has been sent, and that the receiver has knowledge of all the signal parameters, except the signal frequency and time of transmission, can it be detected? Typically, the answer will be no some of the time. Therefore, it is more appropriate to ask: if, when no signal has been sent, the receiver is known to generate false alarms with a certain fixed probability, what is the probability that, when a signal is sent, it will be detected? Since, as the detection probability increases, so does the false alarm probability, thorough performance analysis of any prospective interception receivers must evaluate one as a function of the other.

In this report, the groundwork is laid out for finding the

performance bounds of a spread spectrum interception receiver. This is done by examining the problem of detecting a sinusoid with a discrete frequency distribution. The optimum coherent and noncoherent receivers for such a signal are found, and thus performance limits are established for this problem. It is also shown that another well-known receiver approximates the performance of the optimum receiver extremely well.

In addition, the usefulness of a priori knowledge, and the effects on receiver performance if the received signal is not at one of the predicted frequencies, are considered against the performance bounds established in the report. As well, the limiting detection performance as the number of frequencies becomes infinite is derived.

1.2 LITERATURE REVIEW

In order to establish the significance of the work done in this report, a review of articles in the open literature that have examined the interception of spread spectrum signals, will be conducted.

Glenn [5] examined the interception problem from a military viewpoint, where one end of the communications link is either an airborne command post or a satellite communications system, in both jamming and nonjamming environments. He studies, as a solution, a chip radiometer (energy discriminator) that covers only a portion of the entire transmission spectrum. Particularly, he examines the dependency of the interception range on the radiometer bandwidth when the probabilities of detection (P_D) and false alarm (P_F) are both fixed. It should be noted that to obtain the values of P_F and P_D he uses, high signal-to-noise (SNR) are required. The SNR values that are quoted in his article are measured at the input to the receiver.

Typically, the post-detection SNR at the radiometer, used in this report, will be larger than the input SNR.

Krasner [6] discusses optimal receivers for a general class of digital communications signals, including spread spectrum. He develops likelihood ratio tests for signals of which frequency, phase and symbol sequence is unknown, for both coherent and noncoherent detection. Several approximations for the low SNR case are made. Detectors are compared on the basis of output SNR for a fixed input SNR. While the probability of detection for a fixed P_F is discussed, it is not evaluated.

By far the largest body of work produced on the subject has been by Polydoros, along with several coauthors [7-11]. Most of his work examines the use of autoregressive techniques in noncoherent interception receivers versus the traditional detection theory approach. While the autocorrelation algorithm is admittedly inferior to the optimal receiver, the complexity is much reduced. In addition, there is a significant improvement over the radiometer. Surprisingly, his results indicate that the autoregressive method works better when random tone interference occurs than when there is none. His work also shows that the performance gain of the correlator over the radiometer increases with the SNR.

Most notable is [10] in which he and Weber discuss detector structures for PN and FH signals, considering coherent, noncoherent, synchronous and asynchronous forms. While the block diagram of two of the receivers is given, along with a derivation of the likelihood ratio test for the optimum receivers, no attempt is made to analyze their performances. In another paper [7], wideband detectors for time hopping

and PN signals are considered in more detail while the same is done for FH signals in [8]. As expected, the more filters used to cover the band, the better the performance.

In [12], Chandler and Cooper discuss a PN interception receiver. It uses a single detector that covers only part of the entire spread spectrum. Chandler and Cooper show that the optimum bandwidth is a very weak function of the false alarm probability.

A paper by Dillard [13] discusses an assortment of detection system models: radiometer, an integrate and dump energy detector, and four pulse detection systems. Plots of P_D and SNR versus the time bandwidth product are developed for both coherent and noncoherent detectors in FH, PN and hybrid (FH/PN) environments. It should be noted that all these receivers are suboptimum.

Cooper extends Dillard's work in [14] for noncoherent detection of FH signals in the presence of narrowband interfering signals. He considers the advantages of using multiple observations and an adaptive threshold. The probability of detection is evaluated as a function of the signal power and the number of interfering tones. Degradation in performance from asynchronous detection is also calculated. He concludes by examining the effects of time misalignment and unknown hop rate on the detector performance. He finds that the lack of this information can be counteracted by adaptive thresholding.

Ziemer and Liebetreau [15] study double threshold radiometers and channelized receivers for PN/FH signals from the viewpoint of a transmitter.

1.3 SYSTEM MODEL

As was seen in the previous section, several receivers have been developed for the purpose of intercepting spread spectrum signals. Generally, these can be classified as radiometers, channelized receivers, or autoregressive algorithms for both coherent and noncoherent reception. Although it is acknowledged in the literature that these receivers are not optimum, no performance curves for the optimum receiver have been used for comparison. It would appear, therefore, that no one has developed upper bounds for the interception receiver performance.

To develop the groundwork for these bounds, it is necessary to consider the interception of a sinusoidal signal with a discrete frequency distribution. The optimum receivers for FH or PN signals, which are not discussed in this thesis, will be extensions of the receivers developed for this problem.

In the derivation and analysis of these receivers, the following assumptions are made. Some are idealized but they enable the development of a performance upper bound.

(i) The signal bandwidth and duration is known exactly.

(ii) The frequency distribution is known. It is discrete with frequencies spaced $\frac{1}{T}$ Hz or $\frac{1}{2T}$ Hz apart for noncoherent or coherent systems respectively, where T is the signal duration.

(iii) Each frequency has an equal probability of arrival and only one is active in the detection period.

(iv) The receiver can monitor the entire transmission bandwidth.

(v) The signal is distorted by additive white Gaussian noise (AWGN) of two-sided spectral density, $\frac{N_0}{2}$ W/Hz.

(vi) The unknown factor is the signal frequency.

The problem is to determine if a signal has been sent, and no attempt will be made to estimate the frequency. Therefore, the receiver must be able to differentiate between signal present and no signal present situations only. Or, stated in other words, a receiver must choose between one of two hypotheses which are:

$$H_1: \quad r(t) = A \cos \omega t + n(t) \qquad 0 \leq t \leq T$$

$$H_0: \quad r(t) = n(t) \qquad 0 \leq t \leq T$$

and n(t) is AWGN with zero mean, as mentioned in (v) above. The angular frequency, ω, is unknown but is assumed to have a known discrete distribution as described in (ii).

1.4 PRESENTATION OUTLINE

In Chapter 2, two coherent receivers will be examined. The first is the simple pulse detection system, or maximum likelihood receiver, discussed by Dillard [13]. The optimum, or average likelihood, receiver

is then derived by finding the generalized likelihood test for the system model discussed in the previous section. The performance of each receiver is developed and compared. In addition, this chapter establishes the approach used to design the receivers throughout the report. It should be noted that while evaluating the performance of the optimum receiver, an approximation to the distribution function of a sum of lognormal random variables was found.

The noncoherent versions of the above receivers are derived and analyzed in Chapter 3. For the optimum receiver, the solution of its performance is intractable, so simulations are used to compare its performance to that of the maximum likelihood receiver. In addition, a low SNR receiver is derived, and its degradation relative to the other noncoherent receivers is calculated. The chapter concludes with a comparison of nocoherent and coherent detection methods.

The system model assumes equal probability of arrival and exact knowledge of the hopping frequencies. Chapter 4 investigates receiver performance when these assumptions are no longer valid. The first section examines the change in performance if the detector has a priori knowledge of the signal transmission frequency, and it is used to design a new optimum receiver. The second section of Chapter 4 takes the maximum likelihood receivers and the optimum coherent receiver, and evaluates their performances when the actual transmission frequency does not match the assumed frequency distribution.

The final chapter examines the case when the number of frequencies is large: the case for frequency hopped, spread spectrum. The hopping is assumed to be slow and does not change over the detection period.

Appendix A gives a detailed derivation of the optimum coherent receiver performance. Some details of the Gaussian Quadrature Rule are given in Appendix B while Appendix C describes the simulation of the optimum noncoherent receiver.

CHAPTER 2
COHERENT DETECTION

2.1 INTRODUCTION

This chapter develops two coherent receivers for detecting a sinusoid of unknown frequency, under the assumptions stated in Chapter 1.

The first receiver discussed is not an optimum receiver but is of interest. In [16], Brennan, Reed and Sollfrey develop an average likelihood receiver and a maximum likelihood receiver for radar targets of unknown frequency. They found that the difference between the performance of the two receivers is slight. Therefore, in the next section, the maximum likelihood receiver will be derived to see if that conclusion can also be drawn for this problem.

Section 2.3 carries out a detailed derivation of the generalized likelihood ratio test for this problem, which will give the form of the optimum receiver. The performance analysis of this receiver proves difficult for a large number of frequencies. Thus, the analysis is first carried out for only two frequencies. Several techniques are then tried in order to extend the results to any number of frequencies, using the result for two as a guideline.

Several conclusions are presented at the end of this chapter.

2.2 MAXIMUM LIKELIHOOD RECEIVER

2.2.1 Receiver Description

The maximum likelihood receiver is similar to Dillard's simple pulse detection system [13] when the bandwidth products at both the transmitter and receiver are identical, and energy integration is only over one pulse. The receiver uses a bank of N detectors, which includes an optimum detector for each one of the N possible signals. If any one of these detectors declares a signal present, the receiver will decide a signal has been sent. Otherwise, if none of the detectors declare a signal present, the receiver will conclude that none has been received.

There may be some confusion at this point about the use of the name "maximum likelihood" since it would appear to imply that this receiver is optimum. In [16], this name is given to a receiver that takes the maximum of N outputs and compares this value to a threshold. Only if the threshold is exceeded, will a signal be declared. Consider again the receiver described in the previous paragraph. The decision of that receiver is controlled by the maximum output of the N detectors. Therefore, there will be no difference in performance between the receivers described in this paragraph and the previous one. Since each of the N detectors will be designed by using the average likelihood test, and the receiver's decision is controlled by the maximum output of the N detectors, it will be referred to as the maximum likelihood receiver. If the problem was to estimate the frequency, ω, then this receiver would only need some minor modifications to be optimum. However, it is not optimum for the simple case of detection, as will be

shown in section 2.3.

Before the performance of this receiver can be analyzed, it is necessary to design the optimum detector for a known sinusoid, and find its receiver operating characteristic (ROC). The ROC is simply a plot of the probability of detection versus the probability of false alarm with the SNR as a parameter. It can also be a plot of the probability of detection versus the SNR with probability of false alarm as a parameter.

2.2.2 Detector for a Sinusoid of Known Frequency

The detector must differentiate between noise plus signal and pure noise situations. Therefore, it must decide which of the following hypotheses is true:

$$\begin{aligned} H_1: &\quad r(t) = A\cos\omega t + n(t) && 0 \le t \le T \\ H_0: &\quad r(t) = n(t) && 0 \le t \le T \end{aligned} \qquad (2.1)$$

where n(t) is AWGN with zero mean and spectral height equal to $\frac{N_0}{2}$ W/Hz. r(t) is the received signal and the energy of the transmitted signal, $s(t) = A\cos\omega t$, is equal to $E = \frac{A^2T}{2}$.

To derive the optimum detector, the detection problem is converted to a vector problem, as in [27], so that it becomes a choice between $H_1: \underline{R} = \underline{S} + \underline{N}$ and $H_o: \underline{R} = \underline{N}$, where $\underline{R} = (r_1, r_2)$ and r_i, $i = 1,2$ are the coordinates of r(t) relative to the orthonormal functions, $\left(\frac{2}{T}\right)^{1/2}\cos\omega t$

and $\left(\frac{2}{T}\right)^{1/2} \sin \omega t$. Then the probability density function of the noise vector is

$$p_n(\underline{N}) = \frac{1}{\pi N_o} \exp\left[- \frac{(n_1^2 + n_2^2)}{N_0} \right]$$

$$= \frac{1}{\pi N_0} \exp\left[- \frac{{}_0\int^T n^2(t)\, dt}{N_0} \right]. \qquad (2.2)$$

Under H_1, $n(t) = r(t)-s(t)$. Since $s(t)$ is deterministic, the received signal is a linear transformation of the noise. Therefore, the probability density function of the received signal, under H_1, can be obtained from (2.2). Thus,

$$p_r(\underline{R}|H_1) = p_n(\underline{R} - \underline{S})$$

$$= \frac{1}{\pi N_0} \exp\left[- \frac{{}_0\int^T (r(t)-s(t))^2\, dt}{N_0} \right] \qquad (2.3)$$

which, after multiplying out the expression, becomes

$$p_r(\underline{R}|H_1) = \frac{1}{\pi N_0} \exp\left[\frac{{}_0\int^T r^2(t)\, dt - 2\,{}_0\int^T r(t)\, s(t)\, dt + E}{(- N_0)} \right] \qquad (2.4)$$

since $E = {}_0\int^T s^2(t)\, dt$.

Obviously, the probability density function of the received signal, under H_0, is

$$p_r(\underline{R}|H_0) = p_n(\underline{R})$$

$$= \frac{1}{\pi N_o} \exp\left[-\frac{{}_0\int^T r^2(t)\,dt}{N_0}\right]. \tag{2.5}$$

The likelihood ratio test [17] gives the optimum receiver structure and is

$$L(r) = \frac{p_r(\underline{R}|H_1)}{p_r(\underline{R}|H_0)} \underset{H_0}{\overset{H_1}{\gtrless}} \eta \tag{2.6}$$

where η is the decision threshold. If the ratio exceeds the threshold, the receiver is to decide that H_1 is true. Otherwise, H_0 must be true. For this detector,

$$L(r) = \frac{\frac{1}{\pi N_0} \exp\left[\frac{{}_0\int^T r^2(t)\,dt - 2\,{}_0\int^T r(t)\,s(t)\,dt + E}{(-N_0)}\right]}{\frac{1}{\pi N_0} \exp\left[-\frac{{}_0\int^T r^2(t)\,dt}{N_0}\right]}. \tag{2.7}$$

This simplifies to

$$L(r) = \exp\left[\frac{2}{N_0}\,{}_0\int^T r(t)\,s(t)\,dt - \frac{E}{N_0}\right] \underset{H_0}{\overset{H_1}{\gtrless}} \eta. \tag{2.8}$$

To find the form of the receiver, it is necessary to find the sufficient statistic, ℓ. After some manipulation of the likelihood

ratio test, it is found that

$$\ell = \int_0^T r(t)\, s(t)\, dt \underset{H_0}{\overset{H_1}{\gtrless}} \frac{N_0}{2} \ln \eta + \frac{E}{2} = \gamma. \tag{2.9}$$

Therefore, the optimum detector can be either a correlator or a matched filter, the output of which is compared to a decision threshold. The latter is normally fixed to give a specific probability of false alarm. This detector is used in the maximum likelihood receiver as shown in Figures 2.1 and 2.2.

2.2.3 Performance Analysis of the Detector

To analyze the detector, it is necessary to determine the probability that ℓ exceeds the threshold under each hypothesis. Note that to avoid confusion with the probability of detection and probability of false alarm for the receiver, Q_D and Q_F will be used to denote those of the detector. Now, under H_1, $r(t) = A \cos \omega t + n(t)$. This implies that

$$\ell = \int_0^T A^2 \cos^2 \omega t\, dt + A \int_0^T n(t) \cos \omega t\, dt$$

$$= E + A \int_0^T n(t) \cos \omega t\, dt. \tag{2.10}$$

Therefore, ℓ is a Gaussian random variable with a mean of E and a variance of $\frac{A^2T}{2} \times \frac{N_0}{2} = \frac{EN_0}{2}$. This implies that the probability of

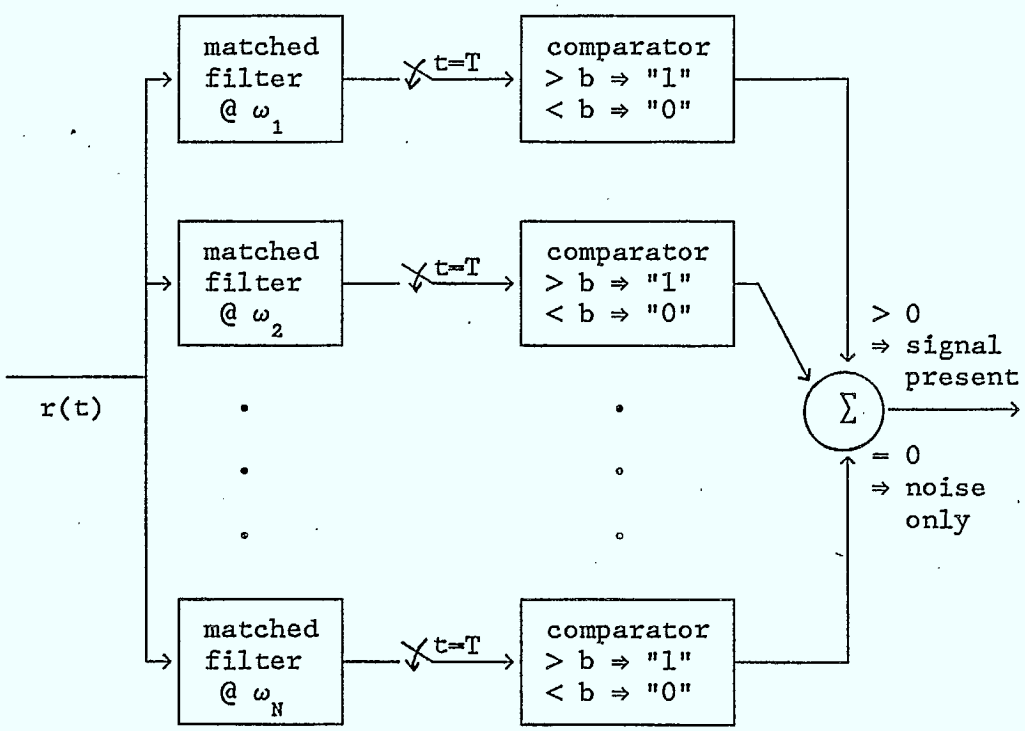

Figure 2.1: Coherent maximum likelihood receiver

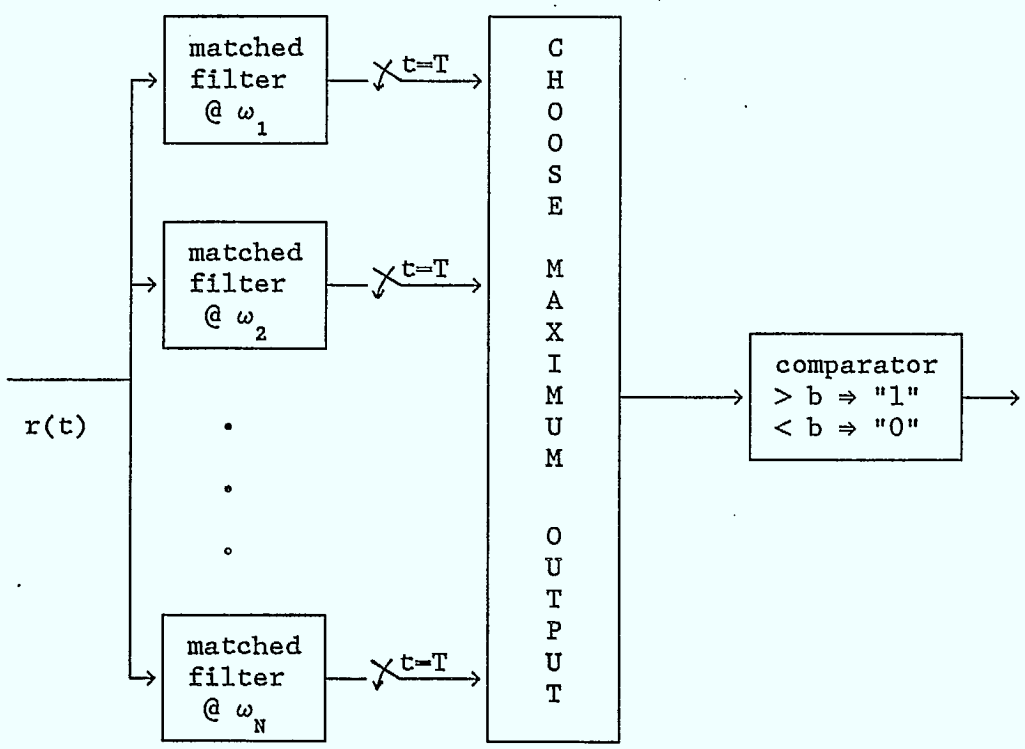

Figure 2.2: Alternate form of the coherent maximum likelihood receiver

detection for this detector is

$$Q_D = \Pr [\ell > \gamma]$$

$$= \int_{\gamma}^{\infty} \frac{1}{(\pi EN_0)^{1/2}} \exp \left[- \frac{(\ell - E)^2}{EN_0} \right] d\ell$$

$$= Q \left[\frac{\gamma - E}{\left(\frac{EN_0}{2} \right)^{1/2}} \right]$$

where Q(x) is the well documented cumulative normal distribution function defined as

$$Q(x) = \int_{x}^{\infty} \frac{1}{(2\pi)^{1/2}} e^{-y^2/2} dy.$$

Define $d = (2E/N_0)^{1/2}$. Then Q_D can be shown to equal, using (2.9) to replace γ,

$$Q_D = Q \left[\frac{\ln \eta}{d} - \frac{d}{2} \right]. \tag{2.11}$$

Under H_0, ℓ will have zero mean and its variance will be identical to that under H_1. So, by a similar method to that used to find Q_D, the probability of false alarm can be shown to equal

$$Q_F = Q \left[\frac{\ln \eta}{d} + \frac{d}{2} \right]. \tag{2.12}$$

Another derivation can be found in [17].

2.2.4 Performance of the Maximum Likelihood Receiver

For the maximum likelihood receiver, as discussed in [13], a false alarm will not occur if none of the detectors generate a false alarm. Therefore, the probability a false alarm will occur is

$$P_F = 1 - (1 - Q_F)^N. \tag{2.13}$$

If a signal is sent, the receiver will not declare a signal present if the detector centered at that frequency misses the signal, and if none of the other detectors generate a false alarm. That is, the probability of a miss is

$$P_M = (1 - Q_D)(1 - Q_F)^{N-1} \tag{2.14}$$

So the probability of detection is

$$\begin{aligned} P_D &= 1 - P_M \\ &= 1 - (1 - Q_D)(1 - Q_F)^{N-1} \end{aligned} \tag{2.15}$$

Some typical values for P_D versus P_F, for SNR = 3 dB, are given in Table 2.1 at the end of the next section.

2.3 OPTIMUM RECEIVER

2.3.1 Likelihood Ratio Test

To find the optimum receiver, it is necessary to first find the likelihood ratio test [17]. As before, this is the ratio of the received signal probability density function under each hypothesis, except now the density functions are averaged over any unwanted parameters, such as the frequency.

$p_r(\underline{R}|H_0)$ is unchanged from the previous section and is given by (2.5). Now, however, the received signal under H_1 is a function of an unknown variable, the frequency. To prevent the likelihood ratio from also becoming a function of the frequency, the conditional probability density function must be averaged over the frequency. That is,

$$p_r(\underline{R}|H_1) = \int_{\omega_{min}}^{\omega_{max}} p_\omega(\omega)\ p_r(\underline{R}|H_1,\omega)\ d\omega. \tag{2.16}$$

From the assumptions made earlier, it is known that the probability density function of the signal frequency is $p_\omega(\omega) = \frac{1}{N}\sum_{i=1}^{N} \delta(\omega - \omega_i)$ where $\delta(x)$ is the Dirac delta function. The conditional probability density function, $p_r(\underline{R}|H_1,\omega)$, is equivalent to $p_r(\underline{R}|H_1)$ from the previous section, as given in (2.3). Therefore,

$$p_r(\underline{R}|H_1) = \frac{1}{N\pi N_o} \sum_{i=1}^{N} \exp\left[\frac{{}_0\int^T r^2(t)\ dt - 2A\ {}_0\int^T r(t)\ \cos\omega_i t\ dt + E}{(-N_0)}\right]. \tag{2.17}$$

Note that in this case, it is assumed that $\omega_i T \gg 1$ so that the signal energy can safely be considered as independent of the frequency. The likelihood ratio test then becomes, by taking the ratio of the two probability density functions,

$$L(r) = \sum_{i=1}^{N} \exp\left[\frac{2A}{N_0} \int_0^T r(t) \cos \omega_i t \, dt\right] \underset{H_0}{\overset{H_1}{\gtrless}} \eta N e^{d^2/2} \tag{2.18}$$

Once again, the sufficient statistic will give the receiver. Denote $\alpha_i = \frac{2A}{N_0} \int_0^T r(t) \cos \omega_i t \, dt$ and $\ell_i = e^{\alpha_i}$. Then the sufficient statistic can be written as

$$\ell = \sum_{i=1}^{N} \ell_i. \tag{2.19}$$

The optimum receiver, then, shown in Figure 2.3, consists of a bank of N matched filters, each centered at one of the N possible frequencies. The output of each is multiplied by $\frac{2A}{N_0}$, to give α_i. Next, e^{α_i} is calculated to give ℓ_i, and the ℓ_i's are summed. The sum is then compared to the decision threshold.

An interesting observation is that the sufficient statistic is a sum of lognormal random variables. While there have been attempts in the literature [18-19] to find its distribution function, no exact solution has been found. In order to be able to determine the accuracy of any approximate solutions, it was decided to carry out the performance analysis for the simple case of two signal frequencies.

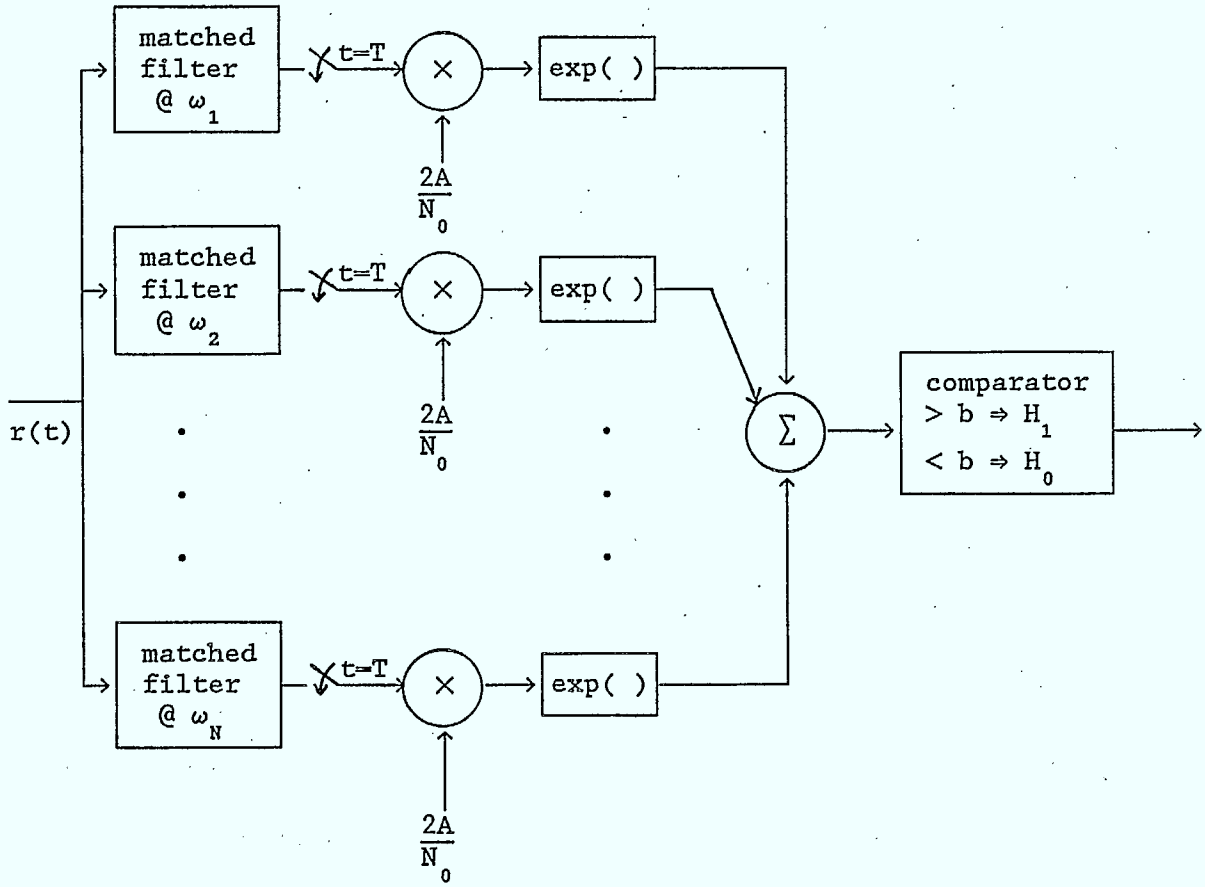

Figure 2.3: Optimum coherent receiver

2.3.2 P_F for Two Frequencies

The false alarm probability can be found in two ways. The first is to find the distribution function of the sufficient statistic, and then integrate this over the region in which ℓ is greater than the decision threshold. The second approach finds the conditional probability, $\Pr[e^{\alpha_1} + e^{\alpha_2} \geq b | \alpha_2]$ which is then averaged over α_2 to find P_F.

For the first approach, the probability density functions of α_i and ℓ_i must be found. Since the former is a linear transformation of a Gaussian random variable, it is also Gaussian. Under H_0, r(t) has a mean of zero. Therefore, α_i will also have a mean of zero and its variance can be shown to equal

$$\text{Var}\ (\alpha_i) = \frac{N_0 T}{4} \left[\frac{2A}{N_0}\right]^2 = \frac{A^2 T}{N_0} = \frac{2E}{N_0} = d^2.$$

This implies that

$$p_{\alpha_i}(\alpha_i | H_0) = \frac{1}{(2\pi d^2)^{1/2}} \exp\left[-\frac{\alpha_i^2}{2d^2}\right]. \tag{2.20}$$

Now, $\alpha_i = \ln \ell_i$. From the theory for the transformation of random variables [20],

$$p_{\ell_i}(\ell_i | H_0) = p_{\alpha_i}(\ell_i | H_0) \frac{d\alpha_i}{d\ell_i}$$

$$= \frac{1}{\ell_i (2\pi d^2)^{1/2}} \exp\left[-\frac{(\ln \ell_i)^2}{2d^2}\right] \tag{2.21}$$

and $p_\ell(\ell|H_0) = p_{\ell_1}(\ell_1|H_0) \otimes p_{\ell_2}(\ell_2|H_0)$ where $\otimes$ denotes convolution. Thus,

$$p_\ell(\ell|H_0) = \int_0^\ell \frac{1}{u(\ell-u)2\pi d^2} \exp\left[-\frac{[(\ln u)^2 + (\ln(\ell-u))^2]}{2d^2}\right] du. \qquad (2.22)$$

The probability of false alarm is the probability that ℓ will exceed the decision threshold when noise alone is present. That is

$$P_F = \int_b^\infty p_\ell(\ell|H_0)\, d\ell \qquad (2.23)$$

where $b = 2\eta e^{d^2/2}$. This is solved in Appendix A to give

$$P_F = Q\left[\frac{\ln b}{d}\right] + \int_{-\infty}^{\ln b} \frac{1}{(2\pi d^2)^{1/2}} \exp\left[-\frac{\alpha_2^2}{2d^2}\right] Q\left[\frac{\ln(b-e^{\alpha_2})}{d}\right] d\alpha_2. \qquad (2.24)$$

This expression can be evaluated by standard numerical integration techniques.

To crosscheck this result, the second approach, mentioned at the beginning of this section, is used. The probability of false alarm can also be expressed as

$$P_F = \Pr[e^{\alpha_1} + e^{\alpha_2} \geq b]$$

$$= \int_{-\infty}^\infty \Pr[e^{\alpha_1} > b - e^{\alpha_2}|\alpha_2, H_0]\, p_{\alpha_2}(\alpha_2|H_0)\, d\alpha_2 \qquad (2.25)$$

The conditional probability is simply

$$\Pr[e^{\alpha_1} + e^{\alpha_2} \geq b | \alpha_2, H_0] = \begin{cases} 1 & \alpha_2 \geq \ln b \\ Q\left[\dfrac{\ln (b-e^{\alpha_2})}{d}\right] & \alpha_2 < \ln b \end{cases} \tag{2.26}$$

Therefore, substitution of (2.20) and (2.26) into (2.25) will give, once again,

$$P_F = Q\left[\frac{\ln b}{d}\right] + \int_{-\infty}^{\ln b} \frac{1}{(2\pi d^2)^{1/2}} \exp\left[-\frac{\alpha_2^2}{2d^2}\right] Q\left[\frac{\ln (b-e^{\alpha_2})}{d}\right] d\alpha_2 \tag{2.27}$$

which is identical to (2.24). Thus, the expression for P_F is verified.

2.3.3 P_D for Two Frequencies

The analysis for the probability of detection is similar to that carried out for the probability of false alarm. Two methods, described at the beginning of section 2.3.2, will be used to find P_D in order to confirm the result.

As before, the probability density function of ℓ is a convolution of those corresponding to ℓ_1 and ℓ_2. Now, however, a signal has been received which is assumed to have a frequency equal to ω_1. This implies that α_1 now has a mean equal to d^2, which can be proved in an identical manner to that used to find the mean for ℓ, under H_1, in section 2.2.3. Therefore,

$$p_{\ell_1}(\ell_1 | H_1) = \frac{1}{\ell_1 (2\pi d^2)^{1/2}} \exp\left[-\frac{(\ln \ell_1 - d^2)^2}{2d^2}\right] \tag{2.28}$$

So, taking the convolution of the probability density functions of ℓ_1 and ℓ_2, given in (2.28) and (2.21) respectively, results in

$$p_{\ell}(\ell|H_1) = \int_0^{\ell} \frac{1}{u(\ell-u)2\pi d^2} \exp\left[-\frac{[(\ln u - d^2)^2 + (\ln(\ell-u))^2]}{2d^2}\right] du. \qquad (2.29)$$

To obtain the probability of detection, it is once again necessary to find the probability that ℓ will exceed the threshold. That is

$$P_D = \int_b^{\infty} p_{\ell}(\ell|H_1)\, d\ell \qquad (2.30)$$

where $b = 2\eta e^{d^2/2}$, as defined earlier. Solving this, as in Appendix A, gives

$$P_D = Q\left[\frac{\ln b}{d}\right] + \int_{-\infty}^{\ln b} \frac{1}{(2\pi d^2)^{1/2}} \exp\left[-\frac{\alpha_2^2}{2d^2}\right] Q\left[\frac{\ln(b-e^{\alpha_2})}{d} - d\right] d\alpha_2. \qquad (2.31)$$

It should be noted that an alternate form of P_D is found if the dummy variable in the integral of (2.29) is allowed to equal ℓ_1 instead. Then P_D can be expressed as

$$P_D = Q\left[\frac{\ln b}{d} - d\right] + \int_{-\infty}^{\ln b} \frac{1}{(2\pi d^2)^{1/2}} \exp\left[-\frac{(\alpha_1 - d^2)^2}{2d^2}\right] Q\left[\frac{\ln(b-e^{\alpha_1})}{d}\right] d\alpha_1. \qquad (2.32)$$

Again, to check the expression, the problem is solved by a second method which begins by recognizing that

$$P_D = \Pr[e^{\alpha_1} + e^{\alpha_2} \geq b]$$
$$= \int_{-\infty}^{\infty} \Pr[e^{\alpha_2} > b - e^{\alpha_1} | \alpha_1, H_1] \; p_{\alpha_1}(\alpha_1 | H_1) \; d\alpha_1. \tag{2.33}$$

This conditional probability is easily solved to give

$$\Pr[e^{\alpha_1} + e^{\alpha_2} \geq b | \alpha_1, H_1] = \begin{cases} 1 & \alpha_1 \geq \ln b \\ Q\left[\dfrac{\ln (b - e^{\alpha_1})}{d}\right] & \alpha_1 < \ln b \end{cases} \tag{2.34}$$

The probability density function of α_1 can be obtained from (2.28), in the same manner (2.21) was derived, and is

$$p_{\alpha_1}(\alpha_1) = \frac{1}{(2\pi d^2)^{1/2}} \exp\left[-\frac{(\alpha_1 - d^2)^2}{2d^2}\right]. \tag{2.35}$$

Substituting (2.34) and (2.35) into (2.33) gives

$$P_D = \int_{-\infty}^{\ln b} \frac{1}{(2\pi d^2)^{1/2}} \exp\left[-\frac{(\alpha_1 - d^2)^2}{2d^2}\right] Q\left[\frac{\ln (b - e^{\alpha_1})}{d}\right] d\alpha_1 + Q\left[\frac{\ln b}{d} - d\right]. \tag{2.36}$$

If, instead, integration is carried out over α_1 first, then

TABLE 2.1: Probability of detection for SNR = 3 dB

P_F	1 freq.	2 freq	
		MLT	ALT
10^{-1}	.552	.443	.448
10^{-2}	.180	.127	.128
10^{-3}	.0467	.0307	.0308
10^{-4}	.0105	6.66×10^{-2}	6.66×10^{-2}
10^{-5}	2.17×10^{-3}	1.33×10^{-3}	1.33×10^{-3}
10^{-6}	5.96×10^{-4}	2.52×10^{-4}	2.52×10^{-4}

$$\Pr[e^{\alpha_1} + e^{\alpha_2} \geq b \,|\, \alpha_2, H_1] = \begin{cases} 1 & \alpha_2 \geq \ln b \\ Q\left[\dfrac{\ln (b-e^{\alpha_2})}{d} - d\right] & \alpha_2 < \ln b \end{cases} \tag{2.37}$$

so that P_D takes a slightly different form

$$P_D = Q\left[\frac{\ln b}{d}\right] + \int_{-\infty}^{\ln b} \frac{1}{(2\pi d^2)^{1/2}} \exp\left[-\frac{\alpha_2^2}{2d^2}\right] Q\left[\frac{\ln (b-e^{\alpha_2})}{d} - d\right] d\alpha_2. \tag{2.38}$$

The expressions in (2.36) and (2.38) are identical to those given in (2.31) and (2.32), respectively. Therefore, these expressions for P_D are correct.

2.3.4 Discussion of Results for Two Signal Frequencies

The expressions of the previous two sections were evaluated using a Gauss Quadrature numerical integration routine. A plot of P_D versus SNR

TABLE 2.2: Probability of detection for SNR = 13 dB

P_F	1 freq.	2 freq	
		MLT	ALT
10^{-1}	.999	.998	.999
10^{-2}	.984	.971	.972
10^{-3}	.916	.880	.880
10^{-4}	.773	.718	.718
10^{-5}	.580	.520	.522
10^{-6}	.387	.336	.356

is given in Figure 2.4 for fixed P_F, along with the results for the single frequency case. As can be seen from the plot, for P_D to exceed 0.5, P_F must be greater than 0.1 for values of SNR around 3 dB. For higher SNR, 13 dB for example, P_F can be as low as 10^{-4} when $P_D = 0.5$.

In section 2.1, it was explained that results in [16] showed, for the particular example examined in that paper, that the maximum likelihood and average likelihood receivers are close in performance. Table 2.1 and Table 2.2 give some typical values for both receivers developed in this chapter, for one and two frequencies when the SNR = 3 dB and 13 dB, respectively. From Table 2.1, it is obvious that in this case as well, the two receivers have nearly identical performance, the discrepancy being on the order of 1% for P_D greater than 0.5, and decreasing for smaller values of P_D. However, for SNR = 13 dB, the loss increases to 6% for very small P_F around 10^{-6}.

Will this hold for a large number of frequencies or is there a better approximation to the performance of the optimum receiver? The

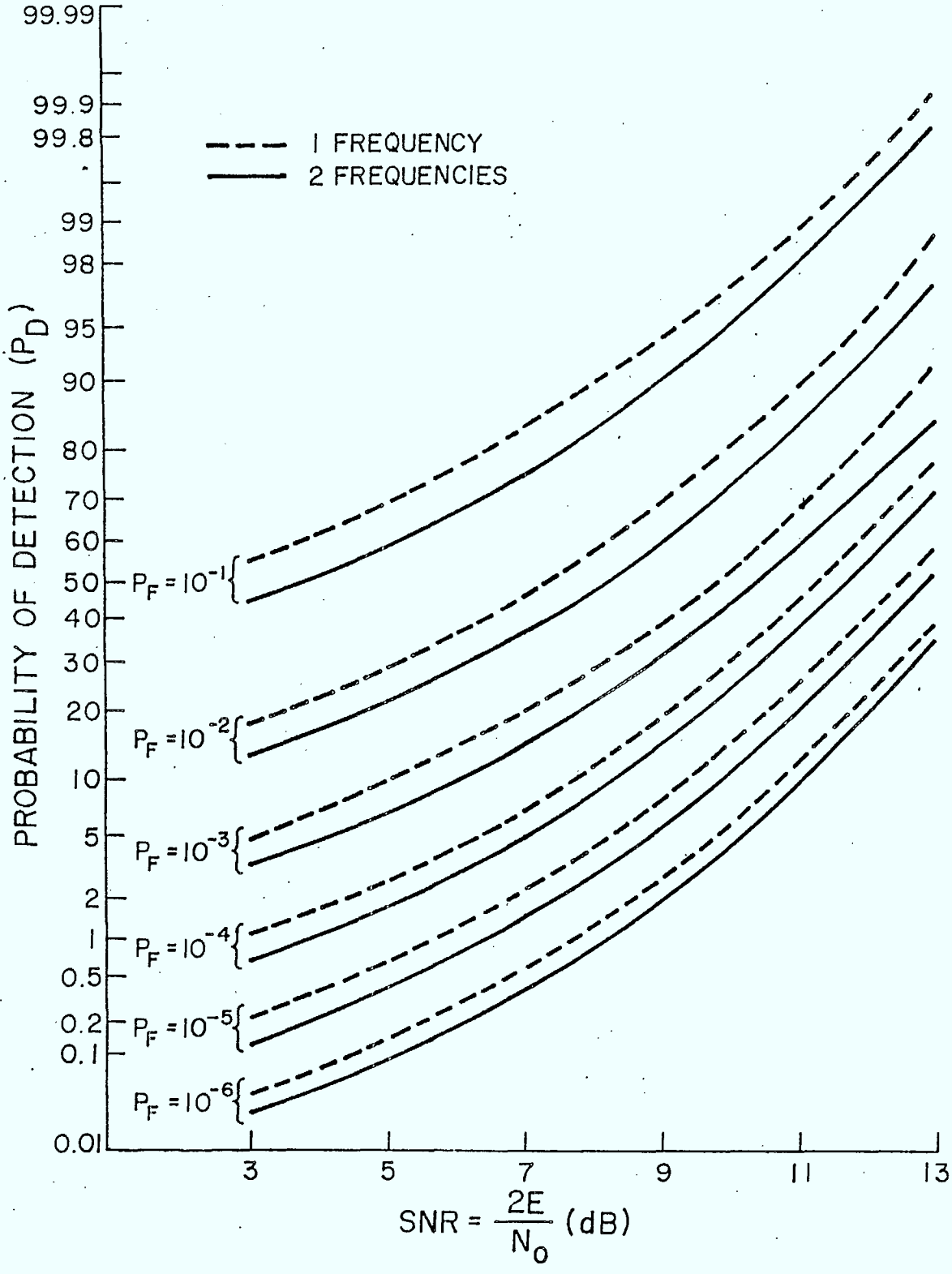

Figure 2.4 Optimum coherent receiver performance plots for one and two frequencies

next few sections address this question.

2.3.5 Gaussian Quadrature Rule

An approach used to evaluate ${}_c\int^d f(x)w(x)\,dx$, the Gaussian Quadrature Rule (GQR) has met with success in solving many problems.

As explained in [18], the GQR uses the fact that w(x) can be approximated by its moments since

$$\mu_i = {}_c\int^d x^i w(x)\,dx = \sum_{j=1}^{M} A_j (t_j)^i \qquad i = 0,1,..,2M. \tag{2.39}$$

Assuming

$$w(x) = \sum_{i=1}^{M} A_i \delta(x - t_i) \tag{2.40}$$

then

$${}_c\int^d f(x)w(x)\,dx = \sum_{i=1}^{M} A_i f(t_i) \qquad c < t_i < d \tag{2.41}$$

if f(x) has continuous derivatives up to order 2M, where 2M is the number of moments used by the algorithm.

Details on the algorithm used to get the weights, A_i, and the nodes, t_i, from the moments of w(x) are given in Appendix B.

Naturally, the question of what are the moments of a sum of lognormals must be answered. Fortunately, that is not difficult to do.

As established in Prabhu [21], the moments of a sum of N

independent random variables can be found recursively. Let $\mu_k(n)$ be the kth moment of a sum of n independent random variables. Then

$$\mu_k(n) = \sum_{i=0}^{k} \begin{bmatrix} k \\ i \end{bmatrix} \mu_i(1)\ \mu_{k-i}(n-1). \tag{2.42}$$

For a lognormal random variable,

$$\mu_k(1) = \exp\left[km_z + \frac{\sigma_z^2 k^2}{2}\right] \tag{2.43}$$

where $\ell = e^z$ and z is normal with mean, m_z, and variance, σ_z^2.

With the moments now established, the algorithm of Appendix B can be carried out to obtain the weights, and nodes, for the GQR of (2.41).

Meyers [18] examines the sum of N lognormal random variables as an example for the GQR. He suggests, in his paper, that to avoid roundoff errors, the moments should be symmetrized. That is, if w(x) is the probability density function of the sum of zero mean lognormals of variance d^2, then let

$$w_e(y) = \frac{1}{2}\ [w(y) + w(-y)]. \tag{2.44}$$

The moments of the even function will then be

$$\begin{aligned} \mu_k^{*} &= \frac{1}{2}\ [\mu_k + (-1)^k \mu_k] \\ &= \begin{cases} e^{d^2k^2/2} & k \text{ even} \\ 0 & k \text{ odd} \end{cases} \end{aligned} \tag{2.45}$$

To transform back,

$$\Pr[y > \gamma] = 2 \int_{\gamma}^{\infty} w_e(x)\, dx.$$

These moments will be referred to as the symmetrical moments.

The GQR was tried with three different sets of moments: central moments, symmetrical moments, and the unmodified or asymmetrical moments. In addition, two different assignments of w(x) and f(x) were used.

In the first case, $w(x) = w\left[\sum_{i=1}^{N} e^{z_i}\right]$ and $f(x) = 1$. Following a suggestion in [18], the value of the integral of (2.41) at each node point was evaluated as

$$I(t_i) - \frac{A_i}{2}$$

where

$$I(t_i) = \sum_{j=1}^{M} A_j u(t_j - t_i).$$

Interpolation is then used between the node points to find Pr $[y > \gamma]$.

In the second case $w(x) = w\left[\sum_{i=1}^{N-1} e^{z_i}\right]$ and $f(x) = w(e^{z_N})$. That is, moments for the sum of N-1 lognormal random variables are used and the GQR is averaged over the Nth variable to give, for example,

$$P_F = \int_0^{\infty} \Pr[\ell_N > \eta N e^{d^2/2} - \sum_{i=1}^{N-1} \ell_i \,|\, \sum_{i=1}^{N-1} \ell_i]\ \Pr[\sum_{i=1}^{N-1} \ell_i]\ d(\sum_{i=1}^{N-1} \ell_i)$$

$$= \sum_{i=1}^{N} A_i\ \Pr[\ell_N > \eta N e^{d^2/2} - t_i \,|\, t_i] \qquad (2.46)$$

where

$$\Pr[\ell_N > \eta N e^{d^2/2} - t_i \mid t_i] = \begin{cases} 1 & t_i > \eta N e^{d^2/2} \\ Q\left[\dfrac{\ln(\eta N e^{d^2/2} - t_i)}{d}\right] & t_i < \eta N e^{d^2/2} \end{cases} \tag{2.47}$$

$\ell_i = e^{z_i}$, and 2M moments are used.

It was hoped that at least one, if not all, of these approaches would give a good approximation. The GQR was executed with 60 moments under each of the alternatives. The results for a single lognormal, and the sum of two lognormals, were compared to the previously established values, as shown in Figures 2.5 - 2.8. Note that the plots for central moments are not included since the results are identical to those for asymmetrical moments.

The approximation to the distribution function of one lognormal variable is poor, five times too large for $\Pr(X > x) = 0.1$ and variance of 5 dB when symmetrical moments are used, for example. This discrepancy becomes worse as the variance increases. Unmodified moments give a much better match which, instead, seems to improve as the variance increases. However, symmetrical moments give a fair approximation when the variance is equal to 0.0 dB.

Of greater interest, however, is the sum of two lognormal random variables. In this case, averaging over one variable gives a better result, which, when combined with unmodified moments, gives the best approximation overall. Looking at a variance of 3 dB and $\Pr(X > x) = 10^{-3}$, when unmodified moments are used and no averaging is performed, the result is three and a half times too large. Yet, when the

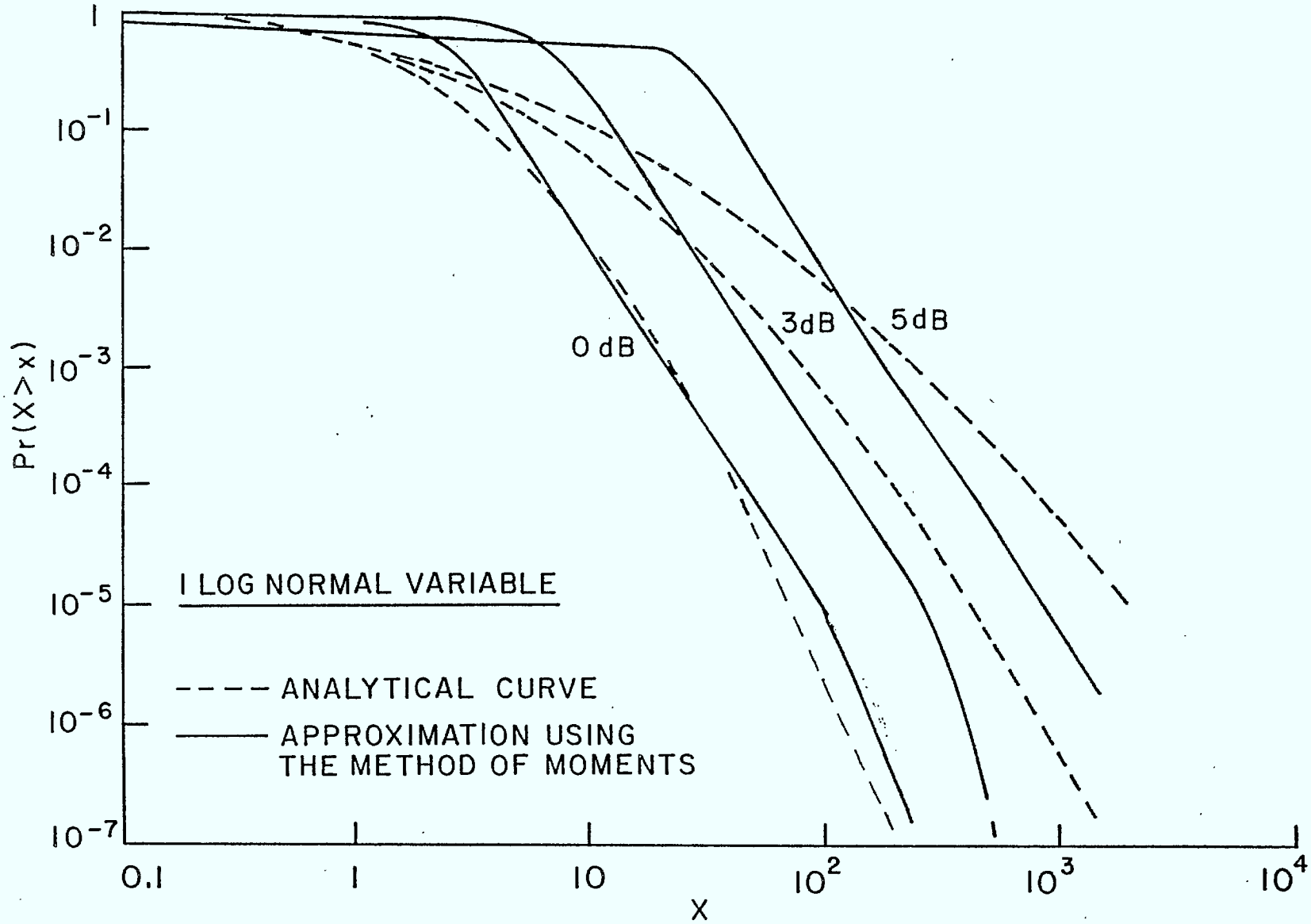

Figure 2.5 GQR approximation of the lognormal distribution function using symmetrical moments

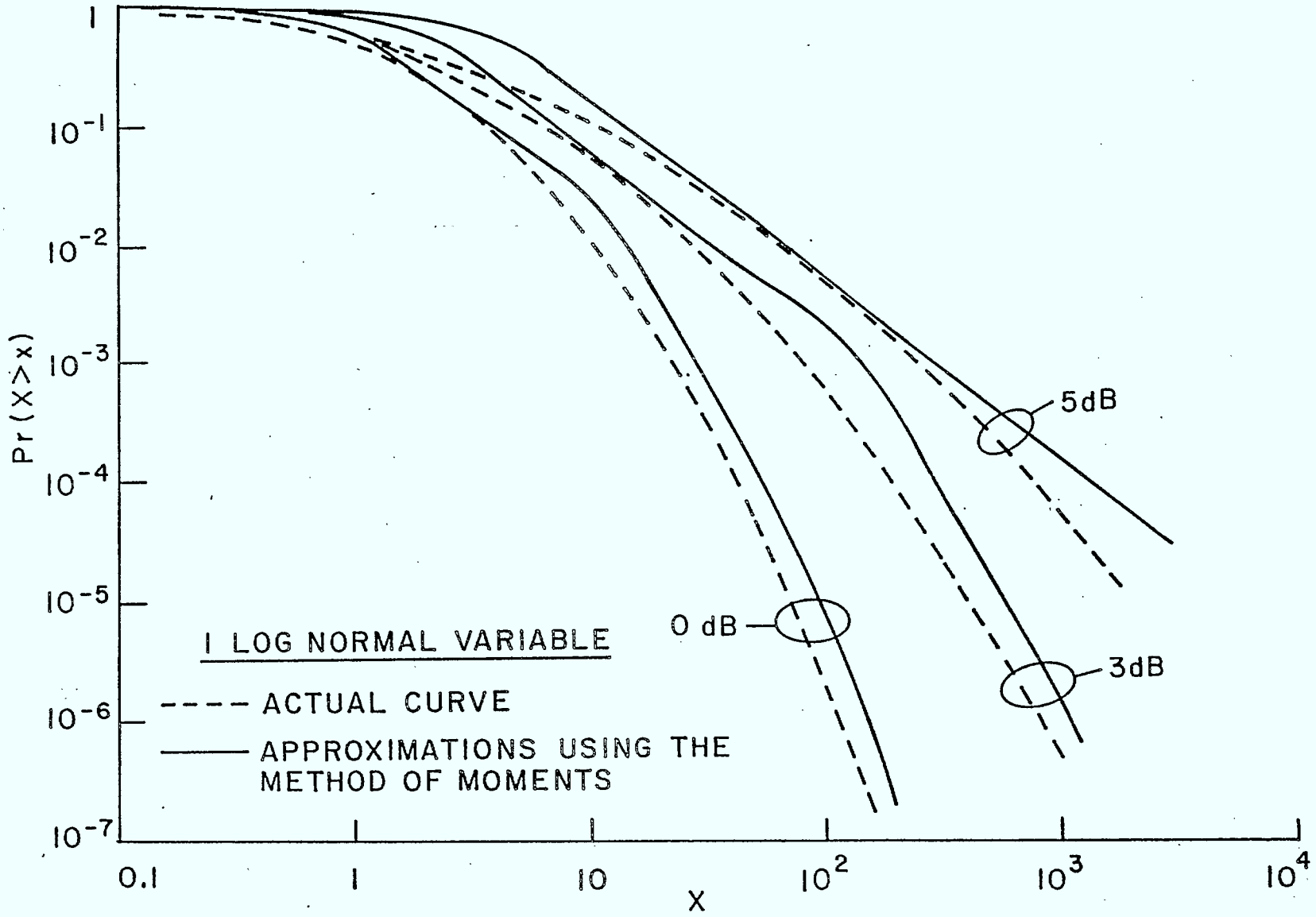

Figure 2.6 GQR approximation of the lognormal distribution function using unmodified moments

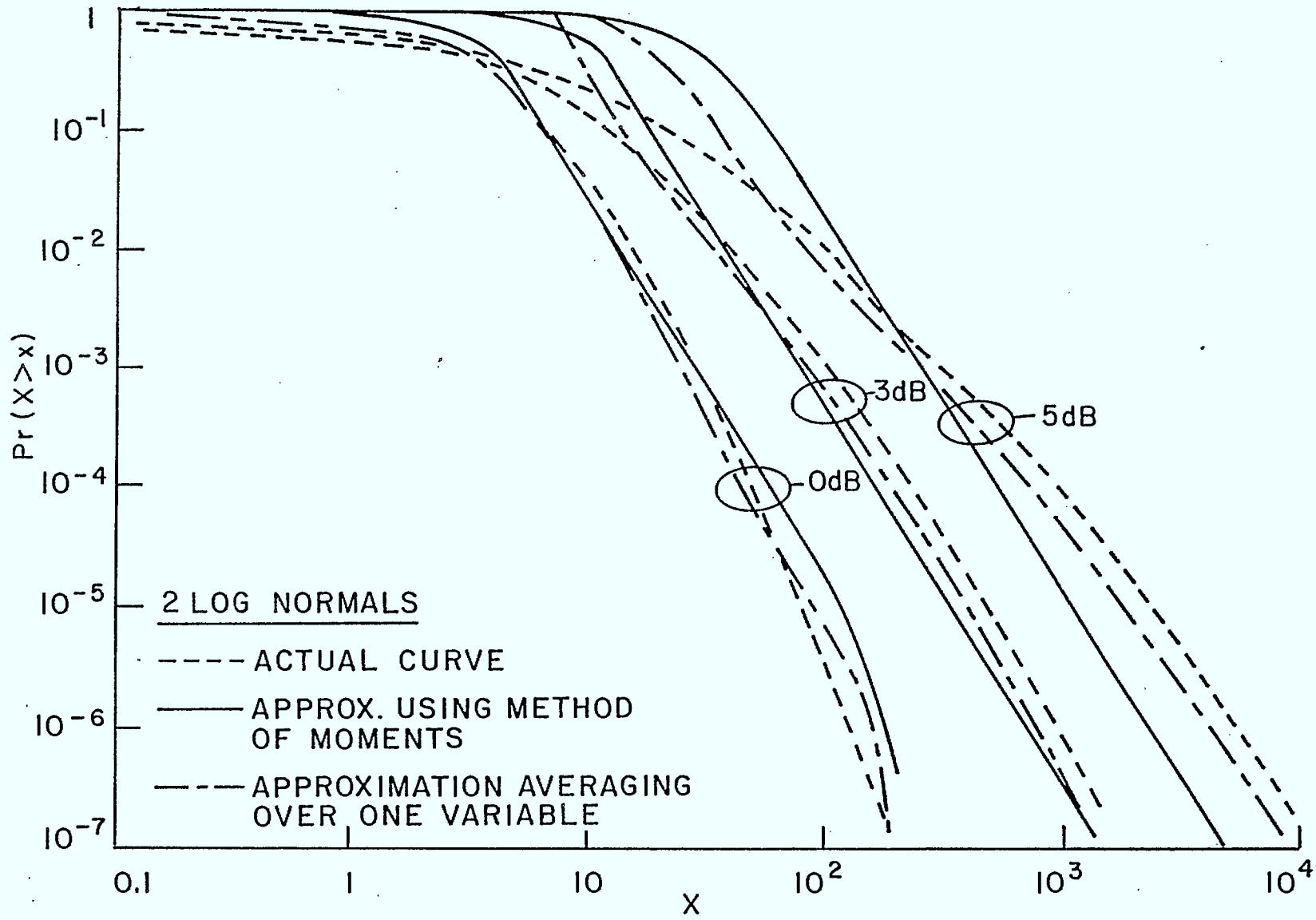

Figure 2.7 GQR approximation, using symmetrical moments, of the distribution function of the sum of two lognormal random variables

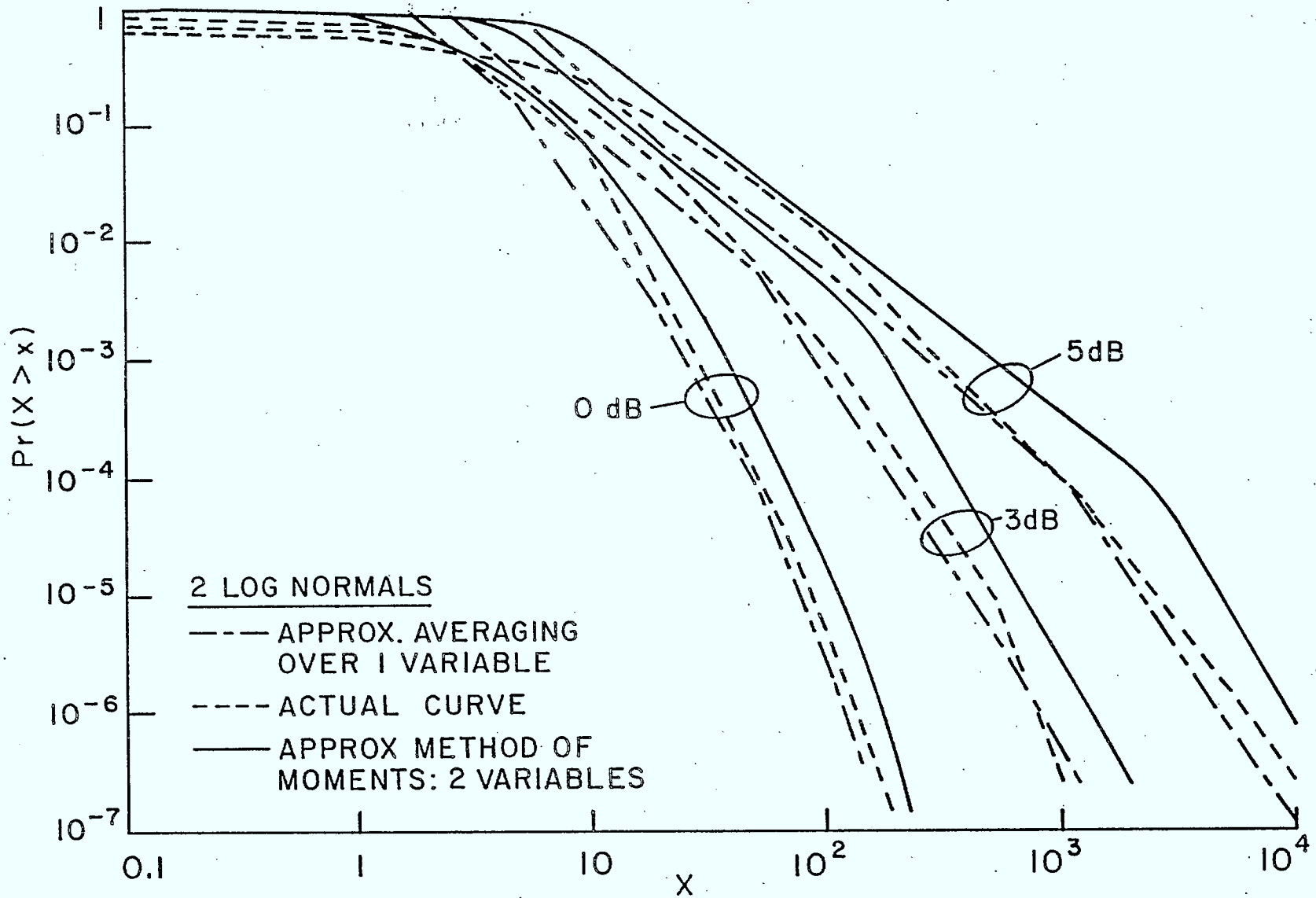

Figure 2.8 GQR approximation, using unmodified moments, of the distribution function of the sum of two lognormal random variables

distribution function is calculated by averaging over one variable , it gives a result that is too small by a factor of 1.6. In comparison, the values found by using symmetrical moments, under similar conditions, are too small by a factor of 2.5 and 1.6 when no averaging and averaging is performed, respectively. As the variance increases, only by averaging over one variable and using the unmodified moments can an approximate solution be obtained, though this approximation can be too large or too small by as much as a factor of two. Using more than sixty moments made no significant change in the results.

The results are surprisingly poor. Why the GQR fails to give a better approximation in this case is unknown. However, the answer may be suggested when the weights at the corresponding nodes are plotted against the lognormal density function. As can be seen from Figure 2.9, the nodes must be concentrated in the tail of the function since at the most one node for each approach appears near the origin, where the function changes the most rapidly. In addition, this node moves further away along the horizontal axis as the variance increases. Using unmodified moments, when the variance is 3 dB, the first node occurs after the probability density function has fallen to 30% of its peak value, well past the range of interest. In contrast, the nodes were evenly distributed across the entire density function when the GQR was run for a Gaussian random variable. It could be that the exponential growth of the moments for a lognormal random variable makes the approximation given in (2.40) very poor.

This approach was abandoned in the hopes of finding a better approximation.

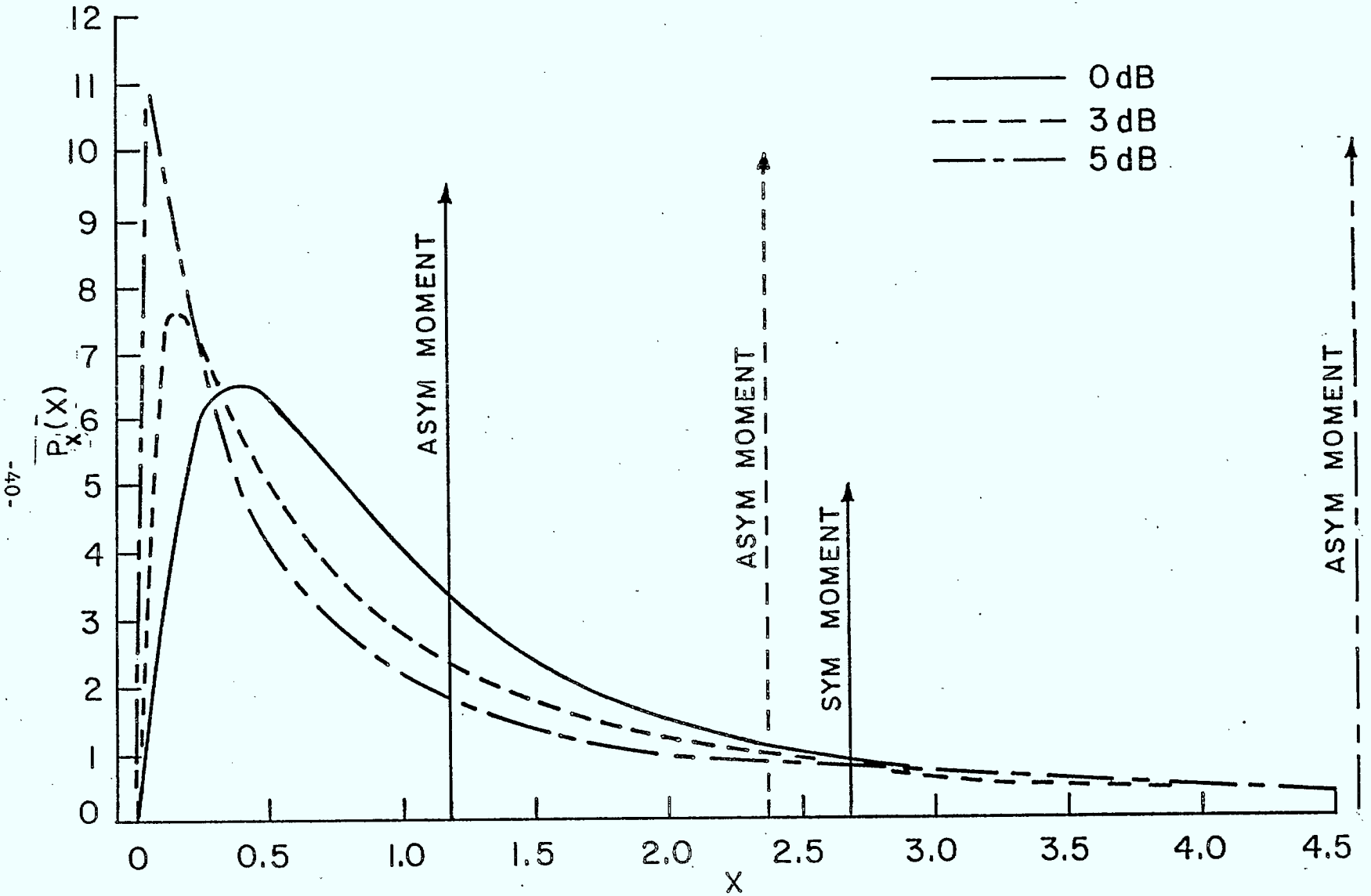

Figure 2.9 A few GQR weights and nodes versus lognormal probability density function for $x < 4.5$

2.3.6 Wilkinson's Approach

In [19], Schwartz and Yeh examined the problem of finding the distribution function of a sum of lognormal variables. They were interested in much smaller variances than those of interest to this report. Denote the variance used in [19] as σ_y^2, and those used here as σ_x^2. Then

$$\sigma_y = .1\ \sigma_x \ln 10. \tag{2.48}$$

For small varainces, the approach the authors recommend is attributed to Wilkinson. He suggested that the sum of lognormals is also lognormal. That is,

$$L = e^z = \sum_{i=1}^{N} e^{z_i}. \tag{2.49}$$

The proof relies on the central limit theorem, as explained in [22]. Let m_1, σ_1^2 be the mean and variance of e^{z_i}, respectively. Then by the central limit theorem,

$$\frac{L - Nm_1}{\sigma_1 N^{1/2}}$$

is asymptotically normal with a mean of zero and a variance equal to one. From the law of large numbers, it can be seen that $\frac{L}{Nm_L} \approx 1$. Since when $x \approx 1$, $\ln x$ can be approximated by $x-1$, then, for large N,

$$\ln\left[\frac{L}{Nm_1}\right] \approx \frac{L}{Nm_1} - 1$$

$$\frac{m_L N^{1/2}}{\sigma_1} \ln\left[\frac{L}{Nm_1}\right] \approx \frac{L - Nm_L}{\sigma_1 N^{1/2}}.$$

So, ln L is normal, which implies that L is lognormal.

If L can indeed be approximated by a lognormal random variable, then the solution is given by

$$\Pr[L > \eta] = Q\left[\frac{\ln \eta - m_z}{\sigma_z}\right]. \tag{2.50}$$

The mean and variance can be found from the moments of L. Denoting the mean of L as $\mu_1(N)$ and the variance as $\mu_2(N)$, from (2.43) it is known that

$$\mu_1(N) = \exp\left[m_z + \frac{\sigma_z^2}{2}\right], \tag{2.51}$$

$$\mu_2(N) = \exp\left[2\, m_z + 2\, \sigma_z^2\right]. \tag{2.52}$$

Solving (2.51) and (2.52) gives

$$m_z = 2 \ln \mu_1(N) - 0.5 \ln \mu_2(N), \tag{2.53}$$

$$\sigma_z^2 = \ln \mu_2(N) - 2 \ln \mu_1(N). \tag{2.54}$$

Therefore, the mean and variance of z can be found since $\mu_1(N)$ and $\mu_2(N)$

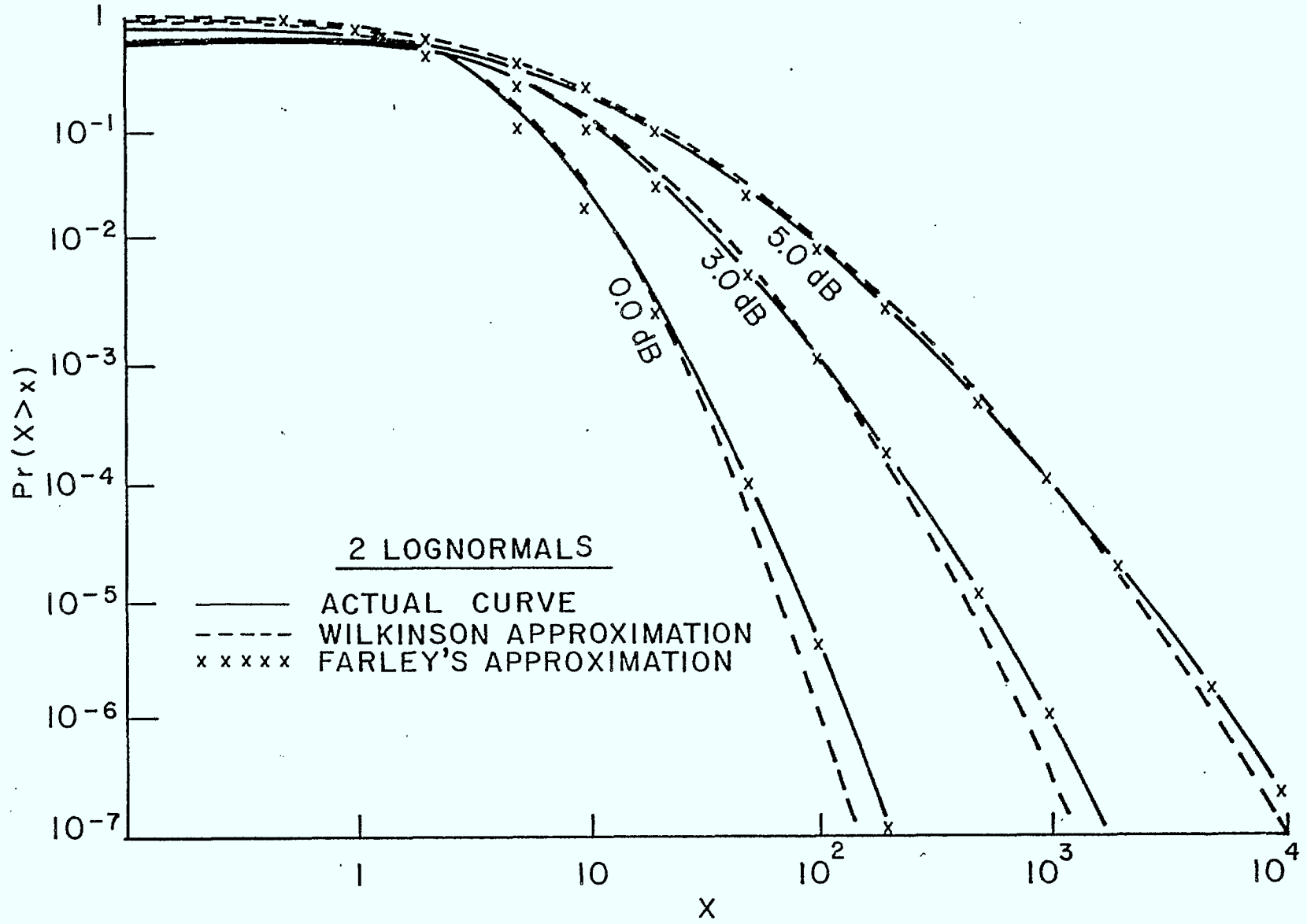

Figure 2.10 The probability distribution function, and two approximations, of the sum of two lognormal random variables

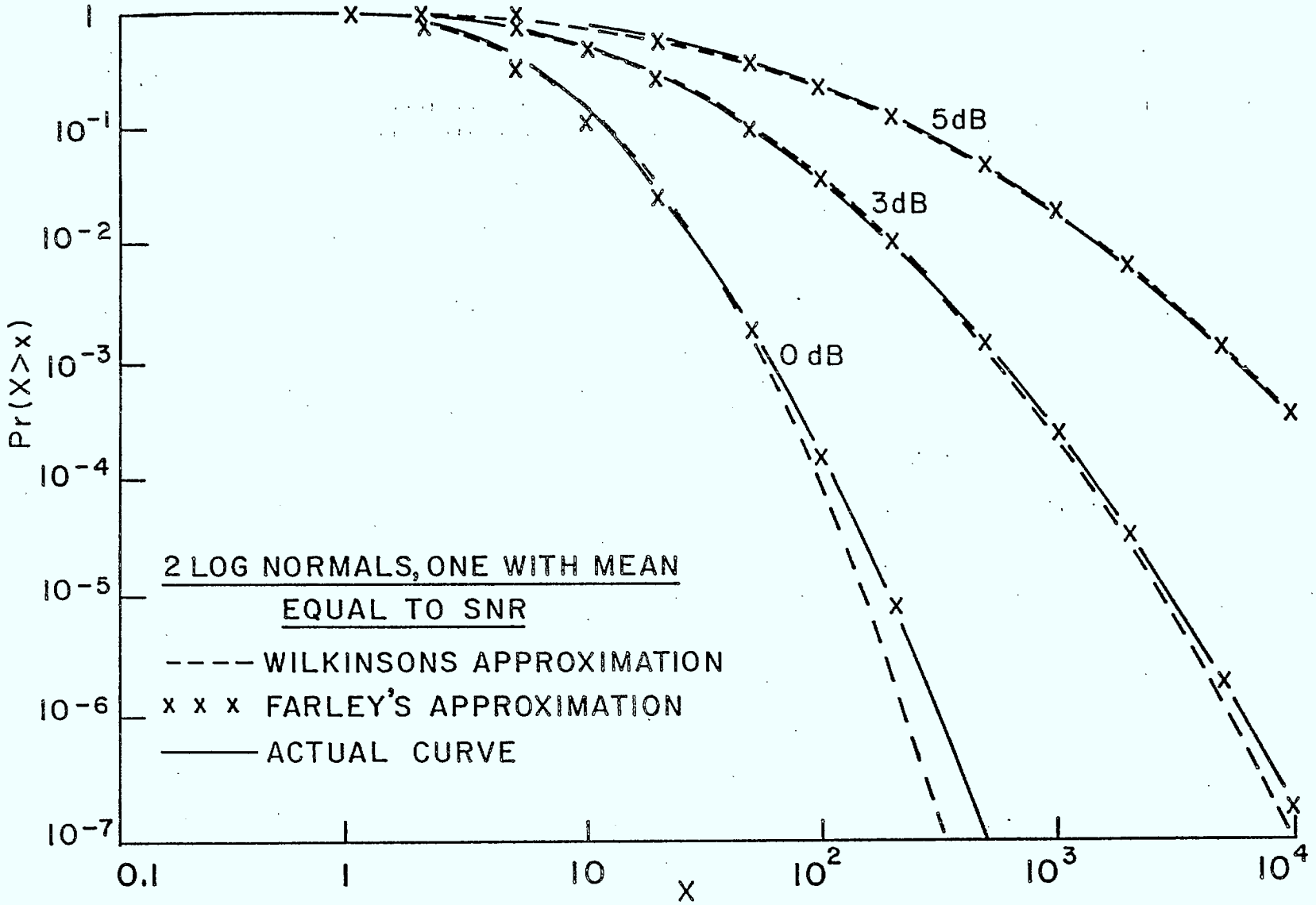

Figure 2.11 The probability distribution function, and two approximations, the sum of two lognormal random variables, one with a nonzero mean

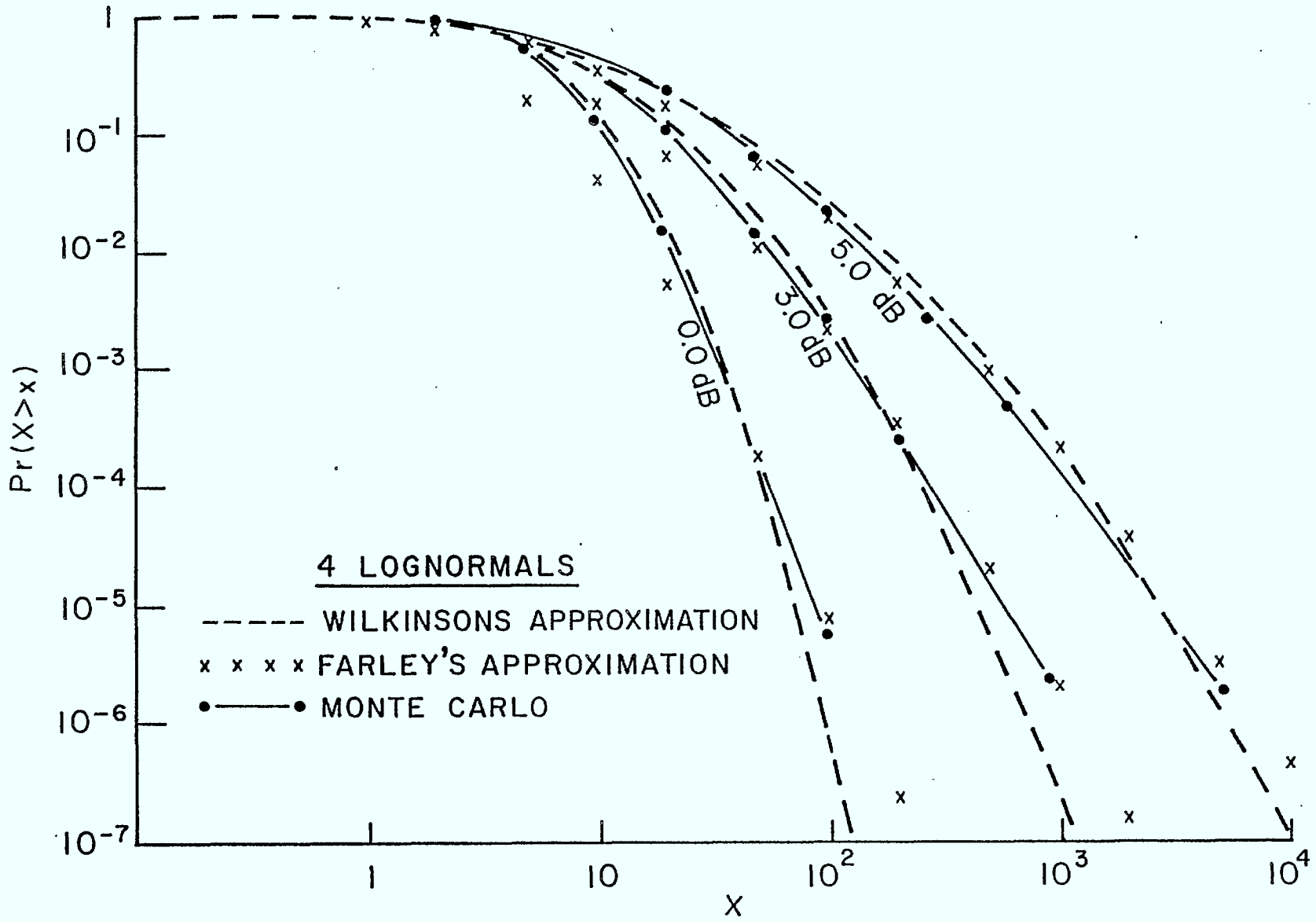

Figure 2.12 The probability distribution function, and two approximations, of the sum of four lognormal random variables

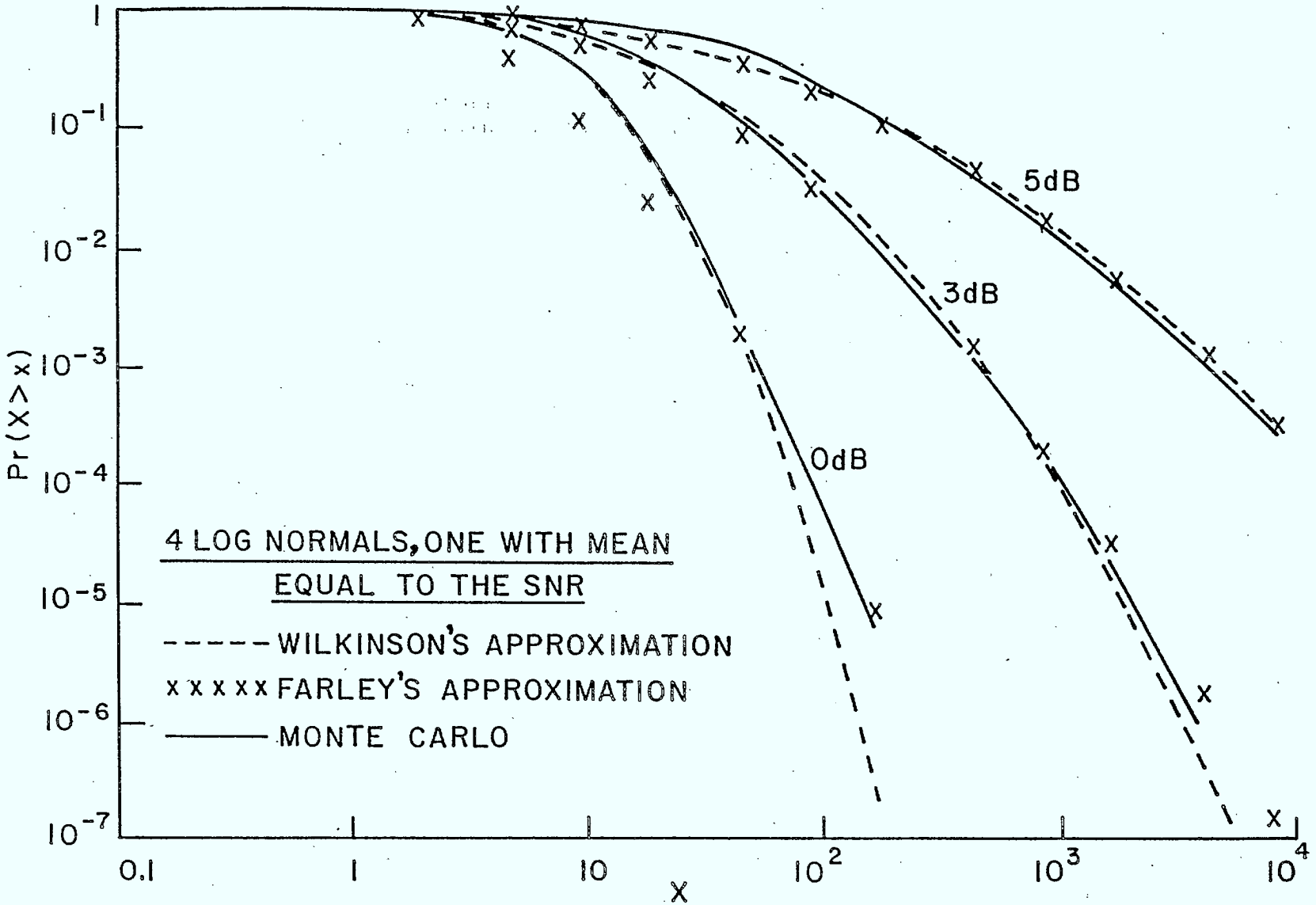

Figure 2.13 The probability distribution function, and two approximations, of the sum of four lognormal random variables, one with a nonzero mean

can be determined by applying (2.42) to (2.49).

According to [19], this approach is good only for variances of -4.5 dB or less. However, since the implementation was not difficult, it was decided to try the algorithm for 2 variables. The results, plotted against the known results in Figures 2.10 and 2.11, are excellent, particularly for probabilities greater than 10^{-3}, for which the approximation is very good. Strangely, the results show that the approximation is better for larger variances, contrary to that indicated by [19]. Two explanations exist. First, Schwartz and Yeh were measuring the degree of accuracy in finding the actual mean and variance of z as opposed to the accuracy in approximating the distribution function of L. Larger probabilities will be less sensitive to any error and so, inaccuracy in the mean and variance may not be significant for probabilities larger than a certain value, such as 10^{-3}. Second, computing facilities have improved in the six or seven years since [19] was written, making roundoff errors less severe. This last point manifested itself during the GQR tests. The roundoff errors, which [18] indicated would result in a very small positive number becoming negative, did not happen.

To see if the results held for a larger number of frequencies, Wilkinson's approach was tested for four variables. A simulation, the approach to which is discussed in Appendix C, was used to find the actual distribution function of the sum. As can be seen from Figures 2.12 and 2.13, the match is still very good for probabilities greater than 10^{-2} but is not as good as found for 2 random variables. At some points, the values are off by as much as much as a factor of 1.4. This is still an improvement over the results obtained with the GQR, however.

It is suggested [19] that to improve the approximation for lower probabilities, higher moments can be used, say the third and fourth moments. This was not attempted because of the results presented in the next section.

2.3.7 Farley's Approximation

The second approach mentioned in [19] and attributed to Farley, says that if the x_i's are independent, identically distributed random variables, then as $\sigma_x \to \infty$,

$$\Pr\left[\frac{1}{\sigma_x}(P_N - m_x) < \alpha\right] = [\Phi(\alpha)]^N \tag{2.55}$$

where $P_N = 10 \log_{10} L$, $L = \sum_{i=1}^{N} 10^{x_i/10}$ and $\Phi(x) = 1-Q(x)$. According to Schwartz and Yeh, this approach is valid for variances greater than -1.5 dB.

At a glance, this appears very similar to the expression found for the P_F of the maximum likelihood receiver given in (2.13). Noting that

$$\sigma_x = \frac{\sigma_z\ 10}{\ln 10} \qquad \text{and} \qquad m_x = \frac{m_z\ 10}{\ln 10} \tag{2.56}$$

the approximation can also be written as

$$\Pr\left[10 \log_{10} L - \frac{m_z\ 10}{\ln 10} < \frac{\sigma_z\ 10}{\ln 10}\alpha\right] = [\Phi(\alpha)]^N$$

which simplifies to

$$\Pr\left[L < 10^{(\alpha\sigma_z + m_z)/\ln 10}\right] = [1-Q(\alpha)]^N.$$

But $e^x = 10^{x/\ln 10}$. So

$$\Pr[L < \exp(\alpha\sigma_z + m_z)] = [1-Q(\alpha)]^N. \tag{2.57}$$

Finally,

$$\Pr[L > \exp(\alpha\sigma_z + m_z)] = 1 - [1-Q(\alpha)]^N. \tag{2.58}$$

Letting $\eta e^{d^2/2} = \exp(\alpha\sigma_z + m_z)$, $Q(\alpha) = Q\left[\dfrac{\ln \eta - m_z}{\sigma_z}\right]$.† But this is Q_F for the maximum likelihood receiver when $\sigma_z = d$ and $m_z = 0$. Therefore,

$$\Pr\,[L > \eta e^{d^2/2}] = P_F(\text{ALT}) \cong 1-(1-Q_F)^N = P_F(\text{MLT}).$$

In other words, Farley's approximation is identical to P_F for the maximum likelihood receiver.

From the data in the tables and Farley's approximation, it would appear the performance of the maximum likelihood receiver is a good approximation of the optimum receiver. The x's in Figures 2.10 - 2.13 indicate points using Farley's approximation. Even when the variables are not identically distributed, the maximum likelihood performance curve closely matches the distribution function of L, particularly in

† The threshold in 2.18 should have ηN replaced by η, the threshold for the ML case.

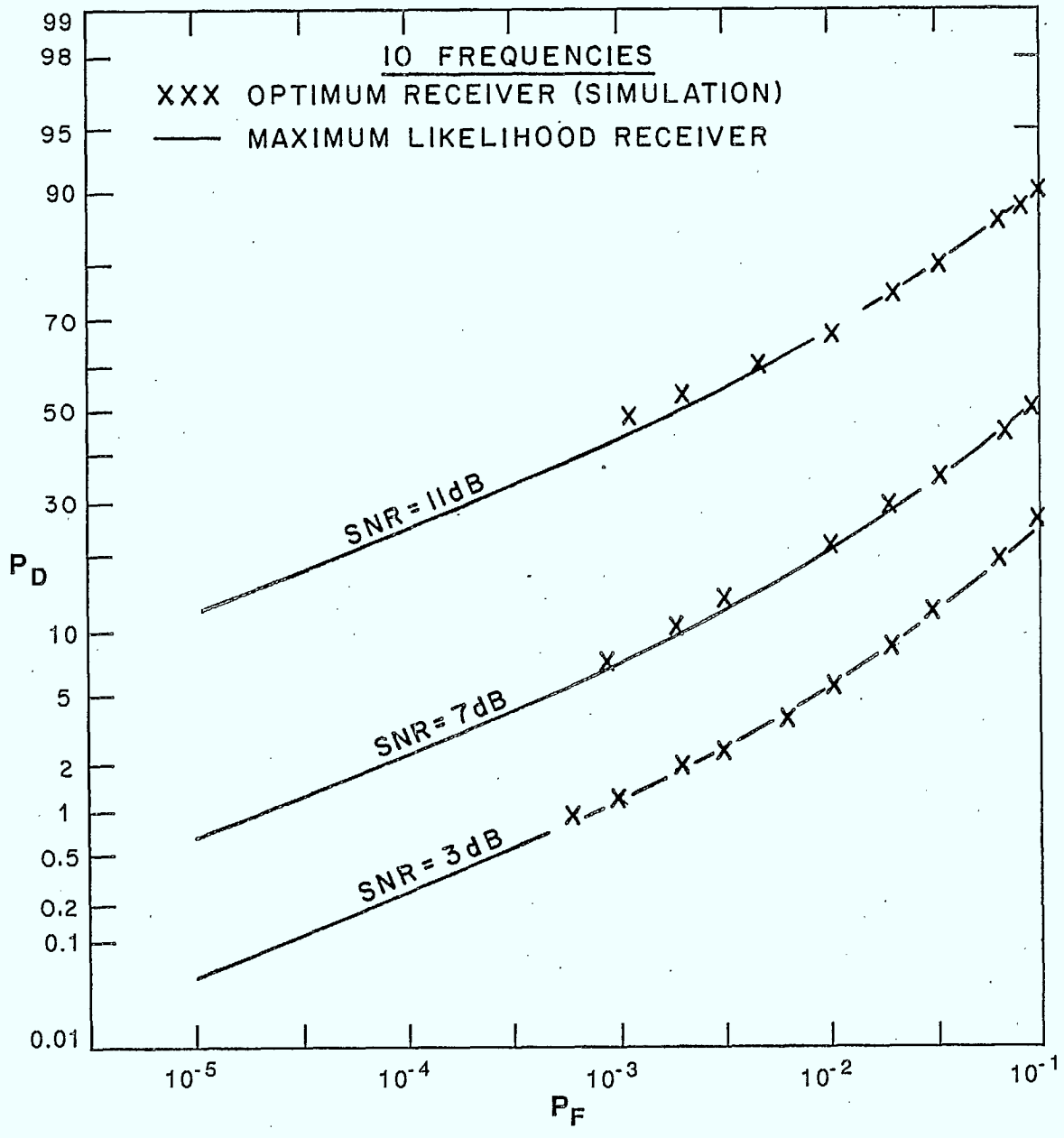

Figure 2.14 Performance curves of optimum and maximum likelihood receivers for ten frequencies

regions where Wilkinson's approach is weak.

2.3.8 Performance of the Optimum Receiver for Large N

The last three subsections each covered a different method of approximating the distribution function of a sum of lognormal random variables. While Wilkinson's approach gives the best approach when $Pr[L > \eta]$ is greater than 10^{-2}, the performance of the optimum receiver and the maximum likelihood receiver is very close when the probability of false alarm is less than 10^{-3}. It is interesting to note that where Farley's approximation is weak, which is for small variance and large probabilities, Wilkinson's approach gives a good approximation. And, when the approximation given by Wilkinson's approach is poor, which is for high SNR values and small probabilities, Farley's approximation is excellent. Simulation results of the optimum receiver for ten frequencies are compared to the exact results for the maximum likelihood receiver in Figure 2.14. These indicate that Farley's approximation improves as the number of frequencies increases. Therefore, it would appear that the performance of the maximum likelihood receiver approximates the optimum receiver performance very closely, at least in the range of SNR values considered here.

While it is surprising to find that the performance of the two receivers is almost identical, it was known that the maximum likelihood receiver is an approximate form of the optimum receiver. As explained in section 2.2, [16] also found the performance of the corresponding two receivers for coherent search radar to be similar. Not only does the performance of the maximum likelihood receiver give a good approximation

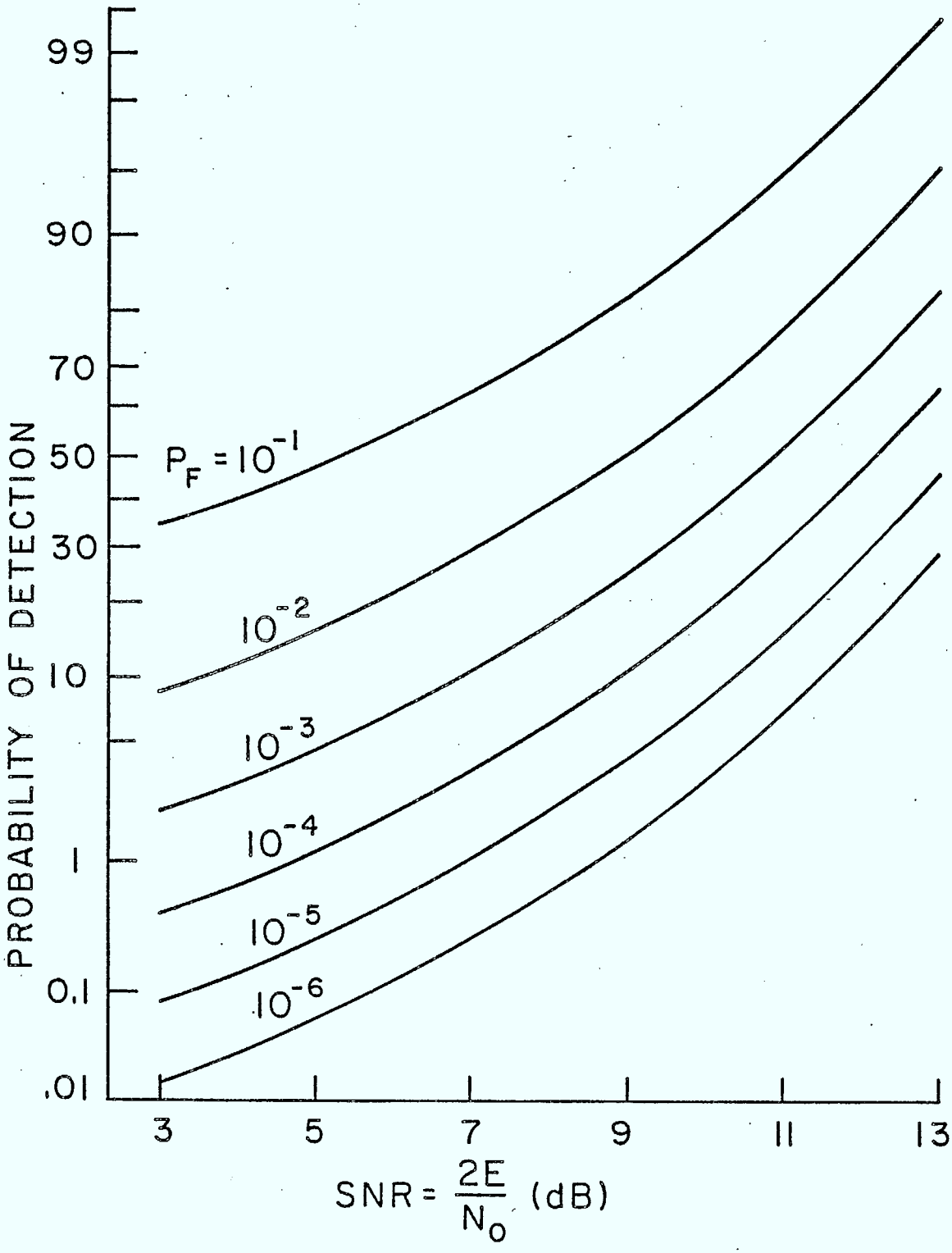

Figure 2.15 Coherent maximum likelihood receiver perfomance curves for four frequencies

of that of the optimum coherent receiver, but (2.13) and (2.15) are easy to evaluate for any number of frequencies. Performance curves for four frequencies are given in Figure 2.15. As can be seen from a comparison between Figures 2.4 and 2.15, the drop in performance between two and four frequencies is less than that between one and two frequencies, though it is nearly equivalent. In Chapter 3, more results for a large number of frequencies are presented when the performance of coherent receivers is compared to that of noncoherent receivers.

2.4 DISCUSSION OF RESULTS

In this chapter, a detailed performance analysis was conducted for the optimum coherent interception receiver. In addition, a second receiver, the maximum likelihood receiver, was analyzed for any number of frequencies.

Attempts to evaluate the performance of the optimum receiver for an arbitrary number of frequencies were discussed. It was shown that the sufficient statistic for the optimum receiver is a sum of lognormal variables and that its distribution function could not be accurately approximated by the Gauss Quadrature Rule. However, for probabilities greater than 10^{-2}, the sufficient statistic can be approximated by a lognormal variable, leading to a trivial solution for the performance. For smaller probabilities, the performance of the maximum likelihood receiver gave an excellent approximation of that for the optimum receiver.

Performance plots for one, two and four frequencies were included, along with a discussion of how to obtain plots for a larger number of

frequencies. While a loss in performance is noted as the number of frequencies increases, the drop is less between two and four frequencies than between one and two frequencies. If this trend continues, some interesting conclusions can be drawn about the benefits of using additional frequencies, from the transmitter's viewpoint. This point is considered in the next chapter.

Results indicate that to have a better than 50% chance of detecting a sinusoid that can take on one of two frequencies when P_F is fixed at 10^{-3}, the SNR must be greater than 10.3 dB. It increases to 10.8 dB for four frequencies. Therefore, for SNR less than 10 dB, the probability of detecting the random frequency sinusoid is less than 0.5, and is less than 0.1 for SNR = 3 dB.

CHAPTER 3

NONCOHERENT DETECTION

3.1 INTRODUCTION

In the last chapter, coherent receivers for signals with a discrete frequency distribution were discussed. However, unless the signal is changing frequency very slowly, it is unrealistic to expect coherent detection to be feasible. The results presented in the last chapter, therefore, are absolute upper bounds to performance.

This chapter examines noncoherent detection methods for these signals, under the assumptions discussed in Chapter 1. Paralleling Chapter 2, the noncoherent version of the maximum likelihood receiver will be developed in the next section, and in section 3.3, the optimum receiver will be derived from the likelihood ratio test. Performance analysis for the latter is very difficult, however. Therefore, conclusions drawn in the last chapter will be used to find a good approximation of the optimum performance.

A third receiver, found by approximating the sufficient statistic of the optimum receiver, gives good performance at low SNR, and is discussed in section 3.4. The chapter concludes with a discussion of the results presented in this chapter, and a comparison of coherent and noncoherent detection methods.

3.2 MAXIMUM LIKELIHOOD RECEIVER

3.2.1 Receiver Description

The noncoherent maximum likelihood receiver, like the coherent version discussed in section 2.2, uses a bank of N detectors. Each detector is matched to the bandwidth and duration of the transmitted signal and there is an optimum detector for each one of the possible signals. Depending on the exact form of the receiver, the maximum output of the N detectors may be used to make the decision, or each of the N outputs will be fed into a separate decision device. In the latter case, if any one of the decision devices declares a signal present, the receiver will conclude the same.

The performance of this receiver is still given by (2.13) and (2.15) except that Q_D and Q_F are no longer given by (2.11) and (2.12). The latter is obvious since the optimum noncoherent detector and the optimum coherent detector are not the same.

3.2.2 Optimum Noncoherent Detector of a Sinusoidal Signal

The noncoherent detector of a sinusoid is well known and is discussed, for example, in [17] and [23]. The derivation of this detector will be presented here for the sake of convenience and in order to present it in a style consistent with that used in the rest of this report.

This detector must decide between one of the following two hypotheses:

$$H_1: r(t) = A \cos(\omega t + \theta) + n(t) \qquad 0 \le t \le T$$
$$H_0: r(t) = n(t) \qquad 0 \le t \le T \tag{3.1}$$

where n(t) is AWGN with zero mean and spectral height equal to $\frac{N_0}{2}$ W/Hz, r(t) is the received signal, and θ is uniform over $[0,2\pi]$.

Following the procedure laid out in Chapter 2, the sufficient statistic for this detector will be derived from the likelihood ratio test. In this case, the unwanted parameter is the phase.

Since H_0 is the same in both (2.1) and (3.1), $p_r(\underline{R}|H_0)$ is still given by (2.5). It is repeated here for convenience.

$$p_r(\underline{R}|H_0) = \frac{1}{\pi N_o} \exp\left[-\frac{{}_0\int^T r^2(t)\,dt}{N_o}\right]. \tag{3.2}$$

As in (2.3),

$$p_r(\underline{R}|H_1,\theta) = p_n(\underline{R}-\underline{S}).$$

For this case, $s(t) = A\cos(\omega t+\theta)$ and so, when the expression is simplified,

$$p_r(\underline{R}|H_1,\theta) = \frac{1}{\pi N_o} \exp\left[\frac{{}_0\int^T r^2(t)\,dt - 2A\,{}_0\int^T r(t)\cos(\omega t+\theta)\,dt + E}{(-N_0)}\right] \tag{3.3}$$

where $E = {}_0\int^T s^2(t)\,dt$ is the signal energy. Finally, averaging

$p_r(\underline{R}|H_1,\theta)$ over θ gives

$$p_r(\underline{R}|H_1) = \frac{1}{\pi N_o}\int_0^{2\pi}\frac{1}{2\pi}\exp\left[\frac{{}_0\int^T r^2(t)\,dt - 2A\,{}_0\int^T r(t)\cos(\omega t+\theta)\,dt + E}{(-N_0)}\right]d\theta. \tag{3.4}$$

The likelihood ratio test, found by taking the ratio of the received signal probability density functions conditioned on each hypothesis, as in (2.6), gives

$$L(r) = e^{-d^2/2}\int_0^{2\pi}\frac{1}{2\pi}\exp\left[\frac{2A}{N_0}\,{}_0\int^T r(t)\cos(\omega t+\theta)\,dt\right]d\theta \underset{H_0}{\overset{H_1}{\gtrless}} \eta \tag{3.5}$$

where $d = (2E/N_0)^{1/2}$ and η is the decision threshold. The sufficient statistic, ℓ, is obtained by first defining

$$\begin{aligned} L_c &= \frac{2A}{N_0}\,{}_0\int^T r(t)\cos\omega t\,dt = q\cos\phi, \\ L_s &= \frac{2A}{N_0}\,{}_0\int^T r(t)\sin\omega t\,dt = q\sin\phi. \end{aligned} \tag{3.6}$$

Thus, (3.5) can be alternatively written as, after some manipulation of trignometric identities,

$$L(r) = I_0(q) \underset{H_0}{\overset{H_1}{\gtrless}} \eta e^{d^2/2} \tag{3.7}$$

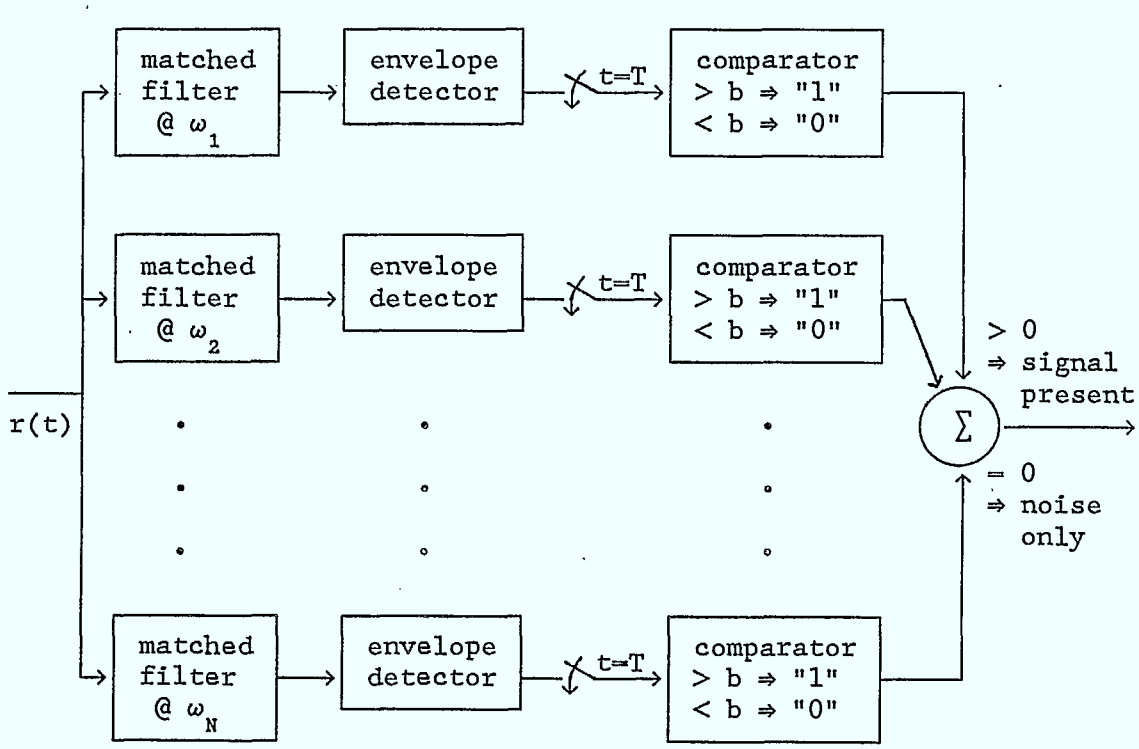

Figure 3.1: Noncoherent maximum likelihood receiver

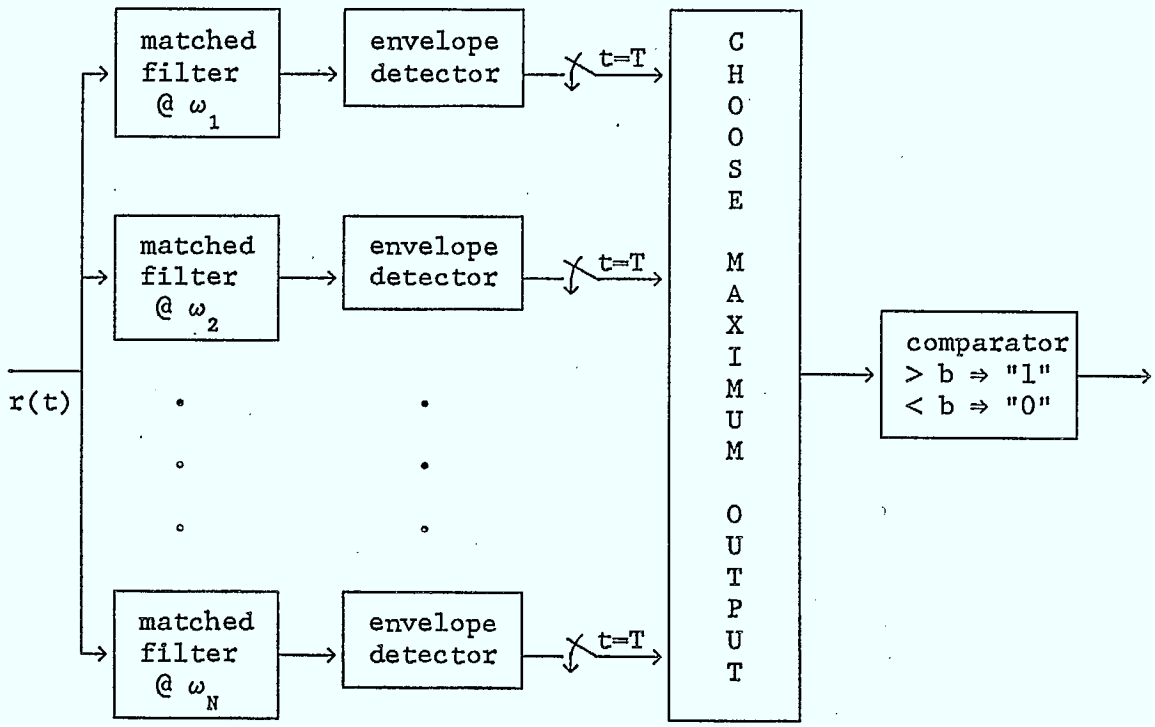

Figure 3.2: Alternate form of the noncoherent maximum likelihood receiver

where $I_0(x)$ is the zero-order modified Bessel function of the first kind, and is defined as

$$I_0(x) = \int_0^{2\pi} \frac{1}{2\pi} e^{x \cos \theta} \, d\theta. \tag{3.8}$$

From (3.7), the sufficient statistic is found to be

$$\ell = q \underset{H_0}{\overset{H_1}{\gtrless}} \gamma = I_0^{-1}(\eta e^{d^2/2}). \tag{3.9}$$

A detailed discussion of how the detector used in the maximum likelihood receiver, shown in Figure 3.1 and an alternate form in Figure 3.2, calculates the sufficient statistic is given in [17]. Note that in these figures, $b = \frac{N_0}{2A} I_o^{-1}(\eta e^{d^2/2})$. If instead the sufficient statistic had been defined as the square of q, then the detector would be the well known quadrature receiver [23], which, therefore, is an equivalent form of the optimum detector.

3.2.3 Detector Performance

There are several methods of evaluation for this detector, two of which are discussed in [17] and [23]. The derivation used here will differ from those in [17,23] by taking advantage of known relationships between random variables.

To derive the performance of the detector, the probability density

function of q must first be found. Note that L_c and L_s are independent, normal random variables and, under H_0, they both have a mean of zero and variance equal to d^2. Now, from (3.6), it is obvious that

$$q = (L_c^2 + L_s^2)^{1/2}. \tag{3.10}$$

This relationship is known to produce a Rayleigh random variable. Therefore, the probability of false alarm for this detector is

$$\begin{aligned} Q_F &= \int_\gamma^\infty p_q(q)\, dq \\ &= \int_\gamma^\infty \frac{q}{d^2} \exp\left[-\frac{q^2}{2d^2}\right] dq. \end{aligned} \tag{3.11}$$

Finally, solving (3.11) gives

$$Q_F = \exp\left[-\frac{\gamma^2}{2d^2}\right]. \tag{3.12}$$

This can be rewritten to define the new threshold, γ, in terms of Q_F. That is,

$$\gamma^2 = -2d^2 \ln Q_F. \tag{3.13}$$

Therefore, it should also be possible to define the probability of detection as a function of Q_F.

To find Q_D, it is necessary to realize that, while L_c and L_s are still normal random variables with a variance of d^2, they no longer have

means equal to zero. The mean of L_c, under H_1, is

$$E(L_c|H_1) = E\left[\frac{2A}{N_0}\left[{}_0\int^T A\cos(\omega t+\theta)\cos\omega t\,dt + {}_0\int^T A\,n(t)\cos\omega t\,dt\right]\right]$$

$$= \frac{2A^2}{N_0}\,{}_0\int^T(\cos^2\omega t\cos\theta - \sin\omega t\cos\omega t\sin\theta)\,dt$$

$$= \frac{A^2T}{N_0}\cos\theta = d^2\cos\theta \qquad (3.14)$$

since $d^2 = \frac{2E}{N_0} = \frac{A^2T}{N_0}$. Similarly, the mean of L_s can be shown to equal $d^2\sin\theta$.

The relationship between q, L_c and L_s [3.10] is the same no matter which hypothesis is true. However, since L_c and L_s no longer have means equal to zero, q is now Ricean. Therefore,

$$p_q(q) = \frac{q}{d^2}\exp\left[-\frac{q^2+d^4}{2d^2}\right] I_0(q) \qquad (3.15)$$

and finally,

$$Q_D = {}_\gamma\int^\infty p_q(q)\,dq$$

$$= \int_\gamma^\infty \frac{q}{d^2}\exp\left[-\frac{q^2+d^4}{2d^2}\right] I_0(q)\,dq \qquad (3.16)$$

$$= Q(d,\tfrac{\gamma}{d})$$

$$= Q(d,(-2\ln Q_F)^{1/2}) \qquad (3.17)$$

where Q(a,b) is the Marcum Q-function which is defined as

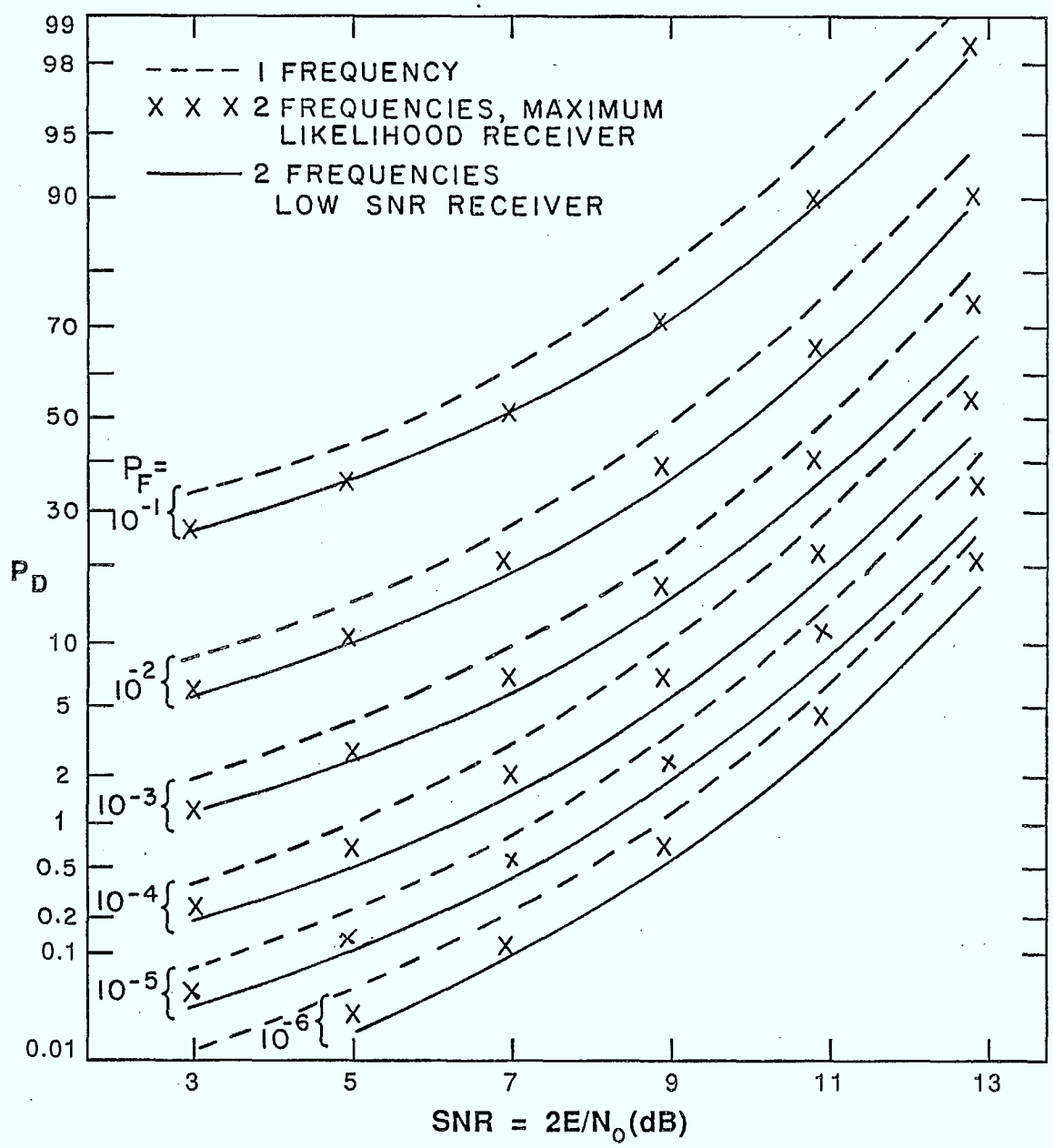

Figure 3.3 Performance curves for noncoherent receivers with one and two frequencies

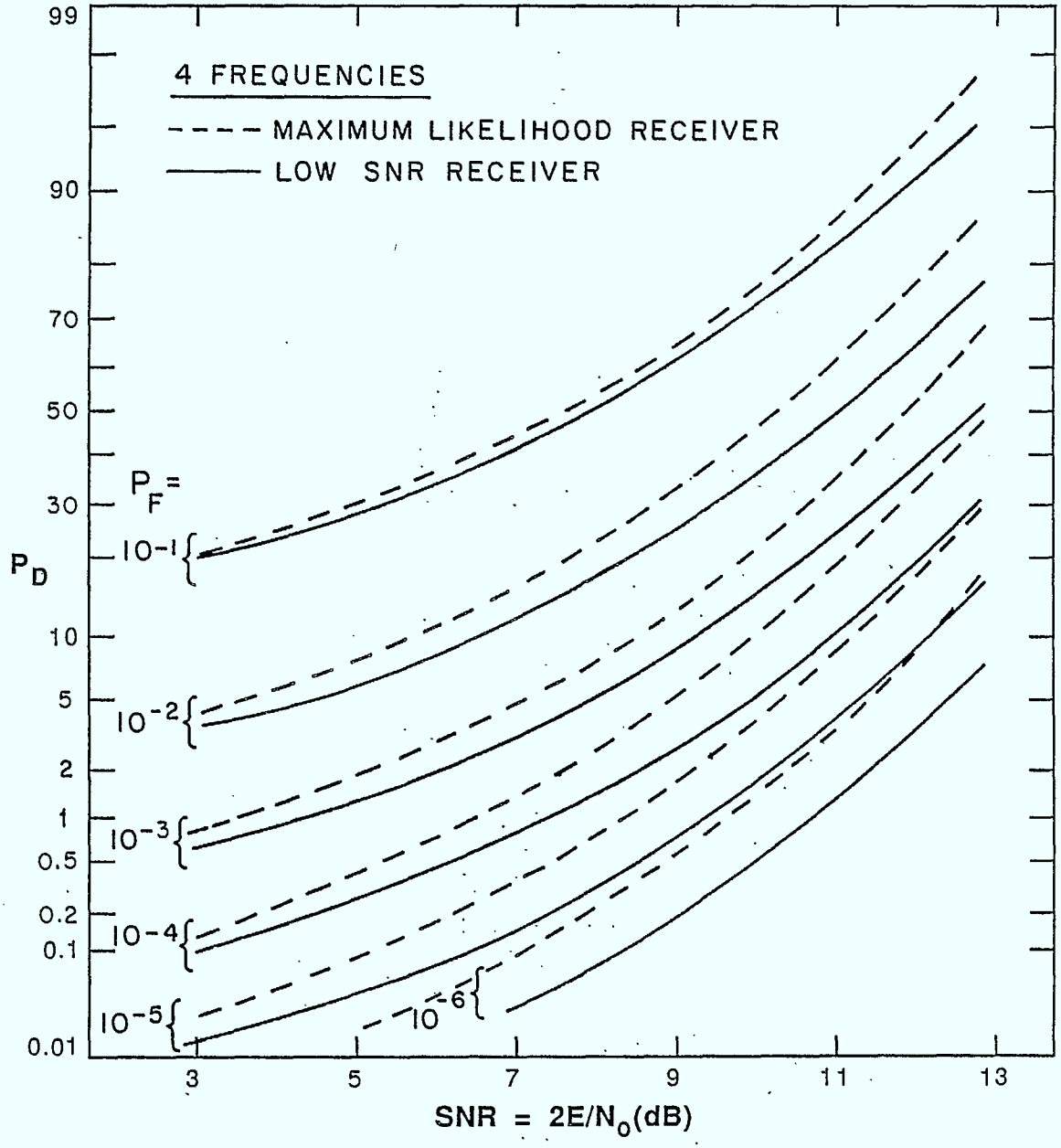

Figure 3.4 Performance curves for noncoherent receivers with four frequencies

$$Q(a,b) = \int_b^\infty x \exp\left[-\frac{x^2 + a^2}{2}\right] I_0(ax)\, dx \qquad (3.17a)$$

which is well documented in [24].

3.2.4 Maximum Likelihood Receiver Performance

The expressions for Q_D and Q_F, (3.17) and (3.12), respectively, are used in (2.13) and (2.15) to find the performance of the maximum likelihood receiver, which is shown in Figures 3.3 and 3.4 for one, two and four frequencies. Figures 3.10 and 3.11, at the end of this chapter, also plot P_D for $P_F = 10^{-2}$ and $P_F = 10^{-4}$, when the transmitter is known to use ten or twenty frequencies. The results for ten and twenty frequencies will be discussed in the chapter conclusion.

Looking at Figures 3.3 and 3.4, the loss between one and two frequencies ranges from 1.5 dB down to .5 dB as the SNR varies from 3 dB to 11 dB, when $P_F = 0.1$. The loss is smaller for smaller values of P_F. The loss between two and four frequencies is marginally less than that between one and two frequencies. To give some typical values of P_D, for two frequencies and $P_F = 10^{-3}$, when the SNR is 3 dB, $P_D = 1.2 \times 10^{-2}$, and when the SNR is 13 dB, $P_D = 0.75$. There is, obviously, a large loss in performance, on the order of 98%, when the SNR decreases from 13 dB to 3 dB.

If the signal is being intercepted, and the transmitter is aware of this, the SNR will normally be quite low, on the order of 3 dB or less. Therefore, P_D will normally be low, greater than P_F by approximately a factor of ten only.

3.3 OPTIMUM RECEIVER

3.3.1 Likelihood Ratio Test

Whalen [23] discusses the optimum noncoherent receiver for a sinusoid that has a discrete frequency distribution, the case under study in this thesis. It should be noted that he only examined the noncoherent version. His result is rederived here, following the approach used in Chapter 2. As before, the likelihood ratio must be determined to find the sufficient statistic, and $p_r(\underline{R}|H_0)$ is unchanged from the previous section.

$p_r(\underline{R}|H_1)$, however, is now dependent on two unwanted parameters, phase and frequency. Since the two parameters are independent, and the phase is uniform between 0 and 2π,

$$p_r(\underline{R}|H_1) = \frac{1}{2\pi} \int_{\omega_{min}}^{\omega_{max}} \int_0^{2\pi} p_\omega(\omega)\ p_r(\underline{R}|H_1,\omega,\theta)\ d\theta\ d\omega. \tag{3.18}$$

From the assumptions given in Chapter 1, it is known that

$$p_\omega(\omega) = \frac{1}{N} \sum_{i=1}^{N} \delta(\omega - \omega_i) \tag{3.19}$$

where $\delta(x)$ is the Dirac delta function and the ω_i's are spaced $\frac{1}{T}$ Hz apart, T being the signal duration. Substituting (3.19) into (3.18) gives

$$p_r(\underline{R}|H_1) = \frac{1}{N} \sum_{i=1}^{N} \frac{1}{2\pi} \int_0^{2\pi} p_r(\underline{R}(\omega_i)|H_1,\theta)\ d\theta.$$

But $p_r(\underline{R}(\omega_i)|H_1,\theta)$ is $p_r(\underline{R}|H_1,\theta)$, given in (3.4), with ω replaced by ω_i. This implies that

$$p_r(\underline{R}|H_1) = \frac{1}{2N\pi^2 N_o} \tag{3.20}$$

$$X \sum_{i=1}^{N} \int_0^{2\pi} \exp\left[\frac{{}_0\int^T r^2(t)\,dt - 2A_0\int^T r(t)\cos(\omega_i t+\theta)\,dt + E}{(-N_0)}\right] d\theta.$$

Again, the likelihood ratio is found by taking the ratio of the received signal probability density functions under each hypothesis. In this case, after some simplification, the likelihood ratio becomes

$$L(r) = \frac{e^{d^2/2}}{N} \sum_{i=1}^{N} \int_0^{2\pi} \frac{1}{2\pi} \exp\left[\frac{2A}{N_0}\,{}_0\int^T r(t)\cos(\omega_i t+\theta)\,dt\right] d\theta. \tag{3.21}$$

Following an identical approach to that used in section 3.2, define

$$\begin{aligned} L_{ci} &= \frac{2A}{N_0}\,{}_0\int^T r(t)\cos\omega_i t\,dt = q_i\cos\phi, \\ L_{si} &= \frac{2A}{N_0}\,{}_0\int^T r(t)\sin\omega_i t\,dt = q_i\sin\phi. \end{aligned} \tag{3.22}$$

Therefore, the likelihood ratio test simplifies to

$$L(r) = \sum_{i=1}^{N} \frac{e^{-d^2/2}}{N} I_0(q_i) \underset{H_0}{\overset{H_1}{\gtrless}} \eta \tag{3.23}$$

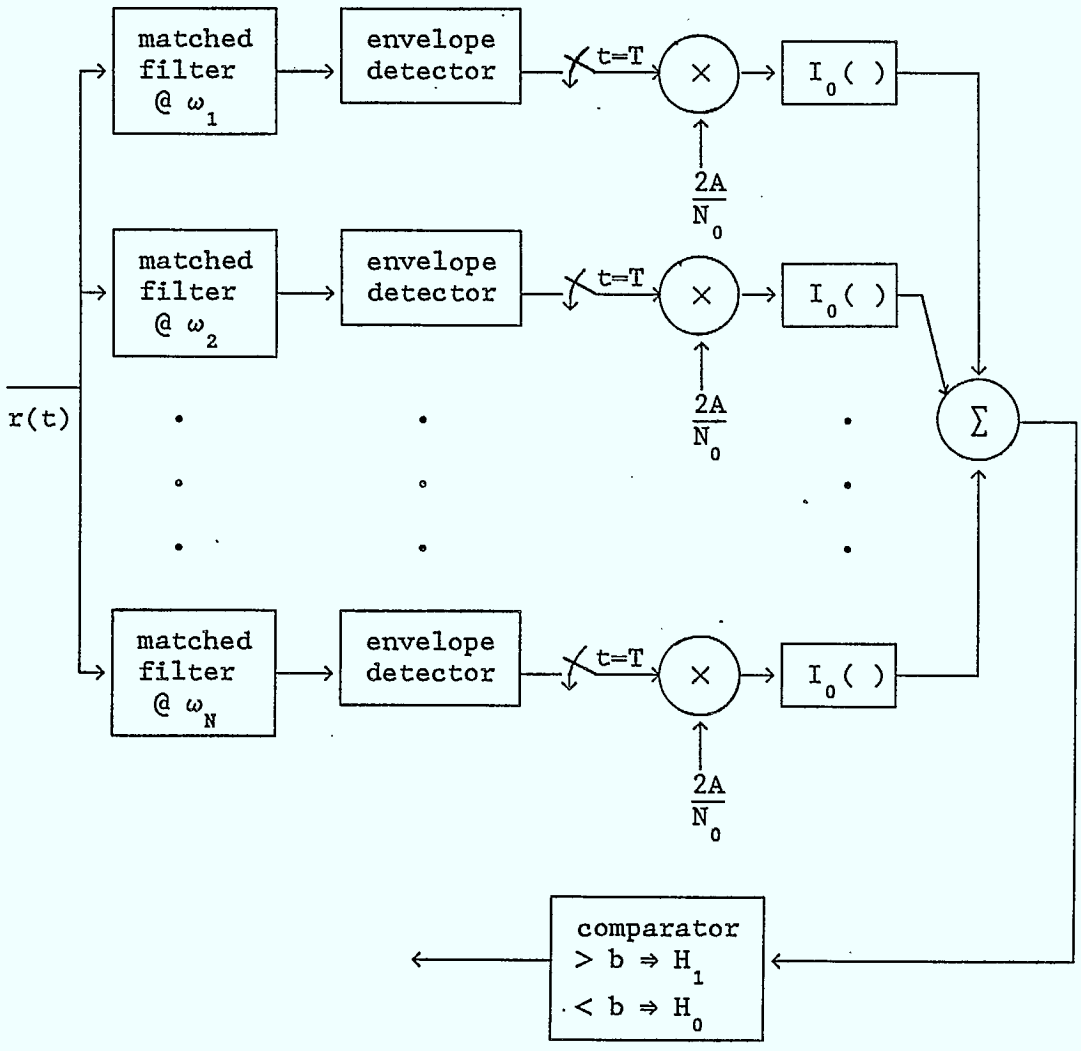

Figure 3.5: Optimum noncoherent receiver

Modifying the test slightly gives the sufficient statistic,

$$\ell = \sum_{i=1}^{N} I_0(q_i) \underset{H_0}{\overset{H_1}{>}} \eta N e^{d^2/2}. \tag{3.24}$$

The noncoherent receiver uses a bank of N detectors, shown in Figure 3.5, identical to those derived for the maximum likelihood receiver. Now, however, each sampler is followed by a multipler, which multiplies the sampler output by $\frac{2A}{N_0}$ to give q_i. The zero-order modified Bessel function of the first kind is then calculated for each output, and the results are summed. Finally, the sum is compared to the threshold, $b = \eta N e^{d^2/2}$, and the receiver decides that a signal has been received only if this sum is larger than the threshold.

3.3.2 Performance Analysis

To find the exact performance of this receiver is difficult since the sufficient statistic is the sum of modified zero-order Bessel functions with Rayleigh or Ricean arguments, and an exact solution could not be found in the same manner as the coherent version. Therefore, a good approximation of the performance was deemed necessary. In Chapter 2, it was shown that the optimum coherent receiver was close in performance to the maximum likelihood receiver. Therefore, if the same conclusion could also be drawn for noncoherent receivers, the performance of the optimum receiver would be adequately approximated. It should be noted that [23] describes the maximum likelihood receiver

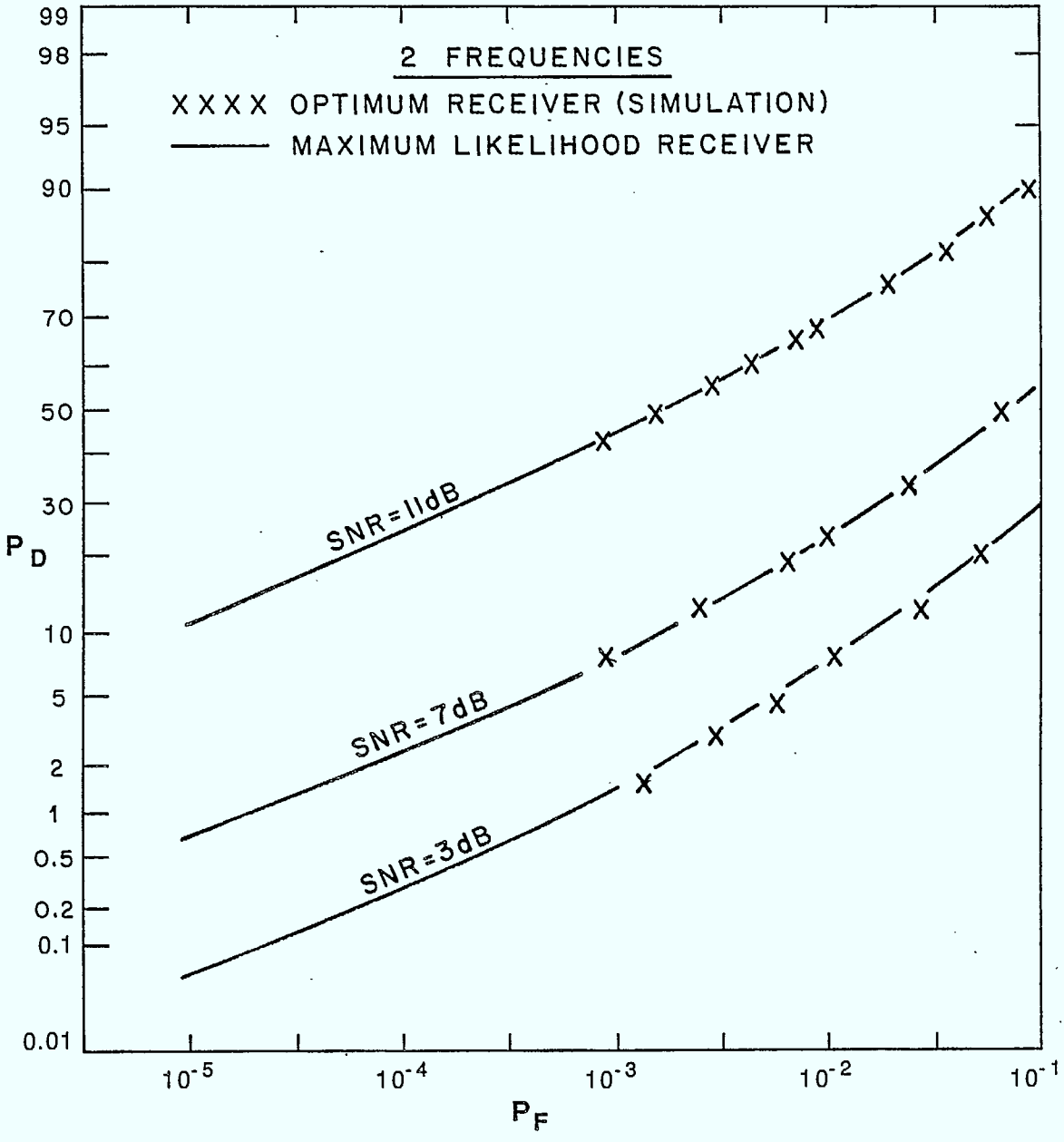

Figure 3.6 Comparison of optimum and maximum likelihood receiver performance for two frequencies

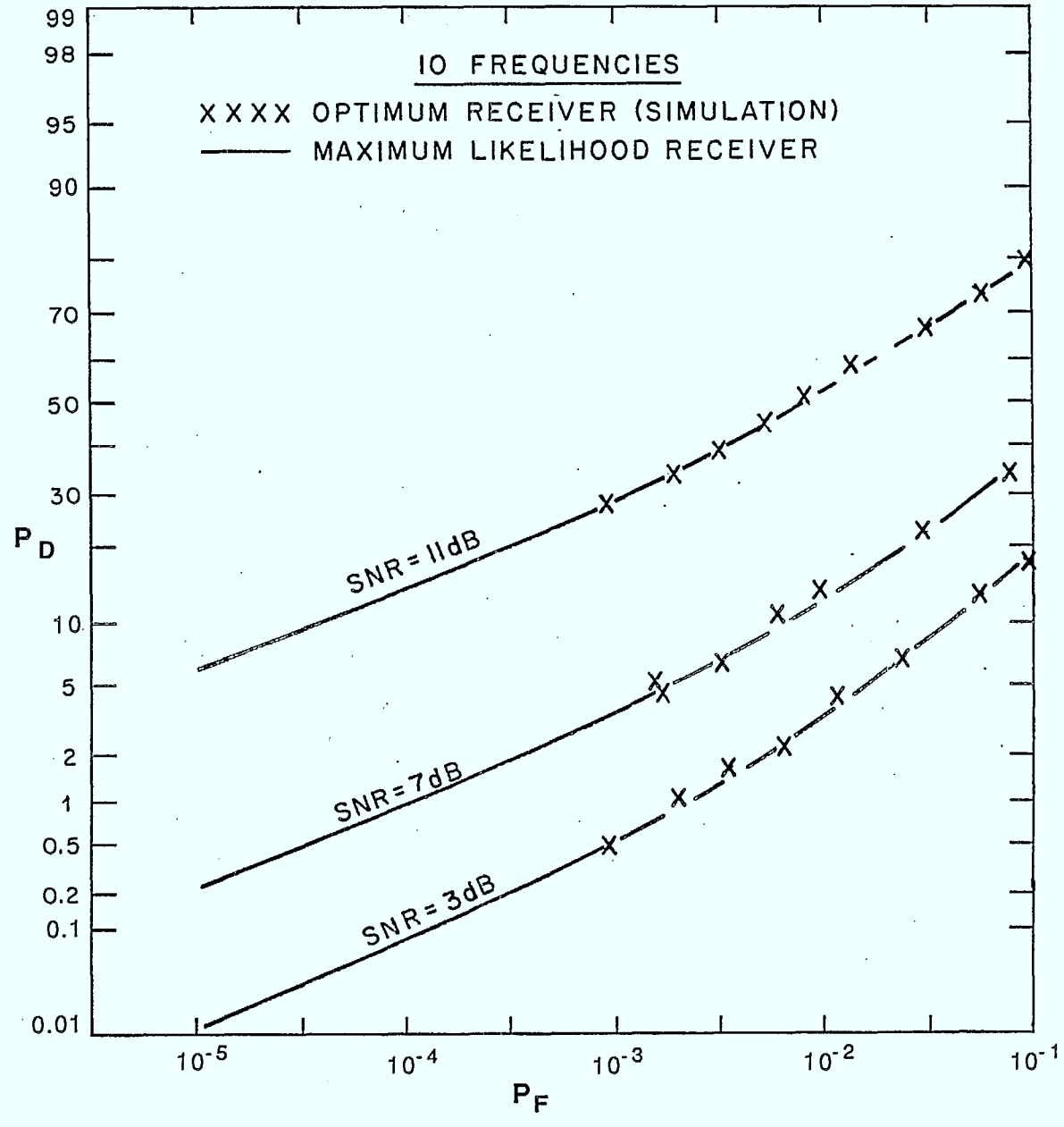

Figure 3.7 Comparison of optimum and maximum likelihood receiver performance for ten frequencies

as an approximate form of the optimum receiver for this case. The author argues that as the threshold increases, the decision region of the optimum receiver for two frequencies is nearly square and that this result can be extended to N frequencies. Thus, the receiver can be approximated by the maximum likelihood receiver.

Without a method to find the exact performance of the optimum receiver it was necessary to simulate the receiver's performance to determine the effectiveness of the approximation. Details on the simulation are given in Appendix C. Simulations for only two frequencies, plotted in Figure 3.6, show that the performance of the two receivers is very close, at least for probabilities of false alarm greater than 10^{-3}. However, of far more interest is the performance of the receivers for a larger number of frequencies. Therefore, simulations were also run for ten frequencies, and the results are plotted in Figure 3.7. Once again, the simulation results match the maximum likelihood receiver performance. Therefore, the maximum likelihood receiver performance offers an excellent approximation of the performance bounds for noncoherent detection methods as well.

3.4 LOW SNR RECEIVER

3.4.1 Derivation of the Receiver

In the last section, only the maximum likelihood receiver was considered as an approximation of the optimum receiver. However, there are two well known approximations to the modified Bessel function that may give two other receivers that are near optimum in performance.

If the SNR is large, q will also be large. Now, a known approximation for $I_0(x)$, when x is large, is

$$I_0(x) \approx \frac{e^x}{(2\pi x)^{1/2}}.$$

There are two reasons that the corresponding receiver will not be examined in this thesis. First, the goal of this thesis is to develop results that are to be extended to the problem of intercepting spread spectrum signals. Therefore, the SNR will usually not be large enough for this large SNR receiver to give near optimum performance. Second, the analysis of this receiver is extremely difficult and would require further approximations or simulations. Since the focus of this thesis is to develop optimum performance bounds, it is felt that further study of this receiver would not aid this goal.

Looking at a second approximation to the modified Bessel function, when the SNR is small, q will also be small. Since for small x, $I_0(x) \approx 1 + (x^2/4)$, the sufficient statistic for the optimum receiver can be rewritten as

$$\ell \approx \sum_{i=1}^{N} \left[1 + \frac{q_i^2}{4} \right] \underset{H_0}{\overset{H_1}{\gtrless}} \eta N e^{d^2/2} \tag{3.25}$$

as discussed in [23]. Therefore, the new sufficient statistic for a receiver that should give the best approximation of optimum performance at low SNR, is

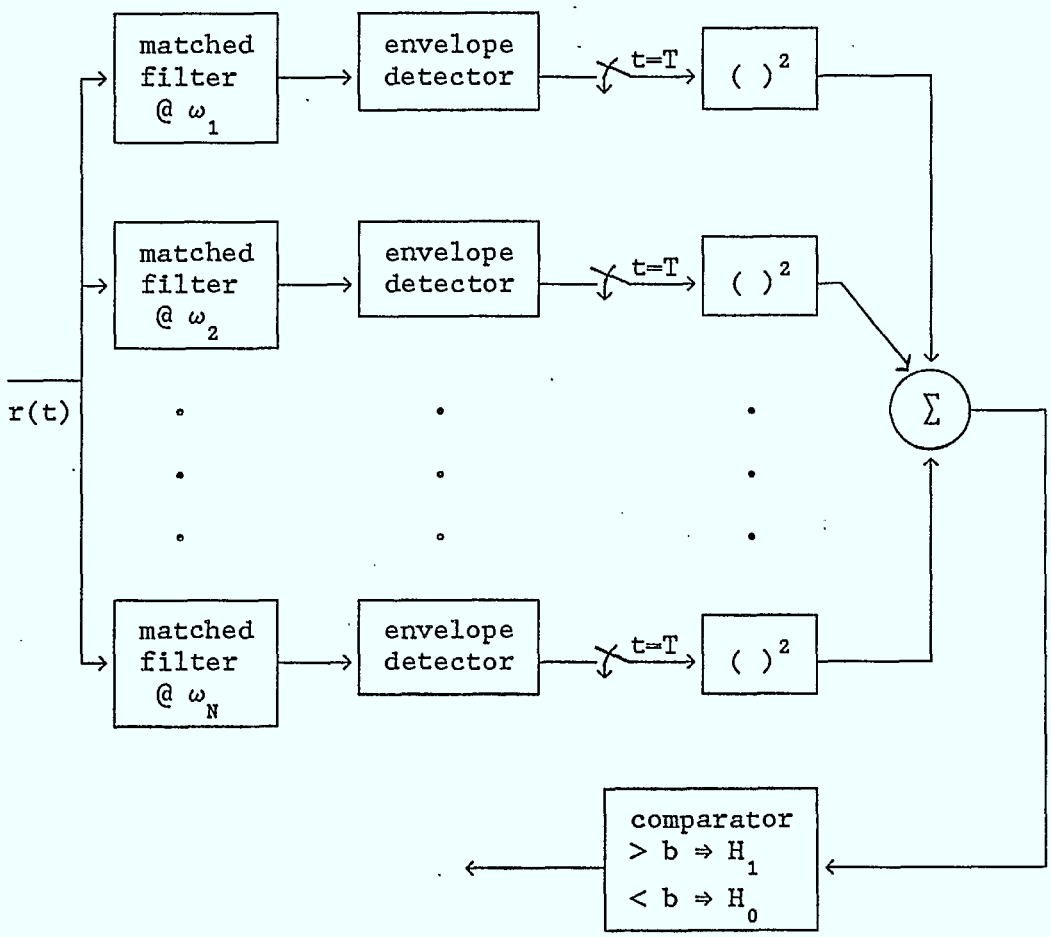

Figure 3.8: Low SNR receiver

$$\mathcal{L} = \sum_{i=1}^{N} q_i^2 \underset{H_0}{\overset{H_1}{>}} 4\eta N e^{d^2/2} - 4N \tag{3.26}$$

This low SNR receiver is a bank of N noncoherent detectors, as described in section 3.2.2, followed by a square law device. Note that the detectors and the square law device could be replaced by the equivalent quadrature receiver. The outputs of the square law devices are summed, as shown in Figure 3.8, and compared to a threshold, $b = \frac{N_0^2}{A^2}(\eta N e^{d^2/2} - N)$. If larger, the receiver will conclude that a signal has been received. Otherwise, the conclusion is that there is only noise present.

3.4.2 Performance Analysis

The derivation of the performance of the low SNR receiver, given in this section, follows an approach outlined in problem 4.5.12 of [17,p.412]. An alternate solution is given in [23].

Under H_0, as shown in section 3.2, q_i is a Rayleigh random variable, the square of which is an exponential random variable. Therefore, the probability density function of the sufficient statistic is the convolution of N exponential probability density functions.

Denote $\mathcal{L}_i = q_i^2$. Now, the easiest method of finding $p_{\mathcal{L}}(\mathcal{L}|H_0)$ is to first find its characteristic function. The characteristic function of an exponential random variable is

$$\Psi_{\mathcal{L}_i}(v) = (1 - jv2d^2)^{-1}. \tag{3.27}$$

Since the characteristic function of a random variable is the Fourier transform of its probability density function, and convolution in one domain is multiplication in the other, the characteristic function of $\mathcal{L}$ is the product of the characteristic functions of the $\mathcal{L}_i$'s. More simply,

$$\Psi_{\mathcal{L}}(v) = \prod_{i=1}^{N} \Psi_{\mathcal{L}_i}(v)$$
$$= (1-jv2d^2)^{-N}. \qquad (3.28)$$

Taking the inverse transform gives [25]

$$p_{\mathcal{L}}(\mathcal{L}|H_0) = \frac{\mathcal{L}^{N-1} e^{-\mathcal{L}/2d^2}}{(2d^2)^N (N-1)!} \qquad \mathcal{L} \geq 0 \qquad (3.29)$$

which is a central chi-square distribution with 2N degrees of freedom.

The probability of false alarm is still the probability that the sufficient statistic exceeds the threshold when noise only is present. That is,

$$P_F = \int_b^{\infty} p_{\mathcal{L}}(\mathcal{L}|H_0)\, d\mathcal{L}$$
$$= \int_b^{\infty} \frac{\mathcal{L}^{N-1} e^{-\mathcal{L}/2d^2}}{(2d^2)^N (N-1)!}\, d\mathcal{L}$$
$$= \exp\left[-\frac{b}{2d^2}\right] \sum_{k=0}^{N-1} \frac{1}{k!} \left[\frac{b}{2d^2}\right]^k \qquad (3.30)$$

where $b = 4N(\eta e^{d^2/2} - 1)$.

Next, P_D is derived. Under H_1, N-1 of the q_i's are Rayleigh random variables. However, for one value of i, the corresponding L_{ci} and L_{si} have means of $d^2\cos\theta$ and $d^2\sin\theta$, respectively, as in section 3.2. Thus, this q_i has a Ricean distribution. Defining this variable as q_1, it can be shown, by application of transformation theory, that $\mathcal{L}_1$ has a non-central chi-square distribution of degree 2 with noncentrality parameter, d^4. This implies that

$$p_{\mathcal{L}_1}(\mathcal{L}_1|H_1) = \frac{1}{2d^2} \exp\left[-\frac{\mathcal{L}_1 + d^4}{2d^2}\right] I_0(\mathcal{L}^{1/2}) \qquad \mathcal{L} \geq 0. \tag{3.31}$$

The easiest approach to finding $p_{\mathcal{L}}(\mathcal{L}|H_1)$ is, again, by finding the characteristic function of $\mathcal{L}$ and taking the inverse Fourier transform. The characteristic function of $\mathcal{L}_1$, the Fourier transform of (3.31), is

$$\Psi_{\mathcal{L}_1}(v) = (1-jv2d^2)^{-1} \exp\left[\frac{jvd^4}{1-jv2d^2}\right]. \tag{3.32}$$

The characteristic functions of the other variables are still given by (3.27). Therefore, the characteristic function of $\mathcal{L}$ is

$$\begin{aligned}\Psi_{\mathcal{L}}(v) &= \prod_{i=1}^{N} \Psi_{\mathcal{L}_i}(v) \\ &= (1-jv2d^2)^{-N} \exp\left[\frac{jvd^4}{1-jv2d^2}\right].\end{aligned} \tag{3.33}$$

Finally, taking the inverse transform [25] gives

$$p_{\mathcal{L}}(\mathcal{L}|H_1) = \frac{1}{2d^2}\left[\frac{\mathcal{L}}{d^4}\right]^{(N-1)/2} \exp\left[-\frac{\mathcal{L}_1 + d^4}{2d^2}\right] I_{N-1}(\mathcal{L}^{1/2}) \tag{3.34}$$

where $I_{N-1}(x)$ is the (N-1)th order modified Bessel function of the first kind, and can be found from lower order modified Bessel functions by the relationship

$$I_n(x) = I_{n-2}(x) - \frac{2(n-1)}{x} I_{n-1}(x). \tag{3.35}$$

The probability of detection, as always, is the probability that the sufficient statistic will exceed the threshold when a signal has been received. So

$$P_D = \int_b^\infty p_{\mathcal{L}}(\mathcal{L}|H_1)\, d\mathcal{L}$$

$$= \int_b^\infty \frac{1}{2d^2}\left[\frac{\mathcal{L}}{d^4}\right]^{(N-1)/2} \exp\left[-\frac{\mathcal{L}_1 + d^4}{2d^2}\right] I_{N-1}(\mathcal{L}^{1/2})\, d\mathcal{L}. \tag{3.36}$$

However, the generalized Q function [25] is defined as

$$Q_m(a,b) = \int_b^\infty x\left[\frac{x}{a}\right]^{m-1} e^{-(a^2+x^2)/2} I_{m-1}(ax)\, dx \tag{3.37}$$

$$= Q(a,b) + e^{(a^2+b^2)/2} \sum_{k=0}^{m-1}\left[\frac{b}{a}\right]^k I_k(ab) \tag{3.38}$$

where m is an integer. Letting $x^2 = \frac{\mathcal{L}}{d^2}$, (3.36) can then be rewritten as

$$P_D = \int_{b/d}^{\infty} x \left(\frac{x}{d}\right)^{N-1} e^{-(x^2+d^2)/2} I_{N-1}(xd)\, dx$$

$$= Q_N\left(d, \frac{b}{d}\right). \qquad (3.39)$$

In Figures 3.3 and 3.4, the performance curves for the low SNR receiver are plotted on the same axes as the performance curves for the maximum likelihood receiver. To obtain these curves, the approximation given in (3.38) was used to find P_D and thus numerical integration was avoided. Note that for one frequency, the performance is naturally identical for both receivers, since the sufficient statistic of the two receivers is also identical.

For two frequencies, as can be seen from Figure 3.3, when the SNR is 3 dB, the two receivers are roughly equivalent in performance. However, for P_F less than 10^{-3}, a small difference in performance appears, with the maximum likelihood receiver consistently giving better results. However, even for SNR as low as 5 dB, a difference in the performance curves can be noticed, with the maximum likelihood receiver having $P_D = 6.3 \times 10^{-3}$ while that for the low SNR receiver is 5×10^{-3}, when $P_F = 10^{-4}$. When the SNR is as large as 13 dB, the performance of the two receivers is still close but the maximum likelihood receiver gives noticeably superior performance. When $P_F = 10^{-3}$, for example, P_D for the maximum likelihood receiver is 0.75 while that for the low SNR receiver is 0.7.

Extending the results to four frequencies, as in Figure 3.4, it can be seen that the difference in performance between the two receivers is larger than for two frequencies. While the two receivers perform

approximately the same for SNR = 3 dB, this cannot be claimed for SNR = 13 dB. Looking at $P_F = 10^{-3}$ again, P_D for the maximum likelihood receiver and the low SNR reciever is 7.773×10^{-3} and 6.293×10^{-3} respectively for SNR = 3 dB. When SNR is 7 dB, these correspondingly become .048 and .031 and increase to .696 and .537 when the SNR is 13 dB. This implies that for a SNR of 3 dB, the low SNR performance gives a 19% degradation in performance, relative to the maximum likelihood receiver, which increases to 23% for SNR = 13 dB, when $P_F = 10^{-3}$. Therefore, since the low SNR receiver never performs better than the maximum likelihood receiver, it is suboptimum for all values of SNR considered.

3.5 DISCUSSION OF RESULTS

3.5.1 Summary of Results for Noncoherent Receivers

This section will not only summarize the results found in this chapter but will also draw comparisons between noncoherent and coherent detection methods, discussing any interesting trends or differences.

In this chapter, three noncoherent receivers were discussed. The optimum receiver was shown to have a sufficient statistic equal to a sum of modified Bessel functions, the arguments of which are either Rayleigh or Ricean random variables. The solution of the performance proved to be even more difficult than for the optimum coherent receiver, and no exact solution was found. However, results from Chapter 2 indicated that for coherent receivers, the performance of the optimum receiver is well approximated by the maximum likelihood receiver. Therefore, the

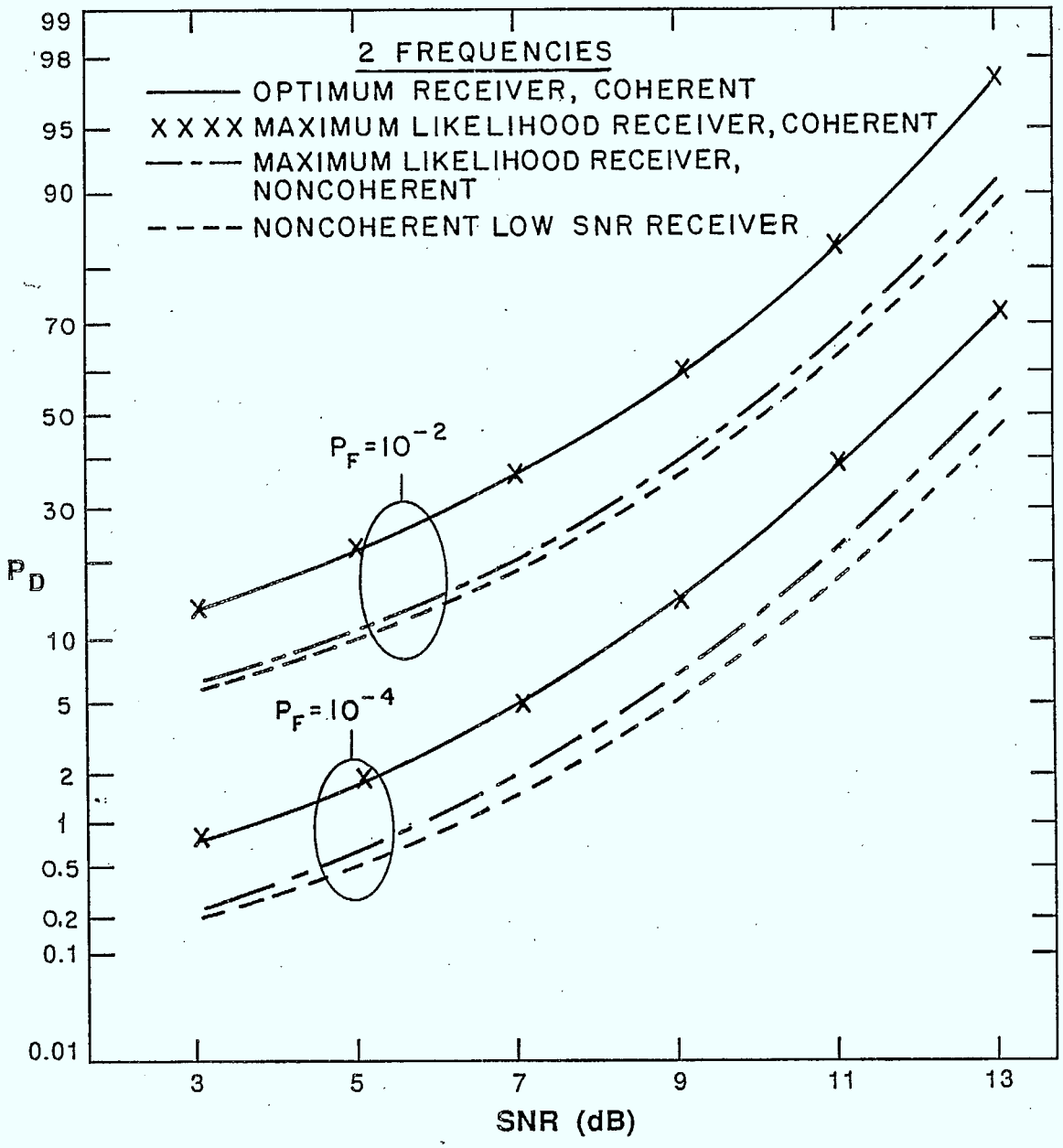

Figure 3.9 Performance plots of noncoherent and coherent receivers for two frequencies

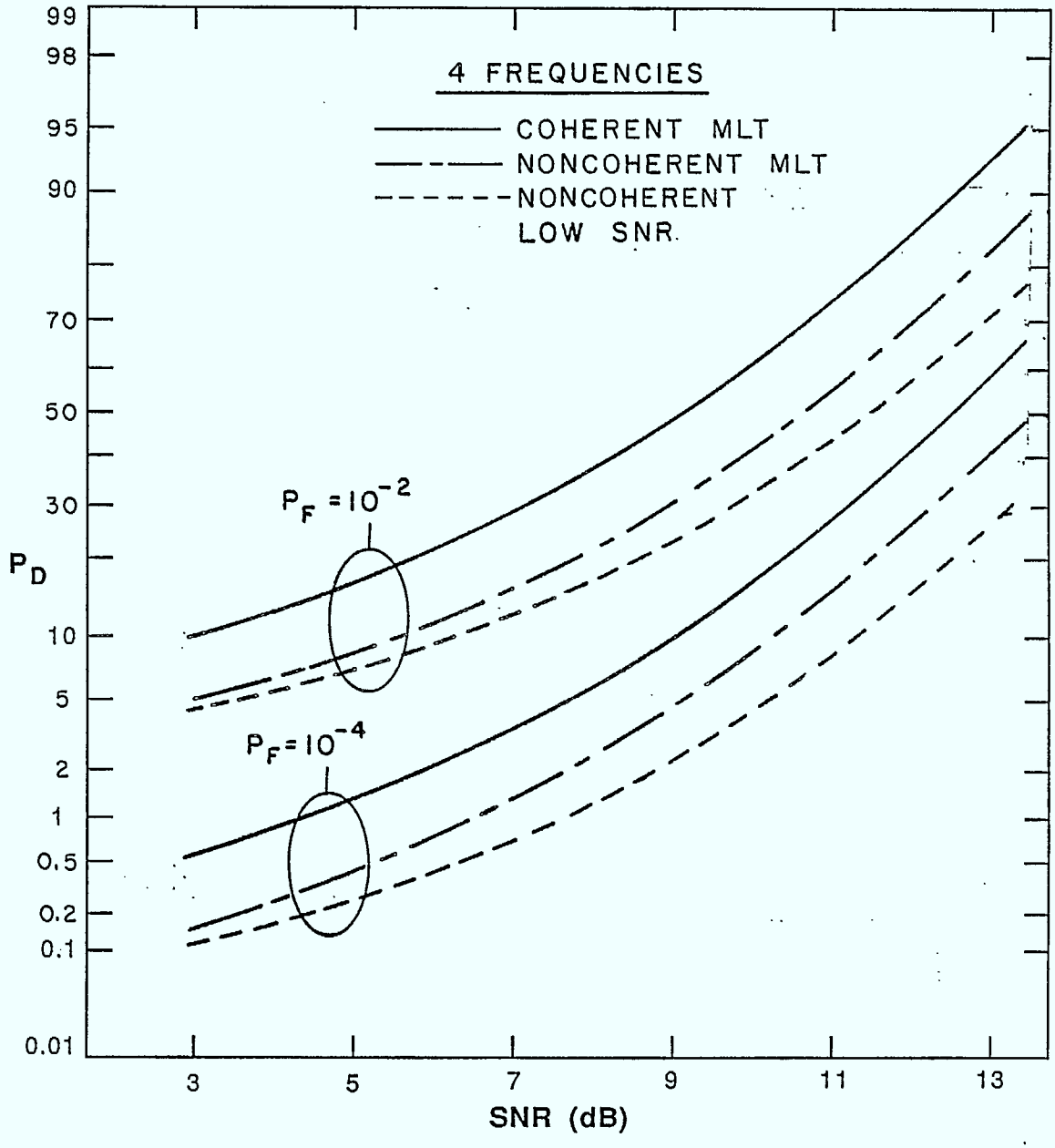

Figure 3.10 Performance plots of noncoherent and coherent receivers for four frequencies

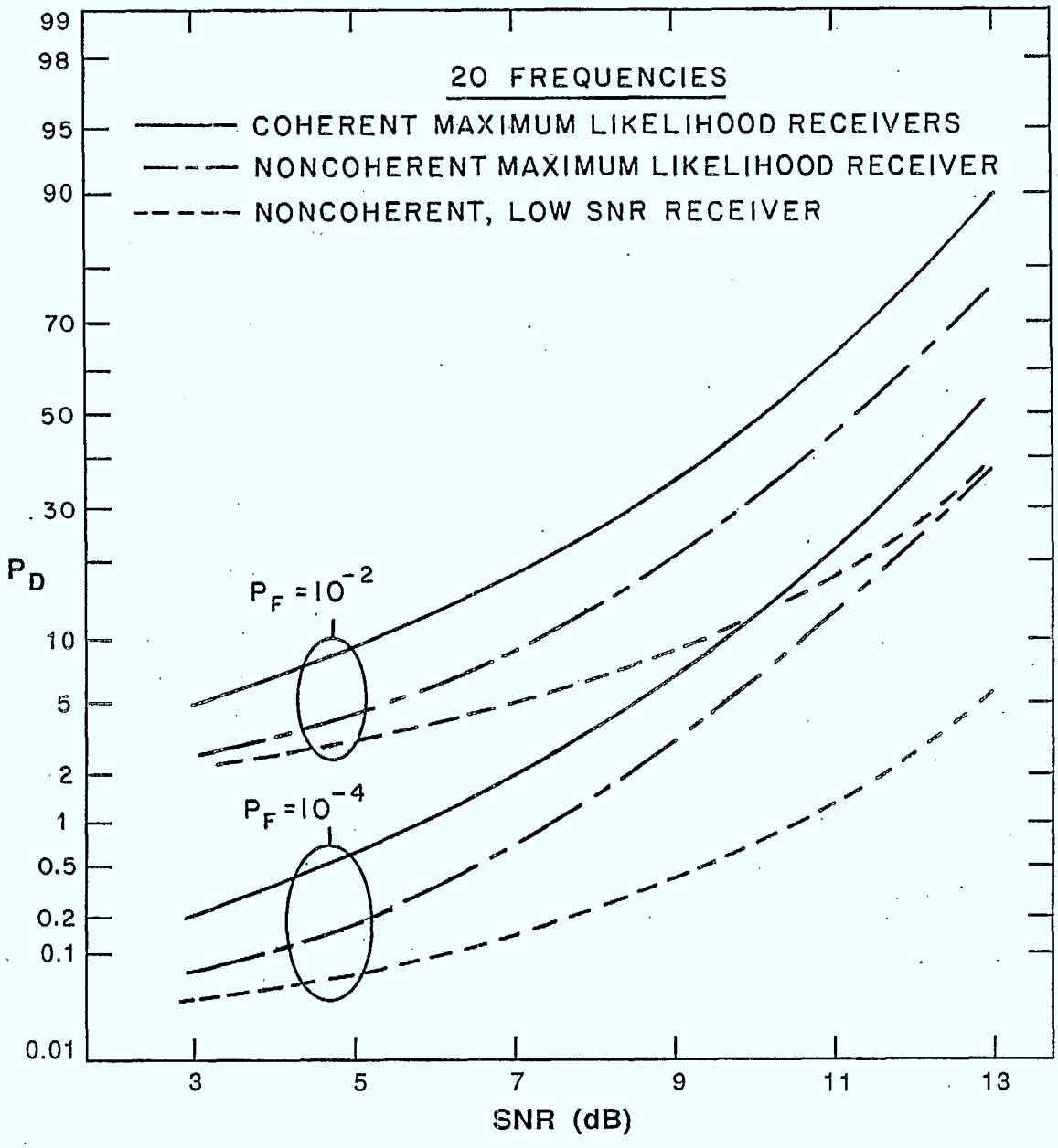

Figure 3.11 Performance plots of noncoherent and coherent receivers for twenty frequencies

noncoherent maximum likelihood receiver was found and its performance derived. Simulations of the optimum receiver performance were compared to that of the maximum likelihood receiver. It was found that for noncoherent receivers as well, the maximum likelihood receiver perfomance is an excellent approximation of the optimum performance.

A third receiver was considered which is derived by an approximation of the sufficient statistic, assuming that the SNR is small. The performance of this receiver was found to either be the same or worse than that of the maximum likelihood receiver. It was found that for a small number of frequencies, around two, this receiver will have an optimum performance for SNR on the order of 5 dB or less. Figures 3.9-3.11 show the loss in performance between the low SNR receiver and the noncoherent maximum likelihood receiver for $P_F = 10^{-2}$ and $P_F = 10^{-4}$. The most interesting, as far as studying the low SNR receiver is concerned, is Figure 3.11 which gives performance curves for twenty frequencies. At 3 dB, when $P_F = 10^{-4}$, P_D is 63% less for the low SNR receiver than for the noncoherent maximum likelihood receiver. At 13 dB, this difference increases to 88%.

It is not surprising that the performance of the low SNR receiver deviates more from that of the maximum likelihood receiver as the number of frequencies increases. Recall that this receiver was found by approximating $I_0(x)$ by $1+(x^2/4)$. The sufficient statistic is a sum of N such terms. Therefore, if the difference between $I_0(x)$ and $1+(x^2/4)$ is ϵ, the sufficient statistics of the two receivers will differ by $N\epsilon$. Thus, the approximation is worse for large N.

3.5.2 Performance Trends

Figures 3.9-3.11 plot the performance of the low SNR receiver and both maximum likelihood receivers for two, four and twenty frequencies, respectively. From these plots, it can be seen that there is a 1 dB loss between coherent and noncoherent receivers when the SNR is in the 13 dB range, and that this increases to 2 dB for SNR values around 3 dB.

Before continuing the analysis of the performance of the receivers, a brief discussion of how the thresholds were set will be undertaken. Simply, all thresholds were set by using the Neyman-Pearson criterion. This criterion finds the threshold for a given P_F. For both maximum likelihood receivers, P_D could be expressed directly in terms of P_F, which simplifies the matter greatly. To find the threshold, note that

$$Q_F = 1-(1-P_F)^{1/N} \tag{3.40}$$

where Q_F is the false alarm probability for a single frequency receiver. This can be solved for the threshold and the threshold then used in the probability of detection expressions. For the noncoherent receiver,

$$Q_D = Q(d, (-2 \ln Q_F)^{1/2}) \tag{3.41}$$

and for the coherent receiver,

$$Q_D = Q\ (Q^{-1}(Q_F) - d) \tag{3.42}$$

where $Q^{-1}(x)$ is the inverse of the error function. Then

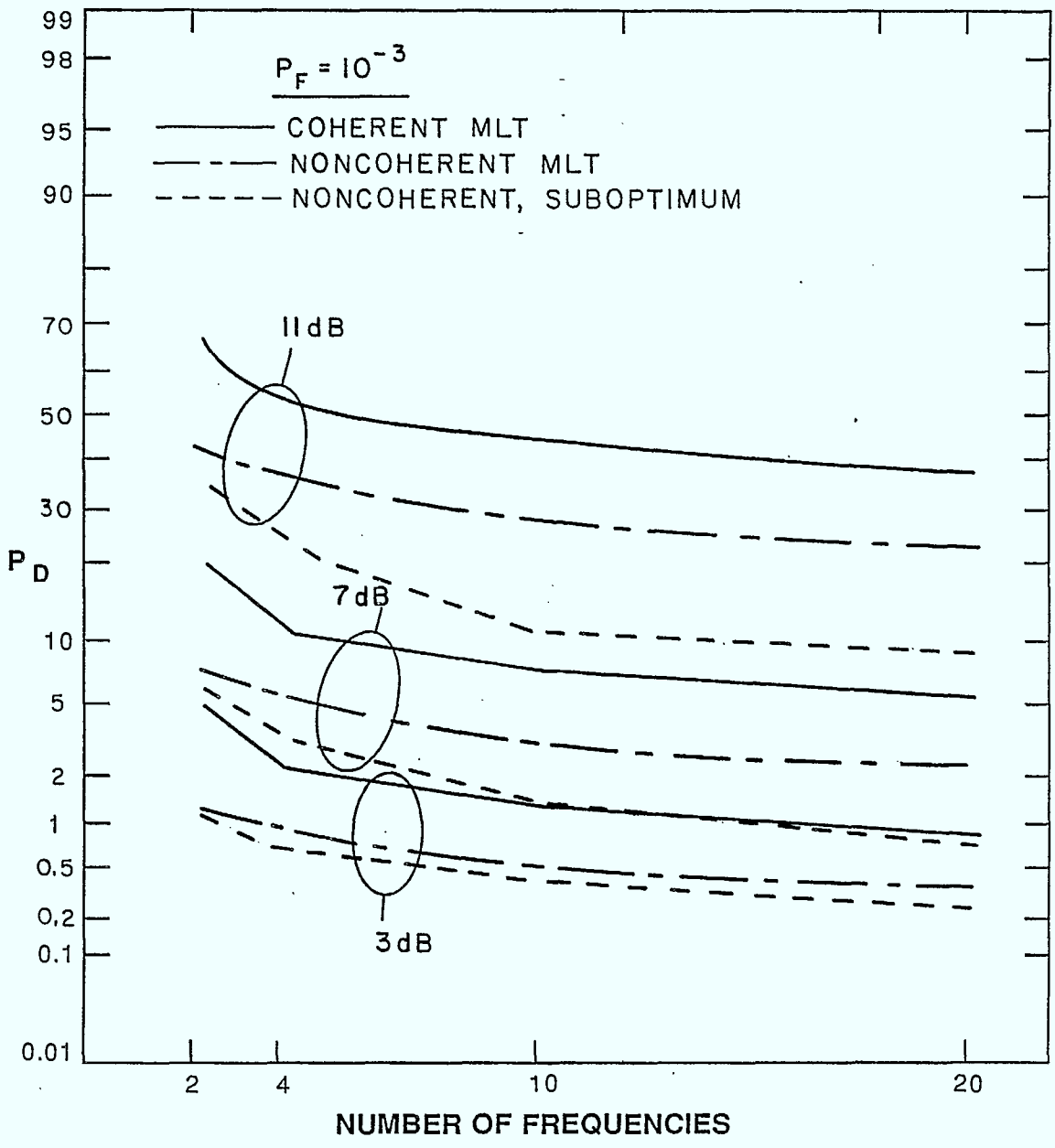

Figure 3.12 Probability of detection as a function of the number of frequencies when $P_F = 10^{-3}$

$$P_D = 1 - (1-Q_D)(1-Q_F)^{N-1} \qquad (3.43)$$

from Chapter 2.

For all the other receivers, P_D and P_F are both calculated across a range of threshold settings in order to find P_D for the desired P_F. An interesting observation can be made about P_D as a function of the number of frequencies, as plotted in Figure 3.12. As would be expected, P_D decreases as the number of frequencies increases. However, the loss in performance as the number of frequencies increases from ten to twenty is less than the loss in performance between two and four frequencies. It will be shown later in Chapter 5 that from (3.40)-(3.43), that as the number of frequencies grow large, P_D has an asymptotic value equal to P_F.

To give some numbers, for noncoherent receivers, P_D drops by 29.5% as the number of frequencies increases from two to four and by 27.7% between ten and twenty frequencies, when $P_F = 10^{-3}$ and SNR = 7 dB. Under similar conditions, the coherent receiver experiences decreases of 26.6% and 28.5% for the increase from two to four and ten to twenty frequencies respectively. Therefore, the performance of the coherent receiver degrades faster than that of the noncoherent receiver except when the number of frequencies is very small, on the order of ten or less. Again, this is not surprising. As stated earlier, P_F behaves as an asymptote for P_D. Since the coherent receiver has a better P_D than the noncoherent receiver, it also has a large potential for performance loss. This would seem to imply, that for a very large number of frequencies, the performance of coherent and noncoherent receivers will be very close.

As well, this shows that, for the transmitter, the addition of

transmission frequencies exemplifies the law of diminishing returns. While each additional frequency does reduce the probability of interception, the amount of the reduction is less for each one. Therefore, it requires more and more frequencies to obtain a significant decrease in the probability of interception.

To conclude, for two frequencies, noncoherent detection methods perform an average of 1.5 dB worse than coherent detection methods. This loss decreases as the number of frequencies increases. It was also found that the low SNR receiver, developed in this chapter, performs well at low SNR values with a small number of frequencies. However, its performance degrades, relative to the optimum, for any given SNR level as the number of frequencies increase. In addition, for the transmitter, each additional frequency will reduce the probability of interception less than the previous one. For the receiver, this means that the loss in P_D is less for each additional frequency.

CHAPTER 4

FREQUENCY OFFSET AND A PRIORI KNOWLEDGE

4.1 INTRODUCTION

Chapters 2 and 3 discussed coherent and noncoherent detection methods developed under the assumptions outlined in Chapter 1. In the current chapter, two deviations and their effect on receiver performance, are considered separately.

In the first case, consider that a priori knowledge of the transmitted signal is available, and it has been used to design a new optimum receiver. Is there a performance improvement over the receiver discussed in Chapter 2? Also, if the a priori knowledge is wrong, is there a loss in performance and if so, what is it?

For the second case, this report examines the performance degradation when a central assumption, used to derive the receivers discussed so far, is invalid. Suppose the actual frequency distribution is not the discrete distribution given in (3.19). If the signal is not at one of the frequencies the receiver was optimized for, what is its probability of detection? This question is answered for the two coherent receivers, and the noncoherent maximum likelihood receiver.

4.2 A PRIORI KNOWLEDGE

4.2.1 The A Priori Receiver

Under the assumption of coherent detection, if a priori knowledge is available, the receiver of section 2.3 is no longer optimum. Therefore, to examine the effects of a priori knowledge on the receiver performance bounds, a new optimum receiver must be developed.

The derivation of this receiver will parallel the derivation done in section 2.3. Therefore, to avoid being repetitious, the derivation presented here will be less detailed. It is recommended that the reader be familiar with section 2.3.1 before continuing.

The receiver must decide between two hypotheses,

$$\begin{aligned} H_1: &\quad r(t) = A\cos\omega_i t + n(t) && 0 \le t \le T \\ H_0: &\quad r(t) = n(t) && 0 \le t \le T \end{aligned} \tag{4.1}$$

where n(t) is AWGN with spectral density $\frac{N_0}{2}$ W/Hzand A is the signal amplitude. It will be assumed that ω still has a discrete distribution. Now, however, the ω_i's no longer have an equal probability of arrival. That is,

$$p_\omega(\omega) = \sum_{i=1}^{N} P_i \delta(\omega - \omega_i) \tag{4.2}$$

where $\sum_{i=1}^{N} P_i = 1$ and $P_i \neq \frac{1}{N}$.

To find the form of the optimum receiver, once again the

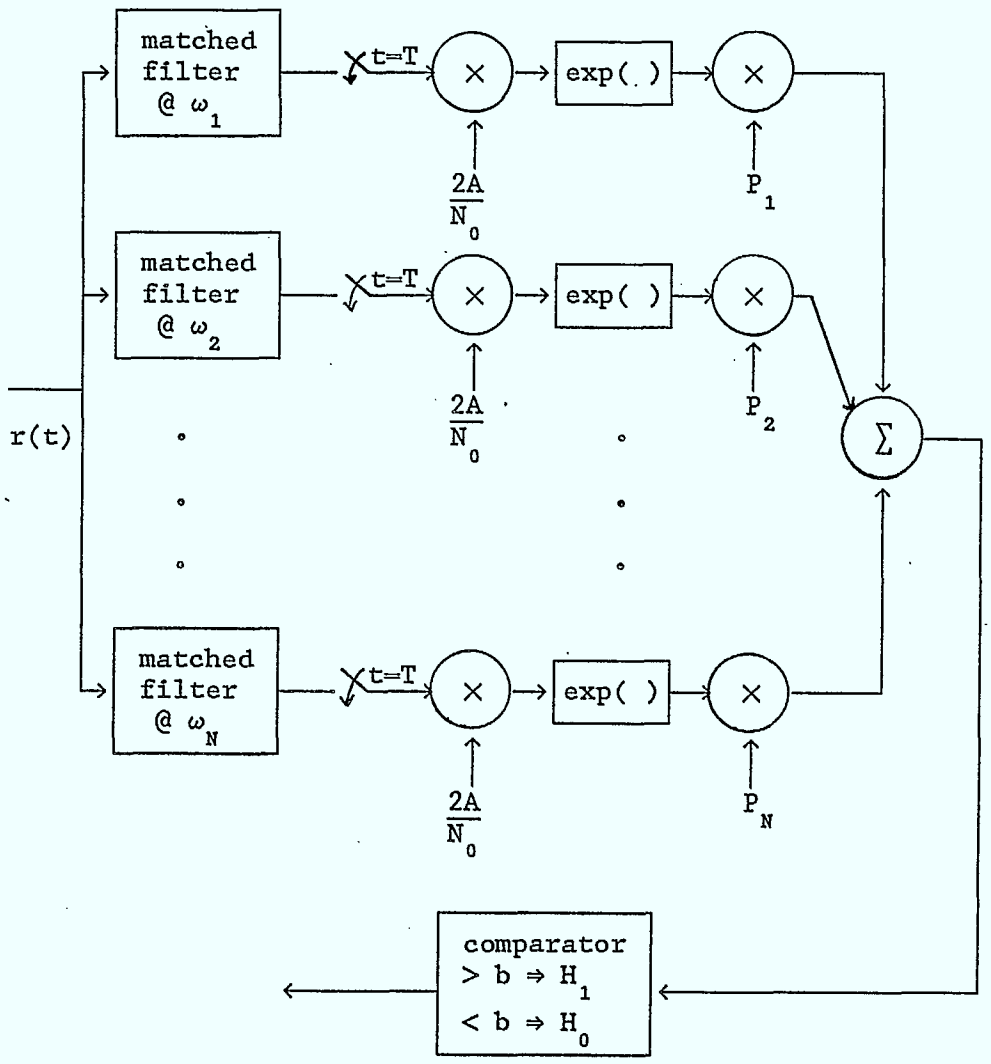

Figure 4.1: Optimum Coherent Receiver Using A Priori Knowledge

generalized likelihood ratio test will be derived. So, following the procedure outlined in Chapter 2, the conditional probability density function of the received signal, under both hypotheses, must be found. $p_r(\underline{R}|H_0)$ is found to be unchanged, since H_0 is the same as before, and is given by (2.5). $p_r(\underline{R}|H_1)$ is once again found by averaging $p_r(\underline{R}|H_1,\omega)$ over ω, as in (2.16) where $p_r(\underline{R}|H_1,\omega)$ is also unchanged from previously. Therefore,

$$p_r(\underline{R}|H_1) = \sum_{i=1}^{N} \frac{P_i}{\pi N_0} \exp\left[\frac{{}_0\int^T r^2(t)\,dt - 2A\,{}_0\int^T r(t)\cos\omega_i t\,dt + E}{-N_0}\right]. \quad (4.3)$$

Taking the ratio of $p_r(\underline{R}|H_1)$ to $p_r(\underline{R}|H_0)$ and simplifying, the likelihood ratio test is found to be

$$L(r) = e^{-d^2/2} \sum_{i=1}^{N} P_i \exp\left[\frac{2A}{N_0}\,{}_0\int^T r(t)\cos\omega_i t\,dt\right] \underset{H_0}{\overset{H_1}{\gtrless}} \eta \quad (4.4)$$

which can be rewritten as

$$\ell = \sum_{i=1}^{N} P_i \ell_i \underset{H_0}{\overset{H_1}{\gtrless}} \eta e^{d^2/2} \quad (4.5)$$

where $\alpha_i = \frac{2A}{N_0}\,{}_0\int^T r(t)\cos\omega_i t\,dt$, $\ell_i = e^{\alpha_i}$ and ℓ is the sufficient statistic for this receiver. Note that ℓ_i is exactly the same as defined in section 2.3.1, and if ℓ, in that section, had been defined as

$\frac{1}{N}\sum_{i=1}^{N}\ell_i$ instead, it would be identical to the sufficient statistic for this receiver. Therefore, the optimum coherent receiver using a priori knowledge, as shown in Figure 4.1, is only slightly different from the one discussed previously in Chapter 2.

4.2.2 Performance Analysis

This receiver has yet another feature in common with the optimum receiver of Chapter 2. The analysis for an arbitrary number of frequencies is unwieldy. Therefore, once again, an exact performance analysis is carried out for only two frequencies. An approximation to a larger number of frequencies is not immediately obvious since no work has been carried out that proves that either Farley's approximation or Wilkinson's approach will hold for a weighted sum of lognormal variables. It is hoped that an analysis of the two frequency case will give a good indication of the effects of a priori knowledge on performance bounds, under more general conditions.

Following the simpler of the two procedures outlined in Chapter 2, the likelihood ratio test for two frequencies is

$$P_1 e^{\alpha_1} + P_2 e^{\alpha_2} \underset{H_0}{\overset{H_1}{\gtrless}} \eta e^{d^2/2}. \tag{4.6}$$

Now, P_F is the probability that ℓ exceeds the threshold when noise only is present. That is,

$$P_F = \Pr\left[P_1 e^{\alpha_1} + P_2 e^{\alpha_2} > \eta e^{d^2/2} \middle| H_0\right]$$

$$= \Pr\left[e^{\alpha_1} > \frac{\eta}{P_1} e^{d^2/2} - \frac{P_2}{P_1} e^{\alpha_2} \middle| H_0\right].$$

Therefore,

$$P_F = \int_{-\infty}^{\infty} \Pr\left[e^{\alpha_1} > \frac{\eta}{P_1} e^{d^2/2} - \frac{P_2}{P_1} e^{\alpha_2} \middle| \alpha_2, H_0\right] p_{\alpha_2}(\alpha_2|H_0)\, d\alpha_2. \tag{4.7}$$

Since α_1 and α_2 are both zero mean normal random variables with a variance of d^2, the conditional probability can easily be found to equal

$$\Pr\left[e^{\alpha_1} > \frac{\eta}{P_1} e^{d^2/2} - \frac{P_2}{P_1} e^{\alpha_2} \middle| \alpha_2, H_0\right] = \begin{cases} 1 & \alpha_2 > \beta \\ f(\alpha_2) & \alpha_2 < \beta \end{cases} \tag{4.8}$$

where

$$\beta = \frac{d^2}{2} + \ln \frac{\eta}{P_2} \tag{4.9}$$

and

$$f(\alpha_2) = Q\left[\frac{\ln\left(\eta - P_2 e^{\alpha_2 - d^2/2}\right) - \ln P_1}{d} + \frac{d}{2}\right]. \tag{4.10}$$

P_F can now be found by substituting (4.8) and (2.20) into (4.7) to

obtain

$$P_F = Q\left[\frac{\beta}{d}\right] + \int_{-\infty}^{\beta} \frac{1}{(2\pi d^2)^{1/2}} \exp\left[-\frac{\alpha_2^2}{2d^2}\right] f(\alpha_2)\, d\alpha_2. \tag{4.11}$$

Since α_1 and α_2 are identically distributed, an alternate form of P_F can be found by switching P_1 and P_2 in the above expression.

Next, P_D must be found. Since the probability of arrival is now assumed higher for some frequencies than for others, the likelihood ratio test will be biased in their favor. This means that P_D is no longer the same for each detector. Those frequencies that are given the lowest probability of arrival will also have the lowest probability of detection. Should the a priori knowledge be incorrect, P_D may actually be less than obtained for the optimum receiver of Chapter 2. Assume that the sinusoid of frequency ω_i arrives with probability $\hat{P}_i$, and P_{Di} is the probability of detection for that signal. Then P_D for the receiver, assuming an arbitrary number of frequencies, N, is

$$P_D = \sum_{i=1}^{N} \hat{P}_i P_{Di} \tag{4.12}$$

In this case, $P_D = \hat{P}_1 P_{D1} + \hat{P}_2 P_{D2}$.

To obtain the individual detection probabilites, P_{Di}, let ω_1 be the frequency of the received signal. Then α_1 will be normal with both mean and variance equal to d^2. α_2 will also be normal with a variance of d^2 but with a mean of zero, as derived previously. Proceeding as in Chapter 2,

$$P_{D1} = \Pr[P_1 e^{\alpha_1} + P_2 e^{\alpha_2} > \eta e^{d^2/2} | H_1]$$

$$= \int_{-\infty}^{\infty} \Pr\left[e^{\alpha_2} > \frac{\eta}{P_2} e^{d^2/2} - \frac{P_1}{P_2} e^{\alpha_1} \middle| \alpha_1, H_1 \right] p_{\alpha_1}(\alpha_1 | H_1)\, d\alpha_1. \tag{4.13}$$

It can easily be shown that

$$\Pr\left[e^{\alpha_2} > \frac{\eta}{P_2} e^{d^2/2} - \frac{P_1}{P_2} e^{\alpha_1} \middle| \alpha_1, H_1 \right] = \begin{cases} 1 & \alpha_1 > \rho \\ g(\alpha_1) & \alpha_1 < \rho \end{cases} \tag{4.14}$$

where

$$\rho = \frac{d^2}{2} + \ln \frac{\eta}{P_1} \tag{4.15}$$

and

$$g(\alpha_1) = Q\left[\frac{\ln (\eta - P_1 e^{\alpha_1 - d^2/2}) - \ln P_2}{d} + \frac{d}{2} \right]. \tag{4.16}$$

Finally, to find P_{D1}, (4.14) and (2.34), where the latter is the probability density function of α_1, are used in (4.13) to give

$$P_{D1} = Q\left[\frac{\rho}{d}\right] + \int_{-\infty}^{\rho} \frac{1}{(2\pi d^2)^{1/2}} \exp\left[- \frac{(\alpha_1 - d^2)^2}{2d^2} \right] g(\alpha_1)\, d\alpha_1. \tag{4.17}$$

The derivation of P_{D2}, when carried out in the same fashion as above, gives an expression almost identical to that of (4.17). In this case, the roles of P_1 and P_2 are reversed.

If, instead, integration is carried out first over α_1, then a slightly different expression for P_{D1} is obtained. Rederiving gives,

$$\Pr\left[e^{\alpha_1} > \frac{\eta}{P_1} e^{d^2/2} - \frac{P_2}{P_1} e^{\alpha_2} \middle| \alpha_2, H_1\right] = \begin{cases} 1 & \alpha_2 > \beta \\ h(\alpha_2) & \alpha_2 < \beta \end{cases} \tag{4.18}$$

where β is given by (4.9) and

$$h(\alpha_2) = Q\left[\frac{\ln\left(\eta - P_2 e^{\alpha_2 - d^2/2}\right) - \ln P_1}{d} - \frac{d}{2}\right]. \tag{4.19}$$

Averaging over α_2, the probability density function of which is found in (2.20), gives

$$P_{D1} = Q\left[\frac{\beta}{d}\right] + \int_{-\infty}^{\beta} \frac{1}{(2\pi d^2)^{1/2}} \exp\left[-\frac{\alpha_2^2}{2d^2}\right] g(\alpha_2)\, d\alpha_2 \tag{4.20}$$

with P_{D2} again being obtained by switching P_1 and P_2.

From (4.12), along with the expressions just derived for P_{D1} and P_{D2}, P_D for the a priori receiver can be calculated. In Table 4.1, values of P_D, when $P_F = 10^{-3}$ and $P_1 = 0.9$, are given for different values of $\hat{P}_1$. The case of $P_1 = 0.5$, which is the equiprobable condition covered in Chapter 2, is also included for comparison purposes.

The improvement in performance is as high as 50%, when SNR = 3 dB, slips to 22% at 7 dB, and drops to 3% for 13 dB. Therefore, the a

TABLE 4.1: Effects of A Priori Knowledge on P_D for $P_F = 10^{-3}$

	$P_1 = 0.9$				$P_1 = 0.5$
SNR \ $\hat{P}_1$	0.5	0.75	0.9	1.0	
3	.0241	.0354	.0421	.0466	.0308
5	.0505	.0724	.0856	.0944	.0658
7	.116	.155	.179	.195	.147
9	.253	.326	.363	.387	.319
11	.546	.606	.642	.666	.602
13	.854	.881	.898	.909	.880

priori knowledge seems to be most beneficial at low SNR. However, if the a priori knowlege is wrong, the loss can be as severe as 22%, when the signals are actually equally probable, or even as large as 95%, if the frequency that was assigned the lowest probability of arrival, arrives all the time. However, an improvement can still be found by using the a priori knowledge if it is not too different from the actual arrival probabilities. For example, examining the data for $\hat{P}_1 = 0.75$, there is a small improvement performance of 15%, when the SNR is 3 dB but this decreases to 0.1% for 13 dB.

It would appear, then, that a priori knowledge improves the performance significantly for SNR values less than 7 dB. Should this knowledge be wrong by a significant margin (in this case if $\hat{P}_1$ is less than 0.75), however, the resulting performance loss could be costly. It is recommended, from the results for two frequencies, if a priori knowledge is available, that it only be used if there is a great deal of

certainty about it. However, further research is necessary in order to determine if these conclusions will extend to more than two frequencies.

4.3 FREQUENCY OFFSET

4.3.1 System Model

In the previous chapters, it was assumed that the frequency distribution was

$$p_{\omega}(\omega) = \sum_{i=1}^{N} \frac{1}{N} \delta(\omega - \omega_i)$$

where the frequency separation is the minimum needed for orthogonality. The performance analysis further assumed that the received signal was at a frequency equal to one of the ω_i's. This section examines the degradation in performance when the latter assumption is not true. More precisely, the frequency of the received signal is $\omega_i+\omega_o$, where ω_o is some frequency offset. Let ω_o be expressed as a fraction of the frequency separation, δ, where the filter frequencies, ω_i, are some integer multiple, k_i, of this separation, and $k_i \geq \frac{1}{T}$. Thus, for coherent detection, $\omega_o = \frac{\pi\delta}{T}$, and for noncoherent detection, $\omega_o = \frac{2\pi\delta}{T}$.

4.3.2 Optimum Coherent Receiver

Due to the difficulty of analysis for a large number of frequencies, it is once again assumed that the receiver is designed for

only two transmission frequencies. Now, however, the received signal frequency is neither.

In order to evaluate the performance of the receiver under these conditions, it is necessary to first find the probability density functions of α_1 and α_2 where $\alpha_i = \frac{2A}{N_0} \int_0^T r(t) \cos \omega_i t \, dt$. Under the conditions outlined at the beginning of this section,

$$r(t) = A \cos (k_i + \delta)\frac{\pi t}{T} + n(t) \tag{4.20}$$

where, since $k_i \gg \frac{1}{T}$, k_i will also be much larger than δ. This implies that

$$\alpha_1 = \frac{2A}{N_0} \int_0^T r(t) \cos \omega_1 t \, dt$$

$$= \frac{2A}{N_0} \int_0^T A \cos (k_1 + \delta)\frac{\pi t}{T} \cos k_1 \frac{\pi t}{T} \, dt + \frac{2A}{N_0} \int_0^T n(t) \cos k_1 \frac{\pi t}{T} \, dt. \tag{4.21}$$

The first term is deterministic and so the second term indicates that α_1 has a normal distribution with a variance of d^2, as before. Since the mean of this term has been established as zero, the first term gives the mean of α_1, which is

$$E(\alpha_1) = \frac{2A^2}{N_0} \int_0^T \left[\cos (2k_1 + \delta)\frac{\pi t}{T} + \cos \frac{\pi \delta t}{T}\right] dt$$

$$= d^2 \frac{2(k_1 + \delta)}{2k_1 + \delta} \frac{\sin \pi\delta}{\pi\delta}. \tag{4.22}$$

Since $k_i \gg \delta$, this reduces to

$$E(\alpha_1) = d^2 \text{ sinc } \delta \tag{4.23}$$

where $\text{sinc } x = \frac{\sin \pi x}{\pi x}$.

α_2 can also be shown to be normal with a variance of d^2. To find its mean, it is important to note that ω_2 is offset from ω_1 by $\frac{1}{2T}$. In other words, $k_2 = k_1+1$. Since the received signal is unchanged,

$$\begin{aligned} E(\alpha_2) &= \frac{2A}{N_0} \int_0^T A \cos (k_1+\delta)\frac{\pi t}{T} \cos (k_1+1)\frac{\pi t}{T}\, dt \\ &= \frac{2A^2}{N_0} \int_0^T \left[\cos (2k_1+\delta+1)\frac{\pi t}{T} + \cos (\delta-1)\frac{\pi t}{T}\right] dt \\ &= d^2 \frac{2(k_1+\delta)}{2k_1+\delta+1} \frac{\sin \pi(\delta-1)}{\pi(\delta-1)}. \end{aligned} \tag{4.24}$$

Again, since $k_1 \gg \delta$, (4.24) becomes

$$E(\alpha_2) = d^2 \text{ sinc } (\delta-1). \tag{4.25}$$

To find P_D, the simpler of the two procedures presented in Chapter 2 is again used. First, the conditional probability is found to be

$$\Pr\left[e^{\alpha_1} + e^{\alpha_2} \geq b \,|\, \alpha_1, H_1\right] = \begin{cases} 1 & \alpha_1 \geq \ln b \\ Q\left[\dfrac{\ln (b-e^{\alpha_1})}{d} - d \text{ sinc } (\delta-1)\right] & \alpha_1 < \ln b \end{cases} \tag{4.26}$$

The probability density function of α_1, from the previous discussion, is known to be

$$p_{\alpha_1}(\alpha_1) = \frac{1}{(2\pi d^2)^{1/2}} \exp\left[-\frac{(\alpha_1 - d^2 \text{ sinc } \delta)^2}{2d^2}\right]. \tag{4.27}$$

Substituting (4.26) and (4.27) into (2.33) gives

$$P_D = Q\left[\frac{\ln b}{d} - d \text{ sinc } \delta\right] + \int_{-\infty}^{\ln b} \frac{1}{(2\pi d^2)^{1/2}} \exp\left[-\frac{(\alpha_1 - d^2 \text{ sinc } \delta)^2}{2d^2}\right]$$

$$\text{X } Q\left[\frac{\ln (b - e^{\alpha_1})}{d} - d \text{ sinc } (\delta - 1)\right] d\alpha_1. \tag{4.28}$$

If the integration had been carried out with respect to α_1 first, then sinc δ and sinc $(\delta-1)$ would be interchanged in the above equation.

Note that no mention has been made, up to this point, of P_F. That is because it has not changed from section 2.3, and is still given by (2.27). Since P_F is dependent on the sufficient statistic, under H_0, and the noise itself alone, neither which have changed from that section, it, too, is unchanged.

Figure 4.2 plots P_D versus δ for 2 frequencies, when $P_F = 10^{-3}$. As expected, P_D is the highest when δ is equal to zero or one, corresponding to the frequencies the receiver was optimized for. Outside the receiver bandwidth, P_D will equal P_F. Inside the receiver bandwidth, the lowest values of P_D occur when $\delta = 0.5$, which is exactly

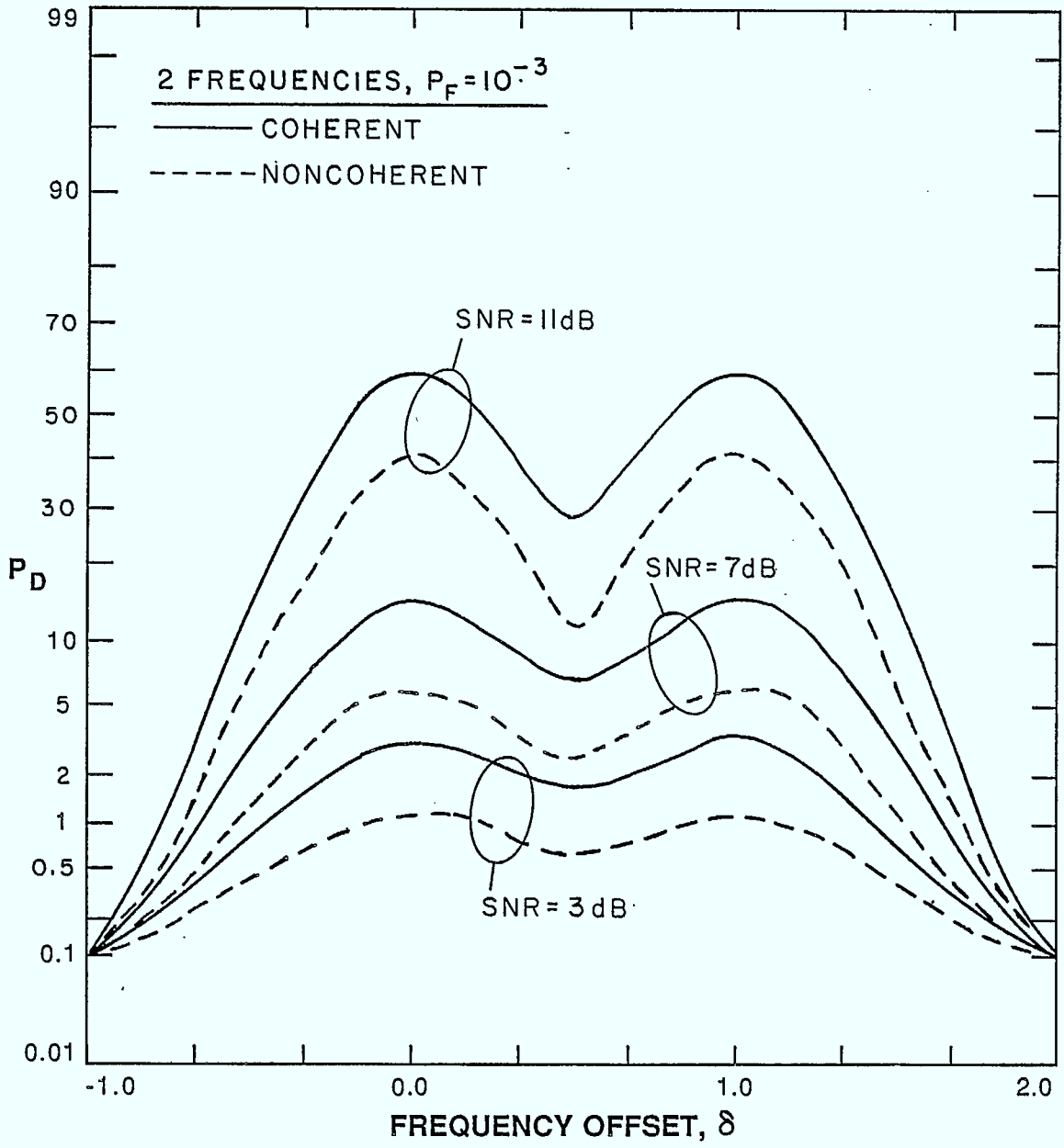

Figure 4.2 Probability of detection as a function of the frequency offset for two frequencies when $P_F = 10^{-3}$

midway between the center frequencies of the detectors. P_D, at these points, is less than half the peak value at the optimum frequency points. Of more interest, however, is the loss in detection probability when δ is small. When δ is only 0.1, the loss is approximately 5 to 6%. It would appear, then, that the receiver can tolerate small frequency errors. This will be discussed in more detail at the end of this section.

4.3.3 Coherent Maximum Likelihood Receiver

For the coherent maximum likelihood receiver described in section 2.2, P_F is unchanged and is given by (2.12) and (2.13). Therefore, it is only necessary to find P_D.

P_D can be defined as the probability that at least one of the individual detectors claims that a signal is present. Letting α_i be as defined previously, P_D can be expressed as

$$P_D = 1 - \prod_{i=1}^{N}(1 - \Pr[\alpha_i > \ln \eta e^{d^2/2}]). \tag{4.29}$$

From the previous section, it is known that α_1 and α_2 are both normal with variance of d^2, where α_1 has a mean of d^2 sinc δ, and α_2 has a mean of d^2 sinc $(\delta-1)$.

To find the probability density function of any arbitrary α_i, observe that the center frequency of the ith detector can be written as

$$\omega_i = (k_1+i-1)\frac{\pi}{T} \tag{4.30}$$

where it is assumed that ω_1 is the smallest frequency in the receiver band. As found for α_1 and α_2, α_i is a normal random variable of variance d^2 and mean

$$E(\alpha_i) = \frac{2A}{N_0} \int_0^T A \cos (k_1+\delta)\frac{\pi t}{T} \cos (k_1+i-1)\frac{\pi t}{T}\, dt$$

$$= d^2 \operatorname{sinc} (\delta+1-i). \tag{4.31}$$

Therefore,

$$\Pr[\alpha_i > \ln \eta e^{d^2/2}] = Q\left[\frac{\ln \eta e^{d^2/2} - d^2 \operatorname{sinc} (\delta+1-i)}{d}\right]. \tag{4.32}$$

This, used in (4.29), will give the probability that a received signal of frequency, $\omega_r = \omega_i + \frac{\pi\delta}{T}$, will be detected.

Results for two frequencies matched those plotted in Figure 4.2 for the optimum receiver. Figure 4.3 shows the performance of the maximum likelihood receiver for four frequencies and Table 4.2 gives some typical values for twenty frequencies. Naturally, the receiver performs best when the received signal frequency matches one of the filter center frequencies. From the figures and the table, it can be seen that when the received frequency falls midway between any two of these frequencies, the degradation in performance is typically greater than 50% which increases as the number of frequencies does. For $\delta = 0.1$, the loss in detection capability is between 5 to 7%, for any number of frequencies. Before discussing the rest of the results presented in these figures and the table, the performance of the noncoherent receiver

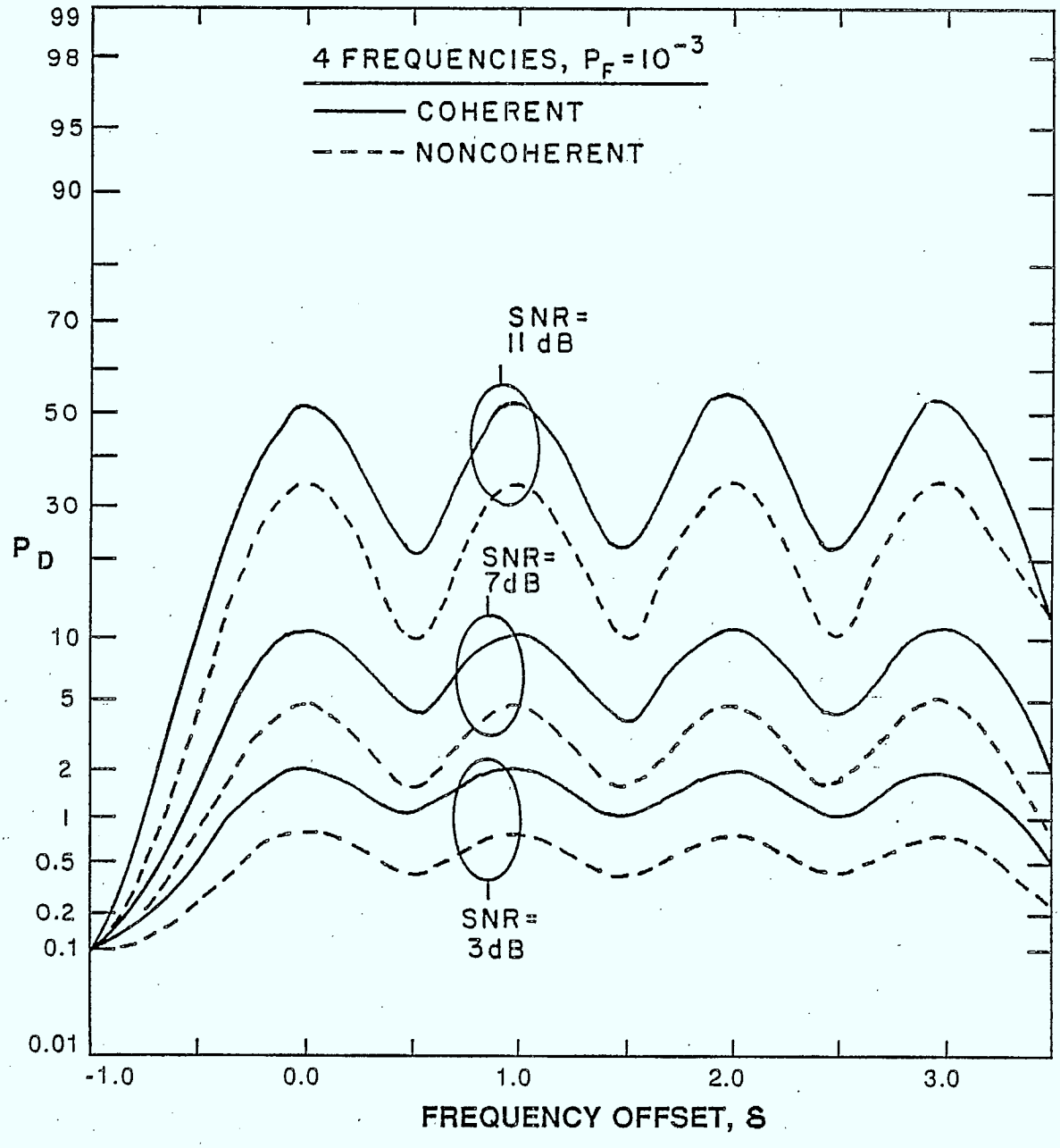

Figure 4.3 Probability of detection as a function of the frequency offset for four frequencies when $P_F = 10^{-3}$

TABLE 4.2 P_D for Frequency Offset when $P_F = 10^{-3}$, N = 20

Note: C = coherent NC = noncoherent

All probability values should be multiplied by 10^{-3}

SNR (dB)	3		7		11	
δ	C	NC	C	NC	C	NC
-.9	1.0	1.0	1.1	1.0	1.2	1.1
-.7	1.3	1.1	2.1	1.4	6.0	2.7
-.5	2.4	1.5	7.9	3.4	53.	22.
-.3	4.7	2.2	25.	10.	200	100
-.1	7.1	2.9	47.	19.	350	210
0	7.6	3.2	50.	21.	370	220
.1	7.2	3.0	46.	19.	350	200
.3	5.0	2.3	26.	11.	200	110
.5	3.7	1.8	15.	5.7	100	43.

will be derived.

4.3.4 Noncoherent Maximum Likelihood Receiver

For the noncoherent maximum likelihood receiver discussed in section 3.2, P_F is still given by (2.13) and (3.12). Due to the similarities between the two maximum likelihood receivers, P_D can be expressed in a similar form to (4.29). In this case,

$$P_D = 1 - \prod_{i=1}^{N}(1 - \Pr[q_i > \gamma]) \tag{4.33}$$

where γ is the decision threshold, and q_i is defined in Chapter 3 as

$$q_i^2 = L_{ci}^2 + L_{si}^2. \tag{4.34}$$

L_{ci} and L_{si} are defined in Chapter 3, which is repeated here for convenience:

$$\begin{aligned} L_{ci} &= \frac{2A}{N_0} \int_0^T r(t) \cos \omega_i t \, dt = q_i \cos \phi, \\ L_{si} &= \frac{2A}{N_0} \int_0^T r(t) \sin \omega_i t \, dt = q_i \sin \phi. \end{aligned} \tag{4.35}$$

The probability that q_i exceeds the threshold will be derived in the same manner as P_D was in Chapter 3. However, unlike the previous section, for the signals to be orthogonal, the ω_i's must be separated by $\frac{1}{T}$ Hz. Therefore, the received signal can be expressed as

$$r(t) = A \cos \left(\omega_1 t + \frac{2\pi\delta}{T} + \theta\right) + n(t) \tag{4.36}$$

where n(t) is unchanged from earlier. ω_i is still an integer multiple of the frequency separation and thus, (4.36) can be rewritten as

$$r(t) = A \cos \left[\frac{2\pi}{T}(k_1+\delta) + \theta\right] + n(t) \tag{4.37}$$

where still $k_1 \gg \frac{1}{T}$.

Next, the probability density function of q_i, and thus that of L_{ci} and L_{si}, is needed. In Chapter 3, it was established that L_{ci} and L_{si}

are normal with a variance of d^2. It is now only necessary to find their means. First,

$$E[L_{ci}|H_1] = \frac{2A}{N_0} \int_0^T A \cos \left[(k_1+\delta)\frac{2\pi}{T} + \theta \right] \cos (k_1+i-1)\frac{2\pi}{T}\, dt$$

which is solved easily to give

$$E[L_{ci}|H_1] = \frac{d^2 \sin 2\pi(\delta-i+1) - \sin \theta}{2\pi(\delta-i+1)}. \tag{4.38}$$

The mean for L_{si} can similarly be found to equal

$$E[L_{si}|H_1] = \frac{d^2 \cos 2\pi(\delta-i+1) - \cos \theta}{2\pi(\delta-i+1)}. \tag{4.39}$$

Finally, it is possible to find the distribution of q_i. Equation (4.34), which defines q_i, describes a Ricean random variable with noncentrality parameter,

$$\begin{aligned} s^2 &= (E[L_{ci}|H_1])^2 + (E[L_{si}|H_1])^2 \\ &= \frac{d^4}{(2\pi)^2(\delta-i+1)^2} (2 - 2 \cos 2\pi(\delta-i+1)) \end{aligned}$$

which simplifies to

$$s^2 = d^4 \operatorname{sinc}^2(\delta-i+1). \tag{4.40}$$

This implies that

$$p_q(q_i) = \frac{q_i}{d^2} \exp\left[-\frac{q_i^2 + d^4\,\mathrm{sinc}^2(\delta - i + 1)}{2d^2}\right] I_0(q_i\ \mathrm{sinc}\ (\delta - i + 1)). \tag{4.41}$$

Things are now set to find P_D. From (3.16), it is obvious that

$$\begin{aligned} \Pr[q_i > \gamma] &= \int_{\gamma}^{\infty} p_{q_i}(q_i)\, dq_i \\ &= Q(d\ \mathrm{sinc}\ (\delta - i + 1), \frac{\gamma}{d}) \end{aligned} \tag{4.42}$$

where Q(a,b) is the Marcum Q-function [24] defined in Chapter 3.

Finally, then, using (4.42) in (4.33) gives

$$P_D = 1 - \prod_{i=1}^{N} (1 - Q(d\ \mathrm{sinc}\ (\delta - i + 1), \frac{\gamma}{d})). \tag{4.43}$$

for the noncoherent maximum likelihood receiver.

Figures 4.2 and 4.3 plot the performance of this receiver, when $P_F = 10^{-3}$, for two and four random variables, respectively, on the same axes as the performance curves for the coherent receiver. Table 4.2 gives P_D when $P_F = 10^{-3}$ and there are twenty frequencies being used by the transmitter. From the figures and the table, it can be seen that the difference in performance between the two receivers will remain constant as long as $\omega_1 < \omega_r < \omega_N$ and the SNR is constant. As found in Chapter 3, this difference is in the range of 2 dB when the SNR is low, decreasing to 1 dB for SNR values in the range of 11 dB when there are

two transmission frequencies. This difference decreases as the number of frequencies increases. Should the frequency of the received signal fall outside of this range, the performance of the both receivers will decrease until $P_D = P_F$, the coherent receiver performance degrading faster than the noncoherent receiver. From the data, it can be seen that small deviations from the transmission frequencies assumed by the receiver, on the order of $\delta = 0.1$, result in a less than 10% decrease in detection capability from optimum levels. Similarly, if the received frequency is between two center frequencies and is not at the edge of the receiver band, large deviations, on the order of $\delta = 0.9$, will result in a less than 10% degradation due to the symmetry exhibited in the problem. However, midrange deviations, around $\delta = 0.5$, result in a greater than 50% decrease in P_D.

However, if the frequency of the received signal does not satisfy $\omega_1 < \omega_r < \omega_N$ then, for a small number of frequencies, it is found that the coherent receiver is less sensitive to small frequency offsets than the noncoherent receiver, as found for four frequencies when the offset was less than 0.25. For larger deviations, the coherent receiver experiences a greater loss in perfomrnace than the noncoherent receiver. Similarly, as the number of frequencies increases, the sensitivity of the coherent receiver to small deviations also increases. Therefore, for a large number of frequencies it is found that the coherent receivers are more sensitive than the noncoherent receivers, even for deviations less than 0.1, as found from the data for twenty frequencies in Table 4.2.

4.4 SUMMARY OF RESULTS

In this chapter, two deviations from the assumptions outlined in Chapter 1 were discussed. The first found that, if a priori knowledge was available and was used, significant performance improvement could be obtained only for SNR less than 7 dB. It was also found that the optimum receiver could tolerate some error in the a priori knowledge. An example used showed that if a frequency was guessed to be used 90% of the time and was actually used 75% of the time, P_D was still larger than if the a priori knowledge had not been used to design the receiver. However, any difference larger than this, and better performance would have been obtained if the a priori knowledge had not been used to design the receiver. It is recommended, on the basis of results obtained for two frequencies and the coherent optimum receiver, that a priori knowledge be used to design a receiver only if the SNR is expected to be less than 7 dB and if there is enough certainty about the a priori knowledge to guarantee that the a receiver using it will not be suboptimum to one not using it.

This chapter also examined the loss in performance if a key assumption, used to derive the receivers of Chapters 2 and 3, was invalid. If the frequency took on values other than those assumed by the detector, then a loss in detection capabilities would occur. Naturally, the largest loss occurs if the transmitted signal falls outside of the receiver bandwidth where it was found that the sensitivity of the coherent receiver to frequency deviations increases at a faster rate than that of the noncoherent receiver as the number of

frequencies increases. If the signal does fall inside the receiver bandwith, the most severe losses occur when δ = k+0.5, where k is an integer. This loss is greater than 50% and increases as either the number of frequencies or the SNR does. However, the receiver can tolerate small frequency errors. For example, a deviaton of 10% of the frequency separation results in a degradation around 10% for noncoherent receivers and 6 to 7% for the coherent receivers. Therefore, the maximum likelihood receivers, and the optimum receivers they approximate, become more sensitive to deviations around 0.5 as the number of frequencies used by the transmitter increases.

To summarize, a priori knowledge, when used to design a receiver, will give superior performance to a receiver that was designed without it. This improvement increases as the SNR decreases. Should it be wrong by a large margin, a loss may result instead. The optimum and maximum likelihood receivers of Chapters 2 and 3 can tolerate small frequency deviations of 0.1, losing less than 10% of their detection capability.

CHAPTER 5

Frequency-Hopped Spread Spectrum Considerations

5.1 INTRODUCTION

Prior to this chapter a modest number of frequencies, N, in the discrete frequency distribution of the signal have been considered. In most frequency-hopped, spread spectrum systems N would be at least 10^3 and more like 10^6. Actually N represents the processing gain of the frequency-hopped, spread spectrum system. In this chapter we consider large N for both the maximum likelihood and the optimum receiver. We show that for a constant false alarm rate, the detection probability of both receivers goes to P_F as $N \to \infty$. For the maximum likelihood receiver we establish N for a given SNR such that $P_D \to P_F$: such a processing gain would render the interception receiver performance as useless since detections cannot be distinguished from false alarms. Hence, signal interception is impossible and a fundamental performance limit has been reached. We establish this performance limit for both the coherent and non-coherent cases. Some approximate results are also given for the optimum receiver. In all cases, slow frequency hopping is assumed as the modulation is not allowed to hop in the detection time period for signal interception.

5.2 P_D as $N \to \infty$: Coherent Maximum Likelihood Receiver

We first establish that $P_D \to P_F$, it's lower bound, as $N \to \infty$. Thus, letting $N \to \infty$, effectively randomizes the signal, $A \cos \omega t$, when ω has the discrete probability density function:

$$p_\omega(\omega) = \frac{1}{N} \sum_{i=1}^{N} \delta(\omega-\omega_i)$$

From equations (2.15) and (2.13) it follows that,

$$P_D = 1 - (1-Q_D)(1-Q_F)^{N-1} \tag{5.1}$$

and

$$P_F = 1 - (1-Q_F)^N \tag{5.2}$$

Recall that Q_D and Q_F are the detection probability and false alarm probability, respectively, for each receiver in the parallel bank of receivers in Fig. 2.1. From (2.11), for the additive, white Gaussian noise model,

$$Q_D = Q\left(\frac{\ell n\ \eta}{d} - \frac{d}{2}\right) \tag{5.3}$$

and from (2.12)

$$Q_F = Q\left(\frac{\ell n\ \eta}{d} + \frac{d}{2}\right) \tag{5.4}$$

where $d = \sqrt{2E/N_o}$.

In our problem it is assumed that a constant false alarm detection probability, P_F, is specified. Thus from (5.2)

$$(1-Q_F)^N = 1 - P_F \tag{5.5}$$

and thus in (5.1)

$$P_D = 1 - (1-Q_D)(1-P_F)^{1-\frac{1}{N}} \tag{5.6}$$

For modest N, $(1-P_F)^{1-1/N} = 1 - P_F$, and

$$P_D = 1 - (1-Q_D)(1-P_F). \tag{5.7}$$

If $Q_D \to 0$ as $N \to \infty$, it follows that $P_D \to P_F$. From (5.4)

$$\frac{\ell n\ \eta}{d} + \frac{d}{2} = Q^{-1}(Q_F)$$

and by use of (5.5)

$$Q_F = 1 - (1-P_F)^{1/N}.$$

Hence,

$$Q_D = Q\{Q^{-1}[1-(1-P_F)^{\frac{1}{N}}]-d\} \tag{5.8}$$

and as $N \to \infty$, $Q_D \to 0$ as $1-(1-P_F)^{1/N} \to 0$, $Q^{-1}(0) = \infty$ and $Q(\infty) = 0$. From (5.7) $P_D \to P_F$ as $N \to \infty$ since $Q_D \to 0$ as $N \to \infty$.

5.3 P_D for Large N: Coherent Maximum Likelihood Receiver

In Figs. 5.1 and 5.2 we plot P_D vs $2E/N_o = d^2$ in dB with P_F and N as parameters. The computations are based on equations (5.1) through (5.4). From Fig. 5.1, when $N = 10^6$ ($\lambda = \log_{10} N = 6$) we see that $P_D = P_F$ when $P_F = 10^{-3}$ for all SNR's less than 6 dB. Thus below this limiting SNR, interception is impossible. For $P_F = 10^{-4}$, in Fig. 5.2, the limiting SNR is 5 dB. For a higher false alarm probability, say $P_F = .1$, from Fig. 5.1 the limiting SNR is 8 dB. Thus the SNR below which interception is impractical increases with the false alarm rate.

We now establish the convergence rate of P_D to P_F as N gets large. From equation (5.7),

$$P_D = P_F + Q_D(1-P_F) \tag{5.9}$$

For large N, the Taylor series for $e^{x\ell n(1-P_F)}$, yields

$$Q_F = 1 - (1-P_F)^{1/N} = \frac{-\ell n(1-P_F)}{N} \tag{5.10}$$

and as

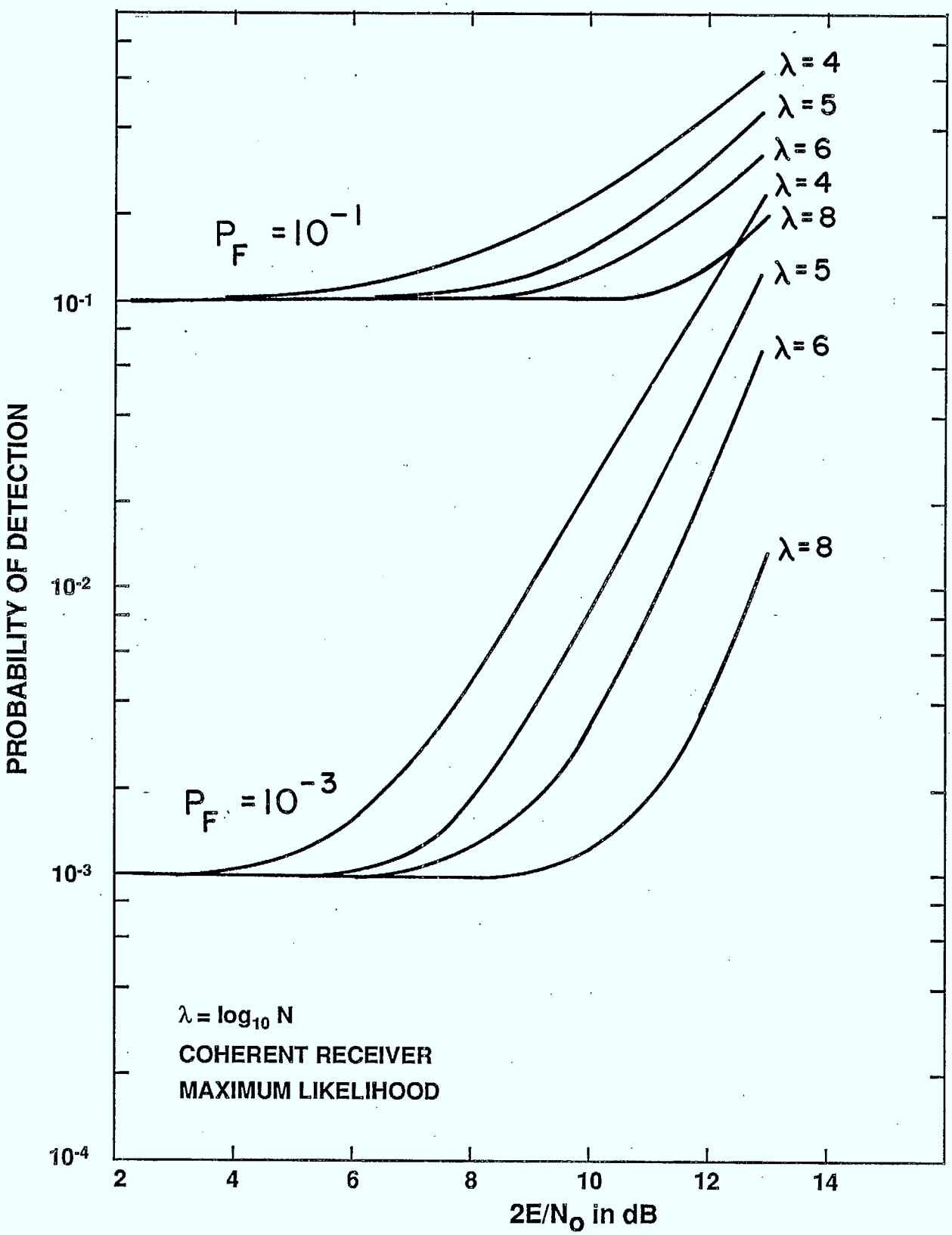

Figure 5.1 Probability of detection as a function of $2E/N_o$ for $P_F = 10^{-1}$, 10^{-3} for the coherent ML receiver

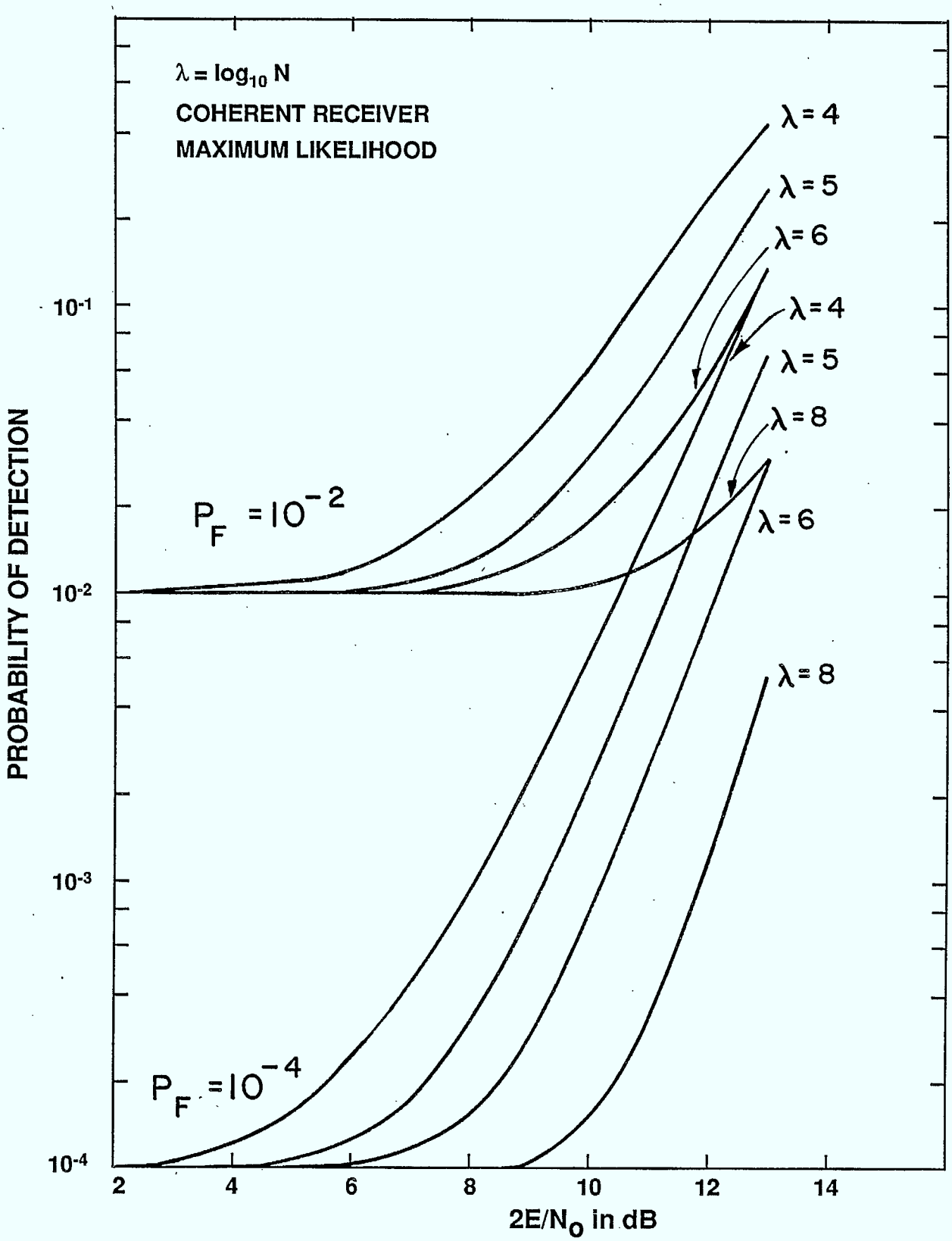

Figure 5.2 Probability of detection as a function of $2E/N_o$ for $P_F = 10^{-2}, 10^{-4}$ for the coherent ML receiver

$$Q^{-1}\,[-\ell n(1-P_F)/N] >> d$$

it follows from (5.8) that

$$Q_D = -\ell n(1-P_F)/N \tag{5.11}$$

Thus, combination of equations (5.9) and (5.11) yields the result

$$P_D = P_F - (1-P_F)\ell n(1-P_F)/N$$

Thus $P_D \to P_F$ as $1/N$ as N gets large. This is the situation for the coherent interception receiver.

5.4 P_D as $N \to \infty$: Non-Coherent Maximum Likelihood Receiver

As in the coherent case P_D and P_F are given by (5.1) and (5.2) respectively. Now, however, Q_D and Q_F are the detection and false alarm probability, respectively, for each individual non-coherent receiver in the parallel bank of receivers in Fig. 3.1. From equation (3.12)

$$Q_F = \exp\{-\frac{\gamma^2}{2d^2}\} \tag{5.12}$$

and from (3.17)

$$Q_D = Q(d, \gamma/d) \tag{5.13}$$

where Q(a,b) is Marcum's Q-function as defined in (3.17a).

Equation (5.7) is still valid for the present consideration. Thus $P_D \to P_F$ if $Q_D \to 0$ as $N \to \infty$. From (5.12),

$$\frac{\gamma}{d} = (-2\ \ell n\ Q_F)^{1/2} \tag{5.14}$$

We will show that $\gamma/d \to \infty$ as $N \to \infty$ and thus $Q_D \to 0$.

From (5.5)

$$Q_F = 1 - (1-P_F)^{1/N}$$

and as $N \to \infty$, $Q_F \to 0$ and $\gamma/d \to \infty$ in (5.14). Thus, Q_D in (5.13) goes to zero and $P_D \to P_F$ as $N \to \infty$, i.e., the lower limit in P_D.

5.5 P_D for Large N: Non-Coherent Maximum Likelihood Receiver

In Figs. 5.3 and 5.4 we plot P_D versus $2E/N_o = d^2$ in dB. The computations are based on equations (5.1), (5.2), (5.12) and (5.13). The algorithm in reference [28] was used to compute Marcum's Q-function. The results are similar to that presented earlier in Figs. 5.1 and 5.2 for the coherent case. However, the non-coherent receiver does not perform as well as the coherent case. The performance is compared in Fig. 5.5 for various N and $P_F = 10^{-4}$. The SNR degradation of the non-coherent case, relative to the coherent case, decreases with N. For N = 100 and $P_D = 10^{-3}$, it is approximately 2 dB, and for $N = 10^6$, and $P_D = 10^{-3}$, it is 1 dB.

We also note that the SNR where $P_D \to P_F$, rendering interception impractical for SNR's smaller than this value, is larger in the non-coherent case. This result is as expected as the non-coherent receiver is inferior in performance to the coherent receiver. For instance, in Fig. 5.3 for $P_F = 10^{-3}$ and $N = 10^6$, this SNR for the non-coherent case is 8 dB. In the coherent case, in Fig. 5.1, for the same parameters this SNR is 6 dB. As expected, interception will fail at a larger SNR for the non-coherent case.

We will now establish the rate of convergence of P_D to P_F as N gets large. Once again, some of our results for the coherent case carry over. For instance, (5.9) and (5.10) remains valid. From (5.13) and (5.14) there follows:

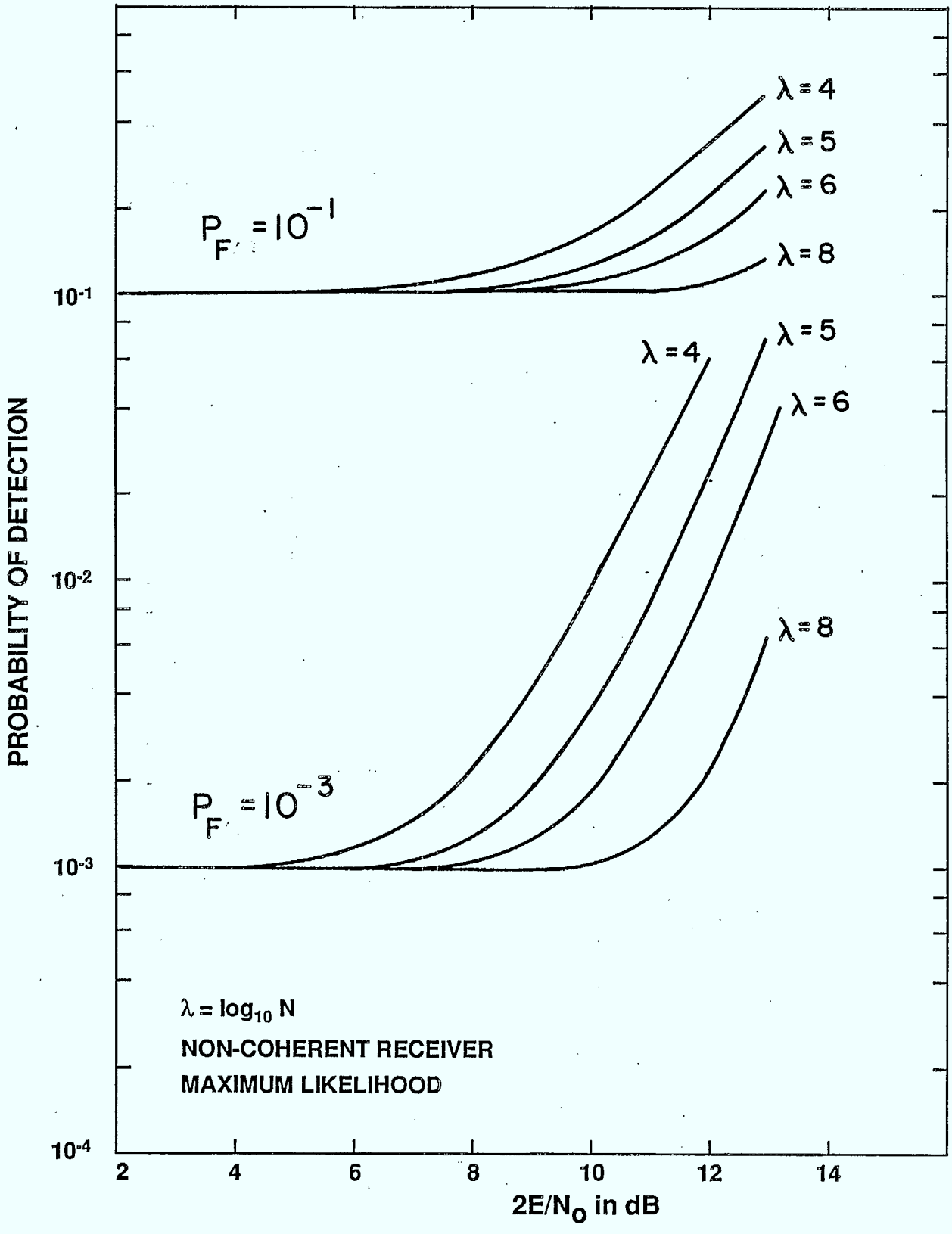

Figure 5.3 Probability of detection as a function of $2E/N_o$ for $P_F = 10^{-1}$, 10^{-3} for the non-coherent ML receiver

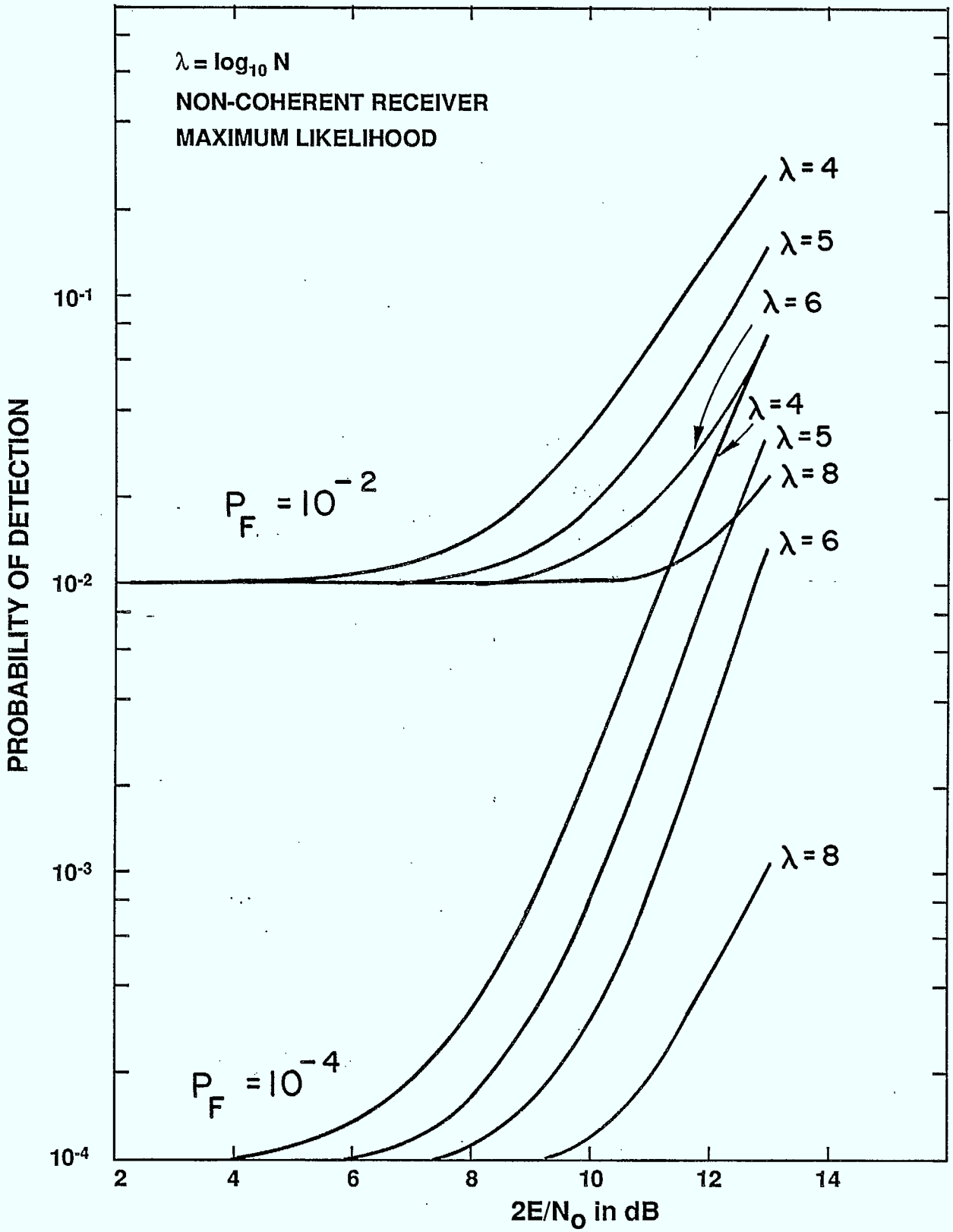

Figure 5.4 Probability of detection as a function of $2E/N_o$ for $P_F = 10^{-2}, 10^{-4}$ for the non-coherent ML receiver

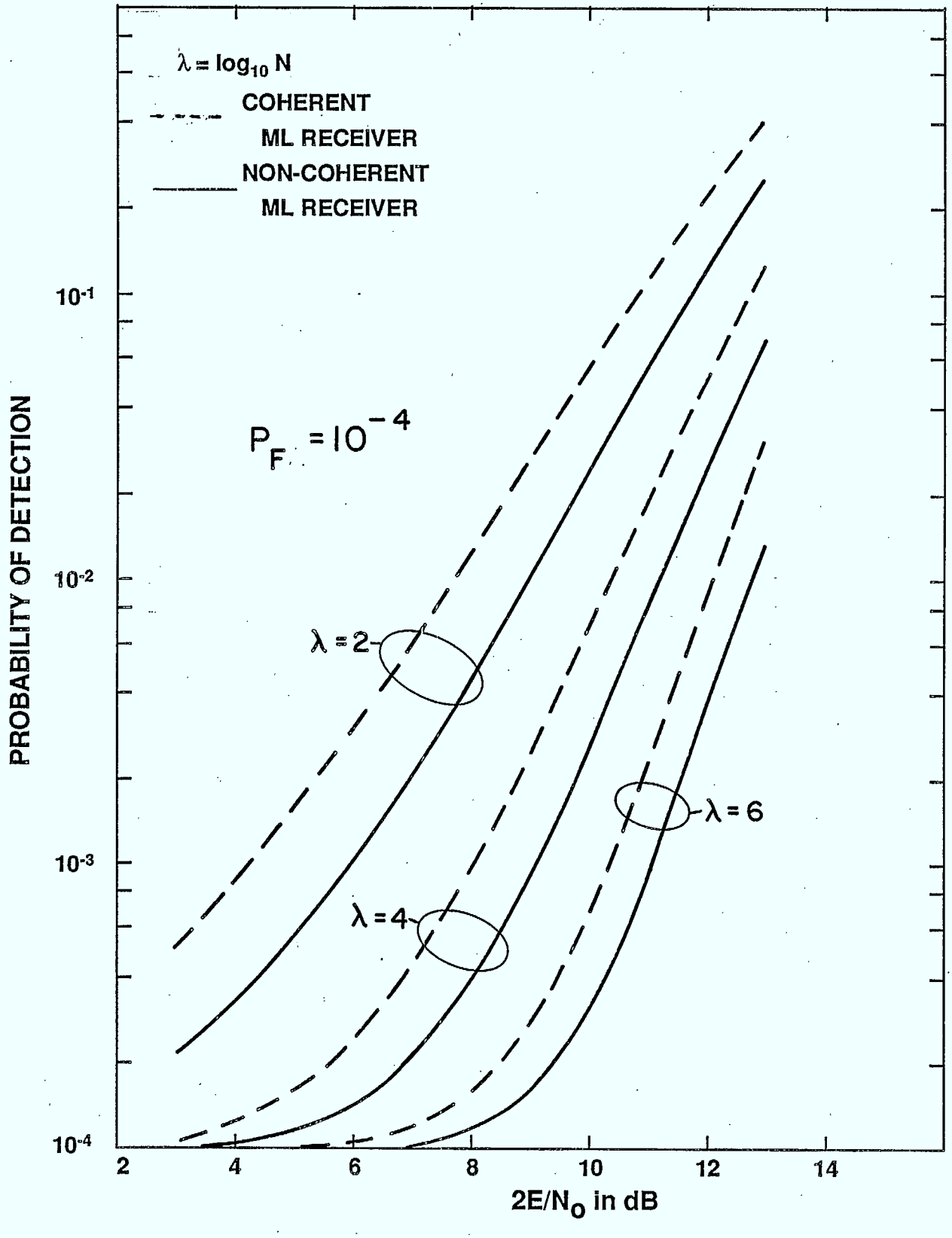

Figure 5.5 Coherent versus non-coherent P_D for the ML receiver

$$Q_D = Q(d, (-2\ell n\ Q_F)^{1/2})$$

and from (5.10),

$$Q_D = Q(d, \{\ell n[\frac{-N}{\ell n(1-P_F)}]^2\}^{1/2}) \qquad (5.15)$$

We consider the case of large SNR or large d. For $\beta >> \alpha$, [29, p.451] states that for

$$Q(\alpha, \beta) \approx \frac{1}{\sqrt{2\pi\alpha\beta}} \exp(-\beta^2/2)$$

In (5.15) we have $\alpha = d$ and

$$\beta^2 = 2\ell n[\frac{-N}{\ell n(1-P_F)}]$$

Hence,

$$Q_D \approx \frac{-\ell n(1-P_F)}{\sqrt{2\pi d}\ N\{2\ell n(\frac{-N}{\ell n(1-P_F)})\}^{1/4}}$$

Now from (5.9),

$$P_D = P_F + \frac{\ell n(1-P_F)^{-1}\ (1-P_F)}{\sqrt{2\pi d}\ N\{2\ell n(\frac{-N}{\ell n(1-P_F)})\}^{1/4}} \qquad (5.16)$$

Thus for the non-coherent case the convergence rate is as $1/(N\{\ell nN\}^{1/4})$. For practical N, this rate is essentially as 1/N.

5.6 P_D as $N \to \infty$: Central Limit Theorem Analysis

Our treatment of P_D as N gets large for the average likelihood, or optimum, receiver will be based a the Central Limit Theorem (CLT), see reference [30, p. 58]. As a prelude to this analysis we reconsider P_D for the maximum likelihood receiver from the point of view of the CLT.

The maximum likelihood receiver computes the decision statistic

$$\ell = \sum_{i=1}^{N} \ell_i ; \qquad \ell_i = 0, 1$$

For the noise only hypothesis, H_o, $\ell = \ell_{H0}$,

$$\ell_i = \ell_{i0} = \begin{cases} 1 & \text{w.p. } Q_F \\ 0 & \text{w.p. } 1-Q_F \end{cases}$$

where w.p. means "with probability" and Q_F is given in (5.4). For the signal present hypothesis, H_1, $\ell = \ell_{H1}$, and

$$\ell_i = \ell_{i1} = \begin{cases} 1 & \text{w.p. } \frac{N-1}{N} Q_F + \frac{Q_D}{N} = p \\ 0 & \text{w.p. } 1-p \end{cases} . \qquad (5.18)$$

The mean and variances below follow from simple derivations,

$$\overline{\ell_{i0}} = Q_F$$

$$\sigma^2_{\ell_{i0}} = Q_F(1-Q_F)$$

$$\overline{\ell_{H0}} = N Q_F$$

$$\sigma^2_{\ell_{H0}} = N Q_F(1-Q_F)$$

$$\overline{\ell_{i1}} = p$$

$$\sigma^2_{\ell_{i1}} = p(1-p)$$

$$\overline{\ell_{H1}} = Np$$

and

$$\sigma^2_{\ell_{H1}} = Np(1-p)$$

Also,

$$\frac{\ell_{H0} - NQ_F}{\sqrt{NQ_F(1-Q_F)}} \to \eta(0, 1) \qquad N \to \infty$$

and

$$\frac{\ell_{H1} - Np}{\sqrt{Np(1-p)}} \to \eta(0, 1) \qquad N \to \infty$$

Thus, for large N,

$$P_F = Q\left(\frac{\eta - NQ_F}{\sqrt{NQ_F(1-Q_F)}}\right) \tag{5.19}$$

and

$$P_D = Q\left(\frac{\eta - Np}{\sqrt{Np(1-p)}}\right).$$

Now from (5.18), $Np = (N-1)Q_F + Q_D$ and thus

$$P_D = Q\left(\frac{\eta - (N-1)\,Q_F - Q_D}{\sqrt{Np(1-p)}}\right). \tag{5.20}$$

A little manipulation of equations (5.19) and (5.20) gives

$$P_D = Q\left\{\frac{Q^{-1}(P_F)}{\lambda}\sqrt{Q_F(1-Q_F)} + \frac{Q_F - Q_D}{\lambda\sqrt{N}}\right\}$$

where

$$\lambda^2 = \left(\frac{N-1}{N}Q_F + \frac{Q_D}{N}\right)\left(1 - \left(\frac{N-1}{N}\right)Q_F - \frac{Q_D}{N}\right).$$

We established earlier that $Q_D \to 0$ as $N \to \infty$. Hence for very small Q_D,

$$P_D = Q\left\{Q^{-1}(P_F) + \frac{Q_F}{\sqrt{N}\sqrt{Q_F(1-Q_F)}}\right\} \tag{5.21}$$

and for large enough N, $P_D \to P_F$.

5.7 P_D, $N \to \infty$: Optimum Coherent Receiver

We now consider the detection random variable in (2.18), namely

$$\ell = \sum_{i=1}^{N} \ell_i$$

where $\ell_i = e^{\alpha_i}$ with $\alpha_i \sim \eta(0, d^2)$, $d^2 = 2E/N_o$. We assume that N is large enough so that ℓ is $\eta(\bar{\ell}, \sigma_\ell^2)$, as a consequence of the Central Limit Theorem. We wish to determine

$$P_F = P(\ell > \eta)$$

given that H_0, the noise only hypothesis is active.

From (2.20) $\bar{\ell}_i = E(e^{\alpha_i})$ is given by $e^{d^2/2}$, where $d^2 = 2E/N_o$. Furthermore, from (2.20),

$$\sigma_{\ell_i}^2 = e^{d^2}(e^{d^2}-1).$$

Thus

$$\bar{\ell}_{H0} = N\, e^{d^2/2}$$

and

$$\sigma_{\ell_{H0}}^2 = N\, e^{d^2}(e^{d^2}-1).$$

Now $P_F = P(\ell > \eta | H_0)$ and thus for N large

$$P_F \simeq Q\{\frac{(\eta - N\, e^{d^2/2})\, e^{-d^2/2}}{\sqrt{N(e^{d^2}-1)}}\} \qquad (5.22)$$

Before we consider the signal present, H_1, hypothesis, it should be noted that only one of the ℓ_i's in the sum for ℓ can have a mean $e^{3d^2/2}$. This is because of the slow hopping assumption, where it follows that the modulation does not frequency hop during the detection period. Hence N-1 of the ℓ_i are independent and identically distributed. The sum of these N-1 variables satisfies the CLT and its distribution is asymptotically Gaussian. Hence, one may write

$$\ell = \sum_{\substack{i=1 \\ i\neq k}}^{N} e^{\alpha_i} + e^{\bar{\alpha}_k} e^{(\alpha_k - \bar{\alpha}_k)} \tag{5.23}$$

where the e^{α_i} are as in the P_F analysis and so is $\alpha_k - \bar{\alpha}_k$: they are all $\mathcal{N}(0, d^2)$ and also, $\bar{\alpha}_k = d^2$. Hence

$$\bar{\ell}_{H1} = (N-1)e^{d^2/2} + e^{d^2} e^{d^2/2}$$

and

$$\sigma_{\ell_{H1}}^2 = e^{d^2} [(N-1) + e^{2d^2}] [e^{d^2} - 1]. \tag{5.24}$$

Thus,

$$P_D = Q\{\frac{\eta - (N-1) e^{\frac{d^2}{2}} - e^{3d^2/2}}{\sigma_{\ell_{H1}}}\}. \tag{5.25}$$

Combination of equations (5.24) and (5.25) with (5.22) yields

$$P_D = Q\{Q^{-1}(P_F) \sqrt{\frac{N}{N + e^{2d^2} - 1}} - \sqrt{\frac{e^{d^2} - 1}{N + e^{2d^2} - 1}}\}. \tag{5.26}$$

For large N, $P_D \to P_F$. We also note that equation (5.26) can be used as an approximation to P_D for large N. We call this the CLT approximation. A better approximation can be obtained by using the Gaussian distribution for α_k in (5.23) and the limit distribution, also Gaussian, for $\sum_{\substack{i=1 \\ i\neq k}}^{N} e^{\alpha_i}$ in (5.23). We call this the CLT + 1 approximation. Data from these approximations are given in Table 5.1. One notes that for

N = 10000 SNR = 3.000000000000000 DB

PF	PDCLT+1	PDCLT	MAXLIKELIHOOD
0.1000000	0.1049900	0.1050987	0.1020163
9.9999998E-03	1.0946072E-02	1.0864927E-02	1.0414147E-02
1.0000000E-03	1.1774122E-03	1.1181121E-03	1.0762307E-03
9.9999997E-05	1.4664898E-04	1.1478132E-04	1.1338558E-04
9.9999997E-06	2.9973244E-05	1.1764009E-05	1.2270002E-05
1.0000000E-06	1.2854009E-05	1.2052842E-06	1.3740269E-06

N = 100000 SNR = 3.000000000000000 DB

PF	PDCLT+1	PDCLT	MAXLIKELIHOOD
0.1000000	0.1014645	0.1014660	0.1003896
9.9999998E-03	1.0235984E-02	1.0231144E-02	1.0075799E-02
1.0000000E-03	1.0323786E-03	1.0299988E-03	1.0133781E-03
9.9999997E-05	1.0457628E-04	1.0360483E-04	1.0226988E-04
9.9999997E-06	1.0865957E-05	1.0415591E-05	1.0374024E-05
1.0000000E-06	1.2977636E-06	1.0475495E-06	1.0601326E-06

N = 1000000 SNR = 3.000000000000000 DB

PF	PDCLT+1	PDCLT	MAXLIKELIHOOD
0.1000000	0.1004491	0.1004491	0.1000714
9.9999998E-03	1.0069225E-02	1.0069034E-02	1.0013304E-02
1.0000000E-03	1.0088673E-03	1.0087990E-03	1.0022686E-03
9.9999997E-05	1.0106216E-04	1.0104196E-04	1.0037400E-04
9.9999997E-06	1.0125486E-05	1.0118617E-05	1.0060132E-05
1.0000000E-06	1.0170654E-06	1.0140127E-06	1.0094639E-06

N = 10000000 SNR = 3.000000000000000 DB

PF	PDCLT+1	PDCLT	MAXLIKELIHOOD
0.1000000	0.1001406	0.1001406	0.1000125
9.9999998E-03	1.0021436E-02	1.0021430E-02	1.0002256E-02
1.0000000E-03	1.0027168E-03	1.0027151E-03	1.0003739E-03
9.9999997E-05	1.0032033E-04	1.0031994E-04	1.0006013E-04
9.9999997E-06	1.0036344E-05	1.0036259E-05	1.0009464E-05
1.0000000E-06	1.0048647E-06	1.0048399E-06	1.0014619E-06

N = 100000000 SNR = 3.000000000000000 DB

PF	PDCLT+1	PDCLT	MAXLIKELIHOOD
0.1000000	0.1000443	0.1000443	0.1000021
9.9999998E-03	1.0006737E-02	1.0006737E-02	1.0000371E-02
1.0000000E-03	1.0008520E-03	1.0008520E-03	1.0000601E-03
9.9999997E-05	1.0010025E-04	1.0010023E-04	1.0000946E-04
9.9999997E-06	1.0011336E-05	1.0011335E-05	1.0001462E-05
1.0000000E-06	1.0020777E-06	1.0020775E-06	1.0002221E-06

N = 1000000000 SNR = 3.000000000000000 DB

PF	PDCLT+1	PDCLT	MAXLIKELIHOOD
0.1000000	0.1000140	0.1000140	0.1000004
9.9999998E-03	1.0002127E-02	1.0002127E-02	1.0000059E-02
1.0000000E-03	1.0002689E-03	1.0002689E-03	1.0000095E-03
9.9999997E-05	1.0003161E-04	1.0003161E-04	1.0000146E-04
9.9999997E-06	1.0003564E-05	1.0003564E-05	1.0000223E-05
1.0000000E-06	1.0012176E-06	1.0012176E-06	1.0000332E-06

Table 5.1a

CLT and CLT+1 approximations to P_D for Coherent Optimum Receiver: SNR = 3 dB.

N = 10000 SNR = 13.000000000000000 DB

PF	PDCLT+1	PDCLT	MAXLIKELIHOOD
0.1000000	0.2334174	0.5000184	0.6261156
9.9999998E-03	0.1265264	0.5000184	0.3937885
1.0000000E-03	0.1039359	0.5000183	0.2328055
9.9999997E-05	9.4743431E-02	0.5000182	0.1262261
9.9999997E-06	8.9055523E-02	0.5000182	6.2943377E-02
1.0000000E-06	8.4900595E-02	0.5000181	2.9106634E-02

N = 100000 SNR = 13.000000000000000 DB

PF	PDCLT+1	PDCLT	MAXLIKELIHOOD
0.1000000	0.1877839	0.5000182	0.4521938
9.9999998E-03	8.3951496E-02	0.5000179	0.2399709
1.0000000E-03	6.5067038E-02	0.5000177	0.1270287
9.9999997E-05	5.8334459E-02	0.5000175	6.3028656E-02
9.9999997E-06	5.4372542E-02	0.5000174	2.9115403E-02
1.0000000E-06	5.1525157E-02	0.5000172	1.2586645E-02

N = 1000000 SNR = 13.000000000000000 DB

PF	PDCLT+1	PDCLT	MAXLIKELIHOOD
0.1000000	0.1548418	0.5000175	0.3114852
9.9999998E-03	5.4436170E-02	0.5000166	0.1330539
1.0000000E-03	3.8704507E-02	0.5000159	6.3880965E-02
9.9999997E-05	3.3962362E-02	0.5000153	2.9203290E-02
9.9999997E-06	3.1365171E-02	0.5000148	1.2595547E-02
1.0000000E-06	2.9537339E-02	0.5000144	5.1270095E-03

Table 5.1b

CLT and CLT+1 approximations to P_D for Coherent Optimum Receiver: SNR = 13 dB

N = 10000000 SNR = 13.000000000000000 DB

PF	PDCLT+1	PDCLT	MAXLIKELIHOOD
0.1000000	0.1325023	0.5000151	0.2152173
9.9999998E-03	3.5252903E-02	0.5000122	7.2404481E-02
1.0000000E-03	2.1956306E-02	0.5000101	3.0081678E-02
9.9999997E-05	1.8685332E-02	0.5000084	1.2684632E-02
9.9999997E-06	1.7075362E-02	0.5000069	5.1359632E-03
1.0000000E-06	1.5975432E-02	0.5000056	1.9798514E-03

N = 100000000 SNR = 13.000000000000000 DB

PF	PDCLT+1	PDCLT	MAXLIKELIHOOD
0.1000000	0.1182626	0.5000075	0.1575911
9.9999998E-03	2.3561163E-02	0.4999985	3.8865324E-02
1.0000000E-03	1.1989110E-02	0.4999919	1.3575445E-02
9.9999997E-05	9.7181918E-03	0.4999865	5.2255932E-03
9.9999997E-06	8.7654199E-03	0.4999818	1.9888338E-03
1.0000000E-06	8.1439465E-03	0.4999776	7.2910078E-04

N = 1000000000 SNR = 13.000000000000000 DB

PF	PDCLT+1	PDCLT	MAXLIKELIHOOD
0.1000000	0.1097260	0.4999836	0.1266779
9.9999998E-03	1.6877392E-02	0.4999551	2.2483438E-02
1.0000000E-03	6.4322571E-03	0.4999343	6.1219237E-03
9.9999997E-05	4.7893496E-03	0.4999171	2.0786556E-03
9.9999997E-06	4.2407899E-03	0.4999023	7.3809421E-04
1.0000000E-06	3.9099250E-03	0.4998890	2.5721898E-04

practical P_F's down to 10^{-3} the approximate P_D via the CLT + 1 approximation is very close to P_D for the maximum likelihood receiver. Thus it appears that, for large N, the average likelihood or optimum receiver performs the same as the maximum likelihood receiver. Our approximate analysis is better at low SNR than large SNR. Also, the CLT approximation at SNR = 13 dB was very poor and is not tabulated. This follows, as [26, p. 194] points out, since a large SNR makes one term in (5.23) dominant, a situation that is poor for CLT approximations.

5.8 P_D as $N \to \infty$; Optimum Receiver: Non-Coherent Case

The decision statistic for the non-coherent, optimum receiver is given by (3.24) as

$$\ell = \sum_{i=1}^{N} I_o(q_i) \tag{5.27}$$

where q_i are defined in (3.22). When r(t) = n(t) in (3.22), i.e., the H_o hypothesis, q_i is Rayleigh distributed. When the signal present hypothesis is active, N - 1, q_i's are Rayleigh distributed and one has a Rician distribution.

The mean and variance of ℓ, in (5.27) under hypotheses H_0 and H_1 cannot all be expressed in terms of known functions as was the situation in the coherent case. However, it is shown herein that if the mean and variance of $\ell_i = I_0(q_i)$ under H_0 and H_1 are finite, then the argument of the previous section can be carried through in general.

To set the stage for this general analysis let $\ell_{i0} = I_0(q_{i0})$ where q_{i0} is the value of q_i under H_0: similarly, $\ell_{i1} = I_0(q_{i1})$ for hypothesis H_1. Then for large N and the CLT referred to earlier

$$P_F = Q\left(\frac{\eta - \bar{\ell}_{H0}}{\sigma_{\ell_{H0}}}\right)$$

where

$$\ell_{H0} = \sum_{i=1}^{N} \ell_{i0} = \sum_{i=1}^{N} I_0(q_{i0}) \tag{5.28}$$

Thus

$$\eta = \sigma_{\ell_{H0}} Q^{-1}(P_F) + \bar{\ell}_{H0} \tag{5.29}$$

Now the probability of detection for large N is given by

$$P_D = Q\left(\frac{\eta - \bar{\ell}_{H1}}{\sigma_{\ell_{H1}}}\right)$$

or by (5.29)

$$P_D = Q\left\{\frac{\sigma_{\ell_{H0}}}{\sigma_{\ell_{H1}}} Q^{-1}(P_F) + \frac{\bar{\ell}_{H0} - \bar{\ell}_{H1}}{\sigma_{\ell_{H1}}}\right\} \tag{5.30}$$

Note that if $\sigma_{\ell_{H0}} \to \sigma_{\ell_{H1}}$ as $N \to \infty$ and if

$$\lim_{N \to \infty} \frac{\bar{\ell}_{H0} - \bar{\ell}_{H1}}{\sigma_{\ell_{H1}}} \to 0$$

one has $P_D \to P_F$ as $N \to \infty$.

We note that equation (5.30) agrees with equation (5.26) for the coherent case. This follows as in that case

$$\ell = \sum_{i=1}^{N} e^{\alpha_i}$$

$$\bar{\ell}_{H0} = N e^{d^2/2},$$

$$\bar{\ell}_{H1} = (N-1) e^{d^2/2} + e^{3d^2/2}$$

$$\sigma_{\ell_{H0}}^2 = N(e^{d^2}-1)\, e^{d^2}$$

and

$$\sigma_{\ell_{H1}}^2 = e^{d^2}[e^{d^2}-1][(N-1)+e^{2d^2}]$$

where $d^2 = 2E/N_o$.

To proceed with the general analysis, it follows from (5.28) that $E(\ell_{H0}) = \bar{\ell}_{H0} = N\,\bar{\ell}_{i0}$ where $\bar{\ell}_{i0} = E\{I_o(q_{i0})\}$: where q_{i0} is Rayleigh distributed.

Under hypothesis H_1,

$$\ell_{H1} = \sum_{i=1}^{N} \ell_{i1} = \sum_{i=1}^{N} I_o(q_{i1}) \tag{5.31}$$

where $N-1$ q_{i1}'s are Rayleigh and one is Rician. Thus

$$\bar{\ell}_{H1} = (N-1)\,\bar{\ell}_{i0} + \bar{\ell}_R \tag{5.32}$$

with $\bar{\ell}_R = E\{I_0(q_R)\}$ with q_R a Rician random variable. Similarly,

$$\sigma_{\ell_{H0}}^2 = N\,\sigma_{\ell_{i0}}^2 = N\{\overline{I_0^2(q_{i0})} - \bar{\ell}_{i0}^2\} \tag{5.33}$$

and

$$\sigma_{\ell_{H1}}^2 = (N-1)\,\sigma_{\ell_{i0}}^2 + \sigma_{\ell_R}^2 \tag{5.34}$$

and $\sigma_{\ell_R}^2$ is the variance of the single Rician term in (5.31); namely

$$\sigma_{\ell_R}^2 = E\{I_0^2(q_R)\} - \bar{\ell}_R^2.$$

It follows from (5.33) and (5.34) that $\sigma_{\ell_{H0}}^2 / \sigma_{\ell_{H1}}^2 \to 1$ as $N \to \infty$ when all other terms in these equations can be defined by a convergent

infinite series. It is shown later that this is true for any finite SNR. Also from (5.32) and the definition of ℓ_{H0} in (5.28),

$$\frac{\bar{\ell}_{H0} - \bar{\ell}_{H1}}{\sigma_{\ell_{H1}}} = \frac{E\{I_0(q_{i0})\} - E\{I_0(q_R)\}}{\sigma_{\ell_{H1}}} \tag{5.35}$$

where q_{i0} is Rayleigh and q_R is Rician. From (5.34), $\sigma_{\ell_{H1}}$ grows as $\sqrt{N-1}$ whereas the numerator in (5.35) is finite for finite SNR. It follows that

$$\frac{\bar{\ell}_{H0} - \bar{\ell}_{H1}}{\sigma_{\ell_{H1}}} \to 0 \quad \text{as} \quad N \to \infty.$$

Thus both of the conditions following equation (5.30) have been satisfied and $P_D \to P_F$ as $N \to \infty$ for the optimum, non-coherent receiver.

There only remains to show that $E\{I_0(q_{i0})\}$, $E\{I_0^2(q_{i0})\}$, $E\{I_0(q_R)\}$ and $E\{I_0^2(q_R)\}$ are finite when q_{i0} is Rayleigh and q_R is Rician.

We first consider $E\{I_0(q_{i0})\}$ where q_{i0} is Rayleigh. That is the pdf for q_{i0} is

$$f_{q_{i0}}(x) = \frac{x}{\sigma^2} \exp(-x^2/2\sigma^2)\, u(x)$$

where $\sigma^2 = d^2 = 2E/N_o$. Thus

$$E\{I_0(q_{i0})\} = \int_o^\infty I_o(x)\, f_{q_{i0}}(x)dx$$

$$= e^{\sigma^2/2} = e^{E/N_o}$$

which follows from [31]. Furthermore, and also from [31],

$$E\{I_0^2(q_{i0})\} = e^{2E/N_o}\, I_0(\tfrac{2E}{N_o})$$

Thus the variance of $I_0(q_{i0})$ is

$$E\{(I_0(q_{i0}) - \overline{I_0(q_{i0})})^2\} = e^{2E/N_o} (I_0(\frac{2E}{N_o})-1)$$

We now consider $E\{I_0(q_R)\}$ where q_R is Rician [26, p. 139]

$$f_{q_R}(x) = \frac{x}{\sigma^2} I_0(\frac{xb}{\sigma^2}) e^{-b^2/2\sigma^2} e^{-\frac{x^2}{2\sigma^2}}$$

where $b = \sigma^2 = d^2 = 2E/N_o$. Then

$$E\{I_0(q_R)\} = \int_o^\infty I_0(x) f_{q_R}(x)\, dx$$

$$= e^{E/N_o} I_0(\frac{2E}{N_o})$$

again by use of [31].

When q_{i0} is Rayleigh, it has been shown that the mean and variance of $I_0(q_{i0})$ can be given in terms of known functions. A similar result holds for the mean of $I_0(q_R)$, when q_R is Rician. For the second moment of $I_0(q_R)$ we can show that,

$$E\{I_0^2(q_R)\} = \int_o^\infty I_0^2(x) f_{q_R}(x)\, dx$$

$$= \sum_{m=0}^{\infty} \sum_{k=0}^{m} \frac{(2m)!(d^2/2)^{k+m}}{(m!)^2(k!)^2(m-k)!}$$

Also, by a comparison test, it can be shown that this doubly infinite series converges for finite d.

We thank L.L. Campbell, Mathematics Department, Queen's University, for his assistance in obtaining the results on $E(I_0^n(x))$, $n = 1, 2$ where x is Rayleigh or Rician.

We have carried out the argument that $P_D \to P_F$ as $N \to \infty$ for $\ell_i = I_0(q_i)$. However, the result is true for any ℓ_{H0} and ℓ_{H1} satisfying the conditions of the CLT and also ℓ_i, under H_0 and H_1, satisfying the two conditions following equation (5.30).

CHAPTER 6

CONCLUSION

6.1 SUMMARY

Chapter 1 introduced the problem of detecting a sinusoid with a discrete frequency distribution by discussing relevant literature, and drawing parallels between that problem and the one of spread spectrum signal interception. It also defined the system model used in the rest of the report.

In Chapter 2, two coherent receivers were derived and their performance analyzed. These were the optimum receiver and the maximum likelihood receiver. In that chapter the theory needed to derive the receivers, which was also used in later chapters, was established. In addition, an approximation of the probability density function of the sum of N lognormal random variables was discussed.

Three noncoherent receivers were examined in Chapter 3. In addition to the noncoherent versions of the optimum receiver and the maximum likelihood receiver, a low SNR receiver was discussed. This chapter also included a comparison of the noncoherent and coherent receivers, and especially noted characteristics exhibited by all the receivers.

Chapter 4 looked at two deviations from the assumptions made in Chapter 1. It first considered the advantages of using a priori knowledge, if it exists. Second, it found the probability of detection for any frequency, regardless of whether the receiver was optimized for it or not. This led to a study of the effects of frequency offset on the

receiver performance. This last was done for both maximum likelihood receivers, and the optimum coherent receiver, though the latter was only studied under the assumption of two transmission frequencies.

6.2 CONCLUSIONS

For a sinusoid with a discrete frequency distribution, it has been shown that any optimum receiver includes a bank of N filters, each one of which is matched to one of the N possible transmission frequencies. The optimum coherent receiver has a sufficient statistic equal to N lognormal random variables, the solution of which is too unwieldy for any number of frequencies greater than two. However, the optimum receiver and the coherent maximum likelihood receiver were shown to have nearly identical receiver operating characteristics (ROC), this being confirmed by simulations of the optimum receiver performance. Therefore, the ROC of the maximum likelihood receiver can be used to give a close approximation of the performance limits for the coherent detection of a random frequency signal. For large SNR values, on the order of 13 dB or larger, P_D is greater than 0.9. However, for SNR less than 10 dB, the signal will be detected less than half the time. This reduces to less than one time in ten when the SNR is less than 3 dB.

Three noncoherent detection methods were considered for this signal. Since the sufficient statistic for the optimum receiver is a sum of modified Bessel functions with Rayleigh or Ricean arguments, an exact performance analysis of the receiver is not straightforward, and one was not found. However, simulations showed that the performance of the noncoherent maximum likelihood receiver gives an excellent

approximation of that of the optimum receiver for the SNR values considered. Using the maximum likelihood receiver performance, a comparison of noncoherent and coherent detection shows that the performance loss between the two methods decreases as the SNR increases. Some typical values are a 1 dB loss when SNR is around 13 dB and a 2 dB loss when the SNR is in the vicinity of 3 dB. Note that this loss decreases as the number of frequencies increases.

The third noncoherent receiver, designed by approximating the sufficient statistic of the optimum receiver by $\sum_{i=1}^{N}(1+(q_i^2/4))$, gives a performance equal or inferior to that of the maximum likelihood receiver. The performance of the low SNR receiver is closest to optimum at SNR levels 3 dB or less. However, the approximation becomes poorer, for any SNR, as the number of frequencies increases. Therefore, this receiver gives near optimum performance only when there is a small number of frequencies and the SNR is low.

The law of diminishing returns is exemplified by P_D as a function of the number of transmission frequencies. As the number of frequencies used by the transmitter increases, P_D decreases. However, the loss is less for each additional frequency. From the transmitter's point of view, it will take more and more frequencies to gain the same reduction in the probability of interception. It should also be noted that the performance of the coherent receiver degrades faster than that of the noncoherent receiver. The drop appears to be between 25% and 30% each time the number of frequencies is doubled.

If a priori knowledge is available, and if it is used to design a new optimum receiver, significant improvement is obtained only for SNR less than 7 dB. This receiver can tolerate some error in the a priori

knowledge. In the example used in this report, when two transmission frequencies were used, if the assumed probability of arrival for one signal was 0.9, and the actual probability was 0.75, the a priori receiver would still give a superior performance than if it had been designed without the a priori knowledge. If the difference between the assumed and actual probability was larger than this, a loss relative to the performance of the other receiver was noted. This was as large as 90% or greater if the arrival probability of the signal assigned the larger probability, was actually zero. It is recommended that a priori knowledge not be used unless there is a great deal of certainty about it, since the penalty of using incorrect information to design a receiver could be a loss in performance greater than 90%.

If the received signal frequency is not equal to one of the detector center frequencies, it is less likely to be detected than if it is. However, the receiver can tolerate small frequency offsets, on the order of 10% of the frequency separation, with less than a 10% loss in detection capability for a fixed false alarm probability. Should the received frequency be offset by half of the frequency separation, the loss is greater than 50%, which increases as the number of frequencies does.

When, N, the number of frequencies is large, P_D tends to P_F with the convergence rate of N^{-1}. In a series of curves the SNR below which signal interception is impossible has been established. Below this SNR, $P_D = P_F$ and the interceptor cannot distinguish detections from false alarms. This SNR grows with N but decreases with P_F.

REFERENCES

[1] R.C.Dixon, *Spread Spectrum Systems, 2nd ed.*, John Wiley & Sons, New York: 1984.

[2] A.J.Viterbi, "Spread Spectrum Communications - Myths and Realities", *IEEE Comm. Mag.*, Vol. 17, May 1979, pp. 11-18.

[3] A.J.Viterbi, "When Not to Spread Spectrum - A Sequel", *IEEE Comm. Mag.*, Vol. 23, April 1985, pp. 12-17.

[4] M.Kavehrad, P.J.McLane, "Spread Spectrum for Indoor Digital Radio", *IEEE Comm. Mag.*, Vol. 25, June 1987, pp. 32-40.

[5] A.B.Glenn, "Low Probability of Intercept", *IEEE Comm. Mag.*, vol. 21, July 1983, pp. 26-33.

[6] N.F.Krasner, "Optimal Detection of Digitally Modulated Signals", *IEEE Trans. Commun.*, Vol. COM-30, May 1982, pp. 885-895.

[7] A.Polydoros, C.L.Weber, "Detection Performance Considerations for Direct-Sequence and Time-Hopping LPI Waveforms", *IEEE J. Sel. Areas Comm.*, Vol. SAC-3, Sept. 1985, pp. 727-744.

[8] A.Polydoros, K.T.Woo, "LPI Detection of Frequency-Hopping Signals Using Autocorrelation Techniques", *IEEE J. Sel. Areas Comm.*, Vol. SAC-3, Sept. 1985, pp. 714-726.

[9] A. Polydoros, J.K.Holmes, "Autocorrelation Techniques for Wideband Detection of FH/DS Waveforms in Random Tone Interference", *MILCOM '83 Proc.*, Oct. 1983, pp. 776-780.

[10] A.Polydoros, C.L.Weber, "Optimal Detection Considerations for Low Probability of Intercept", *MILCOM '82 Proc.*, Oct. 1982, pp. 2.1.1-2.1.5.

[11] A.Polydoros, C.L.Nikias, "Advanced Detection of Unknown Frequency Sinusoids in Broadband Noise", *ICC '86 Proc.*, June 1986, pp. 266-270.

[12] E.W.Chandler, G.R.Cooper, "Direct-Sequence Interceptor Performance Gains Due to a Partial-Band Receiver Approach", *MILCOM '86 Proc.*, pp. 2.2.1-2.2.3, Oct. 1986.

[13] R.A.Dillard, "Detectability of Spread-Spectrum Signals", *IEEE Trans. on Aerospace and Electronic Systems*, Vol. AES-15, July 1979, pp. 526-537.

[14] G.R.Cooper, "Detection of Frequency-Hop Signals", *MILCOM '86 Proc.*, pp.10.2.1-10.2.5, Oct. 1986.

[15] R.E. Ziemer, J.M. Liebetreu, "Spread Spectrum Signal Design for Low Probability of Intercept Communications", ICC '83 Proc., pp. F6.8.1-F6.8.5.

[16] L.E. Brennan, I.S. Reed, W. Sollfrey, "A Comparison of Average Likelihood and Maximum Likelihood Ratio Tests for Detecting Radar Targets of Unknown Doppler Frequency", IEEE Trans. Info. Theo., IT-14, Jan. 1968, pp. 104-110.

[17] H.L. Van Trees, Detection, Estimation, and Modulation Theory - Part I, John Wiley & Sons, New York: 1968.

[18] M.H. Meyers, "Computing the Distribution of a Random Variable via Gaussian Quadrature Rules", Bell Sys. Tech. J., Vol. 61, Nov. 1982, pp. 2245-2261.

[19] S.C. Schwartz, Y.S. Yeh, "On the Distribution Function and Moments of Power Sums With Log-Normal Components", Bell Sys. Tech. J., Vol. 61, September 1982, pp. 1441-1462.

[20] P.Z. Peebles, Jr., Probability, Random Variables, and Random Signal Principles, McGraw-Hill Book Company, New York: 1980.

[21] V.K. Prabhu, "Some Consideration of Error Bounds in Digital Systems", Bell Sys. Tech. J., Vol. 50, Dec. 1971, pp. 3127-3151.

[22] N.A. Marlow, "A Normal Limit Theorem for Power Sums of Independent Random Variables", Bell Sys. Tech. J., Vol. 46, Nov. 1967, pp. 2081-1089.

[23] A.D. Whalen, Detection of Signals in Noise, Academic Press, Inc., New York: 1971.

[24] J. Marcum, "A Statistical Theory of Target Detection by Pulsed Radar", IEEE Trans. Inform. Theory, IT-6, April 1960, pp. 59-267.

[25] J.G. Proakis, Digital Communications, McGraw-Hill Company, New York: 1983.

[26] A. Papoulis, Probability, Random Variables, and Stochastic Processes, 2nd ed., McGraw-Hill Book Company, New York: 1984.

[27] J.M. Wozencraft, I.M. Jacobs, Principles of Communication Engineering, John Wiley & Sons, New York: 1965.

[28] W.F. McGee, "Another Recursive Method for Computing the Q-Function", IEEE Trans. Information Theory, Vol. IT-16, July 1970, pp. 500-501.

[29] C.V. Helstrom, "Statistical Theory of Signal Detection", Pergamon Press, 1968.

[30] H. Cramér, "Random Variables and Probability Distributions", Cambridge University Press, 2nd Edition, 1970.

[31] G.N. Watson, "A Treatise on the Theory of Bessel Functions", Cambridge Univ. Press, 1965.

APPENDIX A

Performance Analysis of the Optimum Coherent Receiver

The probability density function of the sufficient statistic, ℓ, for the optimum coherent interception receiver, when noise only is present, is

$$p_{\ell}(\ell|H_0) = \int_0^{\ell} \frac{1}{2d^2} \frac{1}{\pi u(\ell-u)} \exp\left[-\frac{[(\ln u)^2 + (\ln(\ell-u))^2]}{2d^2}\right] du. \quad (A.1)$$

The probability of false alarm is the probability ℓ exceeds the decision threshold when H_0 is true. That is

$$P_F = \int_b^{\infty} p_{\ell}(\ell|H_0)\, d\ell \quad (A.2)$$

so

$$P_F = \int_b^{\infty} \int_0^{\ell} \frac{1}{2d^2} \frac{1}{\pi u(\ell-u)} \exp\left[-\frac{[(\ln u)^2 + (\ln(\ell-u))^2]}{2d^2}\right] du\, d\ell.$$

Switching the order of integration,

$$P_F = \int_0^{b} \frac{1}{(2\pi d^2)^{1/2} u} \exp\left[-\frac{(\ln u)^2}{2d^2}\right] \int_b^{\infty} \frac{(\ell - u)^{-1}}{(2\pi d^2)^{1/2}} \exp\left[-\frac{(\ln(\ell-u))^2}{2d^2}\right] d\ell\, du$$

$$+ \int_b^{\infty} \frac{1}{(2\pi d^2)^{1/2} u} \exp\left[-\frac{(\ln u)^2}{2d^2}\right] \int_u^{\infty} \frac{(\ell - u)^{-1}}{(2\pi d^2)^{1/2}} \exp\left[-\frac{(\ln(\ell-u))^2}{2d^2}\right] d\ell\, du.$$

Let $\lambda = \ln (\ell - u)$. Then

$$P_F = \int_0^b \frac{1}{(2\pi d^2)^{1/2} u} \exp\left[-\frac{(\ln u)^2}{2d^2}\right] \int_{\ln (b-u)}^{\infty} \frac{1}{(2\pi d^2)^{1/2}} \exp\left[-\frac{\lambda^2}{2d^2}\right] d\lambda \, du$$

$$+ \int_b^{\infty} \frac{1}{(2\pi d^2)^{1/2} u} \exp\left[-\frac{(\ln u)^2}{2d^2}\right] \int_{-\infty}^{\infty} \frac{1}{(2\pi d^2)^{1/2}} \exp\left[-\frac{\lambda^2}{2d^2}\right] d\lambda \, du.$$

This simplifies to

$$P_F = \int_0^b \frac{1}{(2\pi d^2)^{1/2} u} \exp\left[-\frac{(\ln u)^2}{2d^2}\right] Q\left[\frac{\ln (b-u)}{d}\right] du$$

$$+ \int_b^{\infty} \frac{1}{(2\pi d^2)^{1/2} u} \exp\left[-\frac{(\ln u)^2}{2d^2}\right] du.$$

Finally, let $\alpha = \ln u$. This gives

$$P_F = Q\left[\frac{\ln b}{d}\right] + \int_{-\infty}^{\ln b} \frac{1}{(2\pi d^2)^{1/2}} \exp\left[-\frac{\alpha_2^2}{2d^2}\right] Q\left[\frac{\ln (b-e^{\alpha_2})}{d}\right] d\alpha_2. \qquad (A.3)$$

For the probability of detection, the probability density function of the sufficient statistic is

$$p_{\ell}(\ell|H_1) = \int_0^{\ell} \frac{1}{2d^2} \frac{1}{\pi u(\ell-u)} \exp\left[-\frac{[(\ln u - d^2)^2 + (\ln (\ell-u))^2]}{2d^2}\right] du. \qquad (A.4)$$

As with the probability of false alarm,

$$P_D = \int_b^\infty p_\ell(\ell|H_1)\, d\ell \tag{A.5}$$

$$= \int_b^\infty \int_0^\ell \frac{1}{2d^2} \frac{1}{\pi u(\ell-u)} \exp\left[-\frac{[(\ln u - d^2)^2+(\ln(\ell-u))^2]}{2d^2}\right] du\, d\ell.$$

Switching the order of integration,

$$P_D = \int_0^b \int_b^\infty \frac{1}{2d^2} \frac{1}{\pi u(\ell-u)} \exp\left[-\frac{[(\ln u - d^2)^2+(\ln(\ell-u))^2]}{2d^2}\right] d\ell\, du.$$

$$+ \int_b^\infty \int_u^\infty \frac{1}{2d^2} \frac{1}{\pi u(\ell-u)} \exp\left[-\frac{[(\ln u - d^2)^2+(\ln(\ell-u))^2]}{2d^2}\right] d\ell\, du.$$

Again, let $\lambda = \ln(\ell - u)$. Then

$$P_D = \int_0^b \frac{1}{(2\pi d^2)^{1/2} u} \exp\left[-\frac{(\ln u - d^2)^2}{2d^2}\right]$$

$$\times \int_{\ln(b-u)}^\infty \frac{1}{(2\pi d^2)^{1/2}} \exp\left[-\frac{\lambda^2}{2d^2}\right] d\lambda\, du$$

$$+ \int_b^\infty \frac{1}{(2\pi d^2)^{1/2} u} \exp\left[-\frac{(\ln u - d^2)^2}{2d^2}\right] \int_{-\infty}^\infty \frac{1}{(2\pi d^2)^{1/2}} \exp\left[-\frac{\lambda^2}{2d^2}\right] d\lambda\, du.$$

Let $\alpha_1 = \ln u$. Then

$$P_D = Q\left[\frac{\ln b}{d} - d\right] + \int_{-\infty}^{\ln b} \frac{1}{(2\pi d^2)^{1/2}} \exp\left[-\frac{(\alpha_1 - d^2)^2}{2d^2}\right] Q\left[\frac{\ln (b - e^{\alpha_1})}{d}\right] d\alpha_1 . \tag{A.6}$$

An alternate form of the probability density function for ℓ is

$$p_\ell(\ell|H_1) = \int_0^{\ell} \frac{1}{2d^2} \frac{1}{\pi u(\ell - u)} \exp\left[-\frac{[(\ln u)^2 + (\ln (\ell - u) - d^2)^2]}{2d^2}\right] du. \tag{A.7}$$

Substituting this expression in (A.5) and integrating in an identical fashion to that shown above, gives

$$P_D = Q\left[\frac{\ln b}{d}\right] + \int_{-\infty}^{\ln b} \frac{1}{(2\pi d^2)^{1/2}} \exp\left[-\frac{\alpha_2^2}{2d^2}\right] Q\left[\frac{\ln (b - e^{\alpha_2})}{d} - d\right] d\alpha_2 . \tag{A.8}$$

APPENDIX B

GAUSSIAN QUADRATURE RULE

The moments of a function, w(x), as discussed in [18], are

$$\mu_i = \int_a^b x^i w(x)\, dx \qquad i = 0,1,..,2M$$

$$= \sum_{j=1}^{M} A_j (t_j)^i \qquad a < t_j < b$$

The weights, A_j's, and nodes, t_j's, can be used to solve

$$\int_a^b f(x)w(x)\, dx = \sum_{j=1}^{M} A_j f(t_j) \qquad a < t_j < b$$

In order to obtain the weights and nodes from the moments, a moment matrix, M, is created such that

$$M = \begin{bmatrix} 1 & \mu_1 & \mu_2 & \mu_3 & \cdots & \mu_M \\ \mu_1 & \mu_2 & \mu_3 & \cdots & & \cdots \\ \mu_2 & \mu_3 & \cdots & & & \cdot \\ \mu_3 & \cdot & & & & \\ \cdot & & & \cdot & & \\ \mu_M & \cdots & & & \cdot & \mu_{2M} \end{bmatrix}$$

Note that $m_{ij} = \mu_{i+j-2}$ and $\mu_0 = 1$. Next, a Cholesky decompostion must be performed on M:

$$M = R^T R$$
$$= R^{*T}\, \mathrm{diag}(r_{ii}^2)\, R^*$$
$$= R^{*T} D R^*$$

where R^* is a unit upper triangular matrix and D is a positive diagonal matrix. Let $m_{ij}^* = r_{ij}^* d_j$. Then

$$r_{ij}^* = m_{ij}^* / r_{ii}^2$$

Now, the elements of R are related to those of M by

$$r_{ii} = (m_{ii} - \sum_{k=1}^{i-1} r_{ki}^2)^{1/2} \qquad i,j = 1,2 \ldots M$$
$$r_{ij} = (m_{ij} - \sum_{k=1}^{i-1} r_{ki} r_{kj})/r_{ii} \qquad i < j$$

So the new variables are related to each other by

$$m_{ij}^* = m_{ij} - \sum_{k=1}^{j-1} m_{ik}^* r_{jk}^* \qquad j = 1,2,\ldots,i-1$$
$$r_{ii}^2 = m_{ii} - \sum_{k=1}^{i-1} m_{ik}^* r_{ik}$$

This implies that

$$m_{ij}^* = \mu_{i+j-2} - \sum_{k=1}^{j-1} m_{ik}^* r_{jk}^*$$
$$r_{ii}^2 = \mu_{i+j-2} - \sum_{k=1}^{i-1} m_{ik}^* r_{ik}$$

Finally, the elements of R are

$$r_{ij} = r_{ii} r^*_{ij}$$

Next the triadiagonal matrix, J, is formed

$$J = \begin{bmatrix} \alpha_1 & \beta_1 & \cdots & 0 \\ \beta_1 & \alpha_2 & \beta_2 & \cdot \\ \cdot & \beta_2 & & \cdot \\ \cdot & & \cdot & \\ \cdot & & \alpha_{M-1} & \beta_{M-1} \\ 0 & \cdots & \beta_{M-1} & \alpha_N \end{bmatrix}.$$

where

$$\alpha_j = \frac{r_{j,j+1}}{r_{j,j}} - \frac{r_{j-1,j}}{r_{j-1,j-1}}$$

and

$$\beta_j = \frac{r_{j+1,j+1}}{r_{j,j}}$$

where $j = 1,2,\ldots,M$.

By finding the eigenvalues and eigenvectors of the matrix J such that

$$Jq_j = \lambda_j q_j$$

the nodes and weights needed by the Gaussian Quadrature Rule can be obtained since

$$t_i = \lambda_i$$
$$A_i = q_{1i}^2$$

where q_{1i} is the first component of the ith eigenvector.

Therefore, the Gaussian Quadrature Rule can be rewritten as

$$\int_a^b f(x)w(x)\,dx = \sum_{j=1}^{M} q_{1j}^2 f(t_j)$$

APPENDIX C

SIMULATION OF THE PERFORMANCE OF THE OPTIMUM NONCOHERENT RECEIVER

C.1 PROBLEM DESCRIPTION

While this appendix will concentrate on the simulation for the performance of the optimum noncoherent receiver, it should be noted that the simulation of that for the coherent optimum receiver was conducted in a similar manner.

In Chapter 3, the sufficient statistic of the optimum noncoherent receiver was found to be

$$\ell = \sum_{i=1}^{N} I_0(q_i) \underset{H_0}{\overset{H_1}{\gtrless}} \eta N e^{d^2/2}$$

where

$$q_i^2 = L_{ci}^2 + L_{si}^2$$

and

$$L_{ci} = {}_0\int^T r(t) \cos \omega_i t \, dt,$$

$$L_{si} = {}_0\int^T r(t) \sin \omega_i t \, dt.$$

$I_0(x)$ is the zero-order modified Bessel function of the first kind, η is the decision threshold, N is the number of frequencies being used by the

transmitter, and d^2 is the SNR, and r(t) is the received signal.

The receiver makes its decision by calculating the sufficient statistic, ℓ, and comparing it to the threshold. Therefore, the probability of false alarm, P_F, can be found by assuming that no signal has been sent and counting the number of times that ℓ exceeds the threshold. P_F can then be obtained by dividing through by the number of samples taken. In the same manner, the probability of detection, P_D, can be found, where instead it is assumed that a signal has been received.

C.2 ALGORITHM

As indicated above, the algorithm to calculate P_F is nearly identical to that used to calculate P_D. Therefore, the algorithms for both will be described simultaneously, with any differences being noted.

L_{ci} and L_{si} are both normal random variables of variance d^2. For P_D, one of the L_{ci}'s has a mean of $d^2\cos\theta$ while the corresponding L_{si} has a mean of $d^2\sin\theta$. For the other N-1 q_i's, L_{ci} and L_{si} will have zero means. For P_F, all the random variables have nonzero means.

Looking again at P_D, for the variables with the nonzero means, since θ is a uniform random variable between $[0,2\pi]$, a random number generator is used to choose a value of θ. The means of L_{ci} and L_{si} are then calculated and the Gaussian random number generator is called twice, each time with the appropriate mean value.

To generate L_{ci} and L_{si} corresponding to the other q_i's, the Gaussian random number generator is again called twice but now each time with a zero mean. To find q_i, L_{ci} and L_{si} are squared separately and

the squares added together. q_i is then obtained by taking the square root of the sum. Finally, the modified zero-order Bessel function of the first kind is taken of q_i, to give ℓ_i. This is repeated N times and the N ℓ_i's are summed together to give the sufficient statistic.

Next, since there is no easy method of determining the threshold that will give the desired P_F, a set of one hundred threshold are stored in an array, and another array of length one hundred is used to count the number of times each threshold is exceeded by the sufficient statistic under each hypothesis. Note that the simulations for each hypothesis were run separately.

The goal was to obtain a good estimate of the receiver performance when $P_F = 10^{-3}$. Therefore, this would require at least one hundred thousand samples in order to count ten false alarms in the relative frequency estimate of P_F. However, to obtain P_D accurate to two significant figures for values as small as 10^{-3}, it was necessary to take one million samples.